

University of Warwick institutional repository: <http://go.warwick.ac.uk/wrap>

**A Thesis Submitted for the Degree of PhD at the University of Warwick**

<http://go.warwick.ac.uk/wrap/34649>

This thesis is made available online and is protected by original copyright.

Please scroll down to view the document itself.

Please refer to the repository record for this item for information to help you to cite it. Our policy information is available from the repository home page.

**INFLUENCE OF THE MECHANICAL ENVIRONMENT UPON  
THE HEALING OF SEGMENTAL BONE DEFECTS IN THE  
RAT FEMUR**

A THESIS

Submitted in fulfilment of the conditions governing  
candidate for the degree of

DOCTOR OF PHILOSOPHY  
of the  
UNIVERSITY OF WARWICK

by

VAIDA GLATT

AUGUST 2009

Department of Medicine,  
Warwick Medical School,  
Warwick Medical School, University of Warwick Coventry CV4 7AL, UK

Research was Conducted at  
the Center for Advanced Orthopaedic Studies at Harvard Medical School  
99 Brookline Avenue, RN120, Boston, MA, 02215

Supervised by

Professor Damian Griffin and Professor Christopher H. Evans

---

## CONTENTS

<b>TITLE</b> .....	1
<b>CONTENTS</b> .....	2
<b>LIST OF FIGURES</b> .....	6
<b>LIST OF TABLES</b> .....	14
<b>ACKNOWLEDGEMENTS</b> .....	16
<b>DECLARATION</b> .....	17
<b>ABSTRACT</b> .....	18
<b>ABBREVIATIONS</b> .....	19
<b><i>CHAPTER ONE: General Introduction</i></b> .....	21
1.1 The Structure and Function of Bone.....	22
1.2 Bone Regeneration and Repair.....	28
1.3 Current Clinical Management of Large Segmental Defects.....	30
1.4 The Influence of Mechanical Forces on Bone Healing.....	35
1.5 Critical Sized Segmental Defects.....	38
1.5.1 Introduction.....	38
1.5.2 BMP-2 and the healing of critical size defects in the rat femur.....	40
1.5.3 Influence of external fixator properties on fracture healing.....	42
1.6 Hypothesis.....	45
<b><i>PROJECT AIMS</i></b> .....	47
<b><i>CHAPTER TWO: The design and evaluation of a novel external fixator, which allows modulation of the mechanical environment within an experimental, critical-sized, femoral defect in the rat</i></b>	

---

2.1 INTRODUCTION.....	49
2.2 DESIGN OF THE FIXATORS.....	50
2.2.1 First Generation Fixator Design and Surgical Implantation.....	50
2.2.2 Surgical implantation of the First Generation External Fixator.....	51
2.3 NOVEL, SECOND GENERATION FIXATOR DESIGN AND SURGICAL IMPLANTATION.....	53
2.3.1. Second Generation Fixator design.....	53
2.3.2 Surgical implantation of the Second Generation External Fixator.....	58
2.4 DISCUSSION.....	60
 <b><i>CHAPTER THREE: Determination of the in vitro mechanical properties of first and second generation external fixators</i></b>	
3.1 INTRODUCTION.....	64
3.2 MATERIALS AND METHODS.....	68
3.2.1 Materials: External Fixators .....	68
3.2.2 Methods.....	68
3.2.2.1 3-Point-Bending of Stability Bars.....	68
3.2.2.2 Axial Compression Validation Test of Materials.....	70
3.2.2.3 Axial Compression Testing.....	72
3.2.2.4 Statistical Analysis.....	76
3.2 RESULTS.....	77
3.3.1 Three Point Bending of Stability Bars.....	77
3.3.2 Axial Compression Validation Testing.....	78
3.3.3 Axial Compression Testing.....	79
3.4 DISCUSSION.....	84

---

**CHAPTER FOUR: Investigation of the effect of the mechanical environment on the healing of an experimental, critical sized femoral defect in response to rhBMP-2**

4.1 INTRODUCTION.....	88
4.2 MATERIALS AND METHODS.....	90
4.2.1 <i>In-Vivo</i> Studies – Study Design.....	90
4.2.2 Surgical Procedure.....	91
4.2.3 Implants.....	91
4.2.4 External Fixators.....	92
4.2.5 Radiographic Evaluation.....	92
4.2.6 Dual-Energy X-Ray Absorptiometry (DXA).....	93
4.2.7 Micro-Computed Tomography ( $\mu$ CT).....	93
4.2.8 Histology.....	94
4.2.9 <i>Ex-Vivo</i> Torsion Testing.....	95
4.2.10 Statistical Analysis.....	95
4.3 RESULTS.....	96
4.3.1 Radiographic Evaluation.....	96
4.3.2 Dual-Energy X-Ray Absorptiometry (DXA).....	99
4.3.3 Micro-Computed Tomography ( $\mu$ CT).....	100
4.3.4 Histology.....	107
4.3.5 <i>Ex-Vivo</i> Torsion Testing.....	109
4.4 DISCUSSION.....	110

**CHAPTER FIVE: The development of a modulated mechanical environment for bone healing in the rat segmental defect model**

5.1 INTRODUCTION.....	115
5.2 MATERIALS AND METHODS.....	118

---

5.2.1 <i>In-Vivo</i> Study Design.....	118
5.2.1.1 Histological Study.....	118
5.2.1.2 Healing Study.....	119
5.2.1.3 Statistical Analysis.....	120
5.3 RESULTS.....	120
5.3.1 Histological Evolution of Defects during the First 2 Weeks of Healing under Different Stiffness Regimens.....	120
5.3.2 Evaluation of an Improved Healing Regimen.....	127
5.3.2.1 Radiographic Evaluation.....	127
5.3.2.2 Dual-Energy X-Ray Absorptiometry (DXA).....	130
5.3.2.3 Micro-Computed Tomography ( $\mu$ CT).....	131
5.3.2.4 Histology.....	138
5.3.2.5 <i>Ex-Vivo</i> Torsion Testing.....	140
5.4 DISCUSSION.....	141
<b>CHAPTER SIX: General Discussion.....</b>	<b>147</b>
<b>FUTURE WORK.....</b>	<b>158</b>
<b>GRADUATE SCHOOLS SKILLS PROGRAMME.....</b>	<b>159</b>
<b>REFERENCE.....</b>	<b>160</b>
<b>APPENDIX.....</b>	<b>173</b>

---

## LIST OF FIGURES

### CHAPTER ONE: GENERAL INTRODUCTION

1.1	Basic structure of a typical long bone, the femur.....	23
1.2	Key stages in the differentiation of MSCs into osteoblasts.....	25
1.3	Steps in the differentiation of haematopoietic stem cells into osteoclasts...26	
1.4	Key events in the remodelling of bone.....	27
1.5	Main phases in fracture healing.....	28
1.6	BMP receptor and signalling cascade.....	29
1.7	Circular external fixator used for the Ilizarov technique.....	32
1.8	Pauwel's concept of tissue differentiation.....	36
1.9	A radiographic image showing critical sized segmental defect.....	40
1.10	Graph showing proposed hypothesis to optimize bone healing.....	46

### CHAPTER TWO: DESIGN OF THE FIXATORS

2.1	Components of first generation external. The rectangular, aluminium stability bar (A) is fixed to the bone with K-wires (B).....	51
2.2	Surgical implantation of first generation fixator.....	52
2.3	Components of the novel extrnal fixator. Three different stiffness connection elements, main module; titanium mounting pin and external fixator implanted on the femur with the defect.....	53

2.4	Assembly of the new generation external fixator.....	54
2.5	External fixator with a titanium screw inserted into the main module.....	54
2.6	(A) Giggly saw guide; (B) Gigly saw guide clipped onto femur.....	55
2.7	Instruments designed for use with the novel fixator: (A) Screwdriver tip; (B) Screwdriver; (C) Miniature electrical pen drill.....	56
2.8	Implantation of second generation external fixator.....	57
2.9	Surgical implanation of the second generation fixator.....	59
2.10	Novel fixator in place across a rat, femoral 5mm defect.....	60

### **CHAPTER THREE: MATERIALS AND METHODS**

3.1	Images illustrating 3-point-bending rig for testing of the external fixator stability bars: (A) ExFixOLD aluminium stability bar; (B) ExFixHigh PEEK stability bar.....	69
3.2	Representative examples of load-displacement curves from 3-pt-bending test of stability bars.....	70
3.3	Representative examples of load-displacement curves of materials: rubber, low-density polyethylene (LDPE), maple and oak tested in an axial compression mode.....	72
3.4	Representative examples of femur constructs tested in axial compression with variuos stiffness fixators and different materials in the defect gap.....	74
3.5	Data from one representative sample shows load-displacement curves from axial compression test of femur constructs with various stiffness fixators	



---

and different materials in the defect gap: (A) No Defect; (B) Low Density polyethylene (LDPE); (C) Maple.....75

### **CHAPTER THREE: RESULTS**

- 3.6 Stability bar stiffness in 3-point-bending for four different stiffness external fixators: ExFixOld, ExFixLow, Med and High.....78
- 3.7 Young's Moduli calculated from axial compression of four different materials: rubber, low-density polyethylene (LDPE), maple and oak.....79
- 3.8 Stiffnesses created by the different fixators applied to rat femur ExFixOld, and ExFixLow, Med, High were placed upon isolated rat femora. (A) Intact femora and femora with 5mm empty defects, and (B) 5mm defects containing rubber were tested in an axial compression mode.....81
- 3.9 Stiffnesses created by the different fixators applied to rat femur ExFixOld, and ExFixLow, Med, High were placed upon isolated rat femora. (C) Femora with 5mm defects containing low density polyethylene (LDPE) and (D) maple were tested in an axial compression mode.....82
- 3.10 Stiffnesses created by different fixators with various inserts in the CSD simulating stages of bone healing, tested in axial compression.....83

### **CHAPTER FOUR: INTRODUCTION**

- 4.1 Representative 3D (top row) and 2D (second row) longitudinal and transverse (third row)  $\mu$ CT images of femur after 8 weeks of treatment with rhBMP-2 with an external fixator (ExFixOld).....89

---

**CHAPTER FOUR: MATERIALS AND METHODS**

- 4.2 Micro-computed tomography images showing evaluation of central defect after 8 weeks of treatment: (A) Region of interest analyzed in the healed defect; (B) Red line represents contour around external callus. All the data presented were calculated within the red line.....94

**CHAPTER FOUR: RESULTS**

- 4.3A First set of representative radiographic images with low, medium and high stiffness external fixators after 9 days, and 2, 3, 4, 5, 6, 7 and 8 weeks of treatment.....97
- 4.3B Second set of representative radiographic images with low, medium and high stiffness external fixators after 9 days, and 2, 3, 4, 5, 6, 7 and 8 weeks of treatment.....98
- 4.4 Bone mineral content (BMC, g) in the segmental defect region after 8 weeks of treatment with rhBMP-2 was measured by DXA.....99
- 4.5 MicroCT was used to measure Total area/callus (mm<sup>2</sup>) with four different stiffness fixators treated with rhBMP-2.....100
- 4.6 MicroCT was used to measure Bone Area (mm<sup>2</sup>) following healing in the presence of rhBMP-2 under the influence of fixators with four different stiffnesses.....101
- 4.7 MicroCT was used to measure Bone Area/Total Area(%) with four different stiffness fixators across defects treated with treated with rhBMP-2.....102
- 4.8 MicroCT was used to measure polar moment of inertia (pMOI, mm<sup>4</sup>) with four different stiffness fixators treated with rhBMP-2.....103

4.9A	First set of representative 3D (top row) and 2D (second and third rows) longitudinal $\mu$ CT images of femur after 8 weeks of treatment with rhBMP-2 and three different stiffness fixators.....	104
4.9B	Second set of representative 3D (top row) and 2D (second and third rows) longitudinal $\mu$ CT images of femur after 8 weeks of treatment with rhBMP-2 and three different stiffness fixators.....	105
4.10A	First set of representative transverse 2D $\mu$ CT images of femoral defects after 8 weeks of treatment with rhBMP-2 with three different stiffness fixators: top row-distal part of the defect; middle row-middle of the defect; bottom row-proximal part of the defect.....	106
4.10B	Second set of representative transverse 2D $\mu$ CT images of femoral defects after 8 weeks of treatment with rhBMP-2 with three different stiffness fixators: top row-distal part of the defect; middle row-middle of the defect; bottom row-proximal part of the defect.....	106
4.11	Representative longitudinal histological sections of femoral segmental defects after 8 weeks of treatment with rhBMP-2 with three different stiffness fixators. Paraffin embedded sections were stained with Hematoxylin & Eosin (top row) and Safranin Orange-Fast Green (bottom row).....	108
4.12	Torsional stiffness of femurs treated with rhBMP-2 with four different stiffness fixators treated with rhBMP-2 after 8 weeks.....	109
4.13	Maximum Torque of femurs treated with rhBMP-2 with four different stiffness fixators treated with rhBMP-2 after 8 weeks.....	110

## CHAPTER FIVE: RESULTS

5.1	Representative longitudinal histological sections of femoral segmental defects after 6, 9 and 14 days of treatment with rhBMP-2 with three
-----	--

	different stiffness fixators. Parafin embedded sections stained with hematoxylin & eosin.....	121
5.2	Representative longitudinal histological sections of femoral segmental defects after 6, 9 and 14 days of treatment with rhBMP-2 with three different stiffness fixators. Parafin embedded sections stained with Safranin Orange.....	122
5.3	Representative longitudinal histological sections of femoral segmental defects after 6 days of treatment with rhBMP-2 with lower stiffness external fixator. Parafin embedded sections stained with hematoxylin & eosin. (A) Fibrous connective tissue adjacent to the defect 5x magnification; (B) Fibrous connective tissue adjacent to the defect at 40x magnification.....	123
5.4	Representative longitudinal histological sections of femoral segmental defects after 9 days of treatment with rhBMP-2 with lower stiffness external fixator. Parafin embedded sections stained with hematoxylin & eosin. (A) Thickened fibrous tissue bridging the defect at 40x magnification; (B) New bone formation in the defect.....	124
5.5	Representative longitudinal histological sections of femoral segmental defects after 9 days of treatment with rhBMP-2 with ExFixHigh stiffness external fixator. Parafin embedded sections stained with hematoxylin & eosin. (A) Fibrous and sponge material adjacent to the defect at 10x magnification; (B) Fibrous and sponge material in the defect at 20x magnification.....	124
5.6	Representative longitudinal histological sections of femoral segmental defects after 2 weeks of treatment with rhBMP-2 with ExFixLow and Med stiffness external fixator. Parafin embedded sections stained with hematoxylin & eosin (top row) and safranin orange-fast green (bottom row). (A) New woven bone formation in the defect at 20x magnification; (B) Thickened fibrous tissue bridging the defect at 10x magnification; (C&D) Traces of cartilage on the edges of callus at 5x magnification).....	125

---

5.7	Representative longitudinal histological sections of femoral segmental defects after 14 of treatment with rhBMP-2 with ExFixHigh stiffness external fixator. Parafin embedded sections stained with hematoxylin & eosin. (A) Fibrous tissue and traces of cartilage in the defect at 5x magnification; (B) Presence of sponge scaffold and fibrous tissue in the defect at 5x magnification.....	126
5.8A	First set of representative radiographic images in the groups with ExFixLow, ExFixMed, ExFixHigh stiffness external fixator and Modulated group after 9 days, 2, 3, 4, 5, 6, 7 and 8 weeks of treatment with rhBMP-2.....	128
5.8B	Second set of representative radiographic images in the groups with ExFixLow, ExFixMed, ExFixHigh stiffness external fixator and Modulated group after 9 days, 2, 3, 4, 5, 6, 7 and 8 weeks of treatment with rhBMP-2.....	129
5.9	Bone Mineral Content (BMC, g) in the segmental defect region after 8 weeks of treatment with rhBMP-2 was measured by DXA.....	130
5.10	MicroCT was used to measure Total area/Callus size (mm <sup>2</sup> ) in four different groups treated with rhBMP-2 and compared to the Intact Femur.....	131
5.11	MicroCT was used to measure Bone Area (mm <sup>2</sup> ) in four different groups: ExFixLow, ExFixMed, ExFixHigh and in Modulated group and compared to the Intact Femur.....	132
5.12	MicroCT was used to measure Bone Area/Total Area (%) in defects treated with rhBMP-2 and stabilised with various stiffness fixator and Modulated group (mean ± SEM) and compared to the Intact Femur.....	133
5.13	MicroCT was used to measure polar moment of inertia (pMOI, mm <sup>4</sup> ) with various stiffness fixators and the modulated group (mean ± SEM) and compared to the Intact Femur.....	134

---

5.14A	First set of representative 3D (top row) and 2D (second and third rows) longitudinal $\mu$ CT images of femora 8 weeks post-surgery in the Modulated group and three different stiffness fixators.....	135
5.14B	Second set of representative 3D (top row) and 2D (second and third rows) longitudinal $\mu$ CT images of femora 8 weeks post-surgery in the Modulated group and three different stiffness fixators.....	136
5.15A	First set of representative transverse 2D $\mu$ CT images of femora 8 weeks post-surgery in the Modulated group and three different stiffness fixators.....	137
5.15B	Second set of representative transverse 2D $\mu$ CT images of femora 8 weeks post-surgery in the Modulated group and three different stiffness fixators.....	138
5.16	Representative histological sections from femoral mid-defect region 8 weeks post-surgery and stabilised with ExFixLow, ExFixMed, ExFixHigh and in a Modulated group.....	139
5.17	Torsional stiffness of femurs treated with rhBMP-2 in four different groups 8 weeks post-surgery, compared to the intact contralateral femur.....	140
5.18	Maximum Torque of femurs 8 weeks post-surgery compared to the intact contralateral femur.....	141

---

## LIST OF TABLES

### CHAPTER THREE: MATERIALS AND METHODS

- 3.1 Indentation moduli for three tissue types in an unstabilized fracture.....71

### CHAPTER THREE: RESULTS

- 3.2 Young's modulus values for materials: rubber, LDPE, maple and oak reported in the literature and compared to the axial compression test performed in the laboratory.....78

### CHAPTER FOUR: RESULTS

- 4.1 Bone mineral content segmental healing characteristic of intact femur, ExFixOld, ExFixLow, ExFixMed and ExFixHigh treated with rhBMP-2 as measured by MicroCT.....99
- 4.2 Segmental healing characteristics of Intact femur, ExFixOld, ExFixLow, ExFixMed and ExFixHigh treated with rhBMP-2 as measured by MicroCT.....103

### CHAPTER FIVE: RESULTS

- 5.1 Bone mineral content segmental healing characteristic of intact femur, ExFixOld, ExFixLow, ExFixMed and ExFixHigh treated with rhBMP-2 as measured by MicroCT.....131
- 5.2 Segmental healing characteristics of Intact femur, ExFixOld, ExFixLow, ExFixMed and ExFixHigh treated with rhBMP-2 as measured by MicroCT.....134

---

5.3	<i>In-vivo</i> segmental healing characteristics of Intact femur, Modulated, ExFixLow, ExFixMed and ExFixHigh treated with rhBMP-2 as measured by MicroCT (n=9-10), DXA (n=9-10), Torsional testing (n=7-8), (mean $\pm$ SEM); and <i>in-vitro</i> results from axial compression construct testing: no defect, 5mm empty defect and with different inserts such as rubber, LDPE, wood (mean $\pm$ SEM, n=6). Asterisks indicate statistical significance from intact, contralateral femur, dollar signs indicate statistical significant difference from Modulated, and hash signs indicate significant difference from ExFixHigh ( $p < 0.05$ ).....	146
-----	--	-----



## ACKNOWLEDGMENTS

First and foremost I would like to thank my primary supervisor and good friend Prof. Christopher Evans from Harvard Medical School. Because my background was concentrated in Biomedical Engineering, I had little knowledge about BMPs, gene therapy and using these therapies to enhance the treatment of larger osseous defects. Chris took it upon himself to teach and explain the needed aspects of biology related to this thesis. I am eternally grateful for all the knowledge, support and excellent supervision he has provided me. Most importantly, I'd like to thank him for his editing and critical review of several drafts for this Lit-English thesis.

I would also like to thank my secondary supervisor Prof. Damian Griffin for his suggestions and for all the support he has given me. His critical review of this thesis was very helpful.

Moreover, I'd like to thank Dr. Mark Vrahas, Partners Chief of Orthopaedic Trauma at Massachusetts General Hospital, for his helpful review of my data from a medical perspective, and for including my husband and I in so many family gatherings when we could not be with our own.

Special thanks goes to my husband and best friend, Michael Glatt, for all his support. He has been so understanding of my absences during so many evenings and weekends over the past four years. I would especially like to thank him for all the help he provided me with the graphics for this thesis. As a professional photographer, he has an amazing talent for colour correction, and his almost magical ability to make my images look amazing, specifically all of the X-Ray and histological images, is astounding. I so appreciate the weeks of work he put in to help make this thesis possible - I will be forever grateful!

I would like to say a special thanks to veterinary pathologist Nicola Parry at the Massachusetts Institute of Technology. She was very helpful with her explanations on how to interpret histology slides.

I would also like to thank members of the Center for Advanced Orthopaedic Studies at Harvard Medical School where all of my research was carried out, and for making the laboratory such an enjoyable place to work. I would like to thank Paula Cohen for all of her help, which extended far beyond just ordering supplies and administration. Alan Ivkovic and Micah Miller for helping and assisting with all of the surgeries. In particular, I would like to thank Ben Roberts and John Muller for all of their help providing mechanical testing and MatLab analyses - without you things would not have gone so smoothly.

---

## DECLARATION

I declare that the thesis titled “Influence of the mechanical environment upon the healing of segmental bone defects in a rat model” is my own work except where I have stated otherwise. I am confirming that this thesis has not been submitted for a degree at any other university.

The idea and the initial design of a novel, external fixator with various stiffnesses for this project is entirely mine. Although, for the final version of the fixator I received help from Romano Matthys, an Innovator at the AO Foundation Research and Development Institute. After presenting him with my idea and design, he worked with me to tweak the design of the prototype. He then collaborated with me in back-and-forth fine-tuning for the final design of the novel external fixator until the fixator was able to meet the specific needs of my research. The AO foundation also assisted me with the actual manufacture of all the parts and needed tools.

To pay for my thesis research I applied for a grant from the AO foundation and was awarded grant S-08-42G (see appendix for attached approval letter).

No part of this research has been published in any scientific journals. However, part of this work has been presented at international conferences as a poster and as podium presentations. Preliminary work of this thesis was also presented at the Biologic Science Postgraduate Symposium, Warwick University, Coventry, UK (see appendix for the abstracts).

### LIST OF ABSTRACTS

Glatt, V. (May 2008) “Influence of Mechanical Environment upon the Healing of Segmental Bone Defects in the Rat Model. Preliminary Report”: *Biologic Science Postgraduate Symposium, Warwick University, Coventry, UK.*

Glatt, V., Matthys, R., Ivkovic, A., Evans, C. (February 2009) “Influence of Mechanical Environment upon the Healing of Segmental Bone Defects in the Rat Model Studied with a Novel, Customized, External Fixator”: *55<sup>th</sup> Annual Meeting of Orthopaedic Research Society, Las Vegas, Nevada, USA.*

Glatt, V., Matthys, R., Ivkovic, A., Evans, C. (June 2008) “Influence of Mechanical Environment upon the Healing of Segmental Bone Defects in the Rat Model Studied with a Novel, Customized, External Fixator. Preliminary data”: *8<sup>th</sup> Annual European Cells and Materials Conference, Davos Switzerland.*

## ABSTRACT

Loss of large segments of bone creates critical size defects (CSDs). These fail to heal spontaneously and present major clinical challenges to orthopaedic surgeons. The research described in this thesis is based upon the hypothesis that the healing of CSDs is responsive to the ambient mechanical environment, and can be accelerated by mechanical modulation. This hypothesis was tested in rat, femoral CSDs treated with recombinant, human, bone morphogenetic protein-2.

For this study I designed novel external fixators allowing experimental control over the local mechanical environment. These were characterised by extensive mechanical testing prior to evaluation in the rat model.

Low stiffness fixators induced callus formation 9 days after surgery, whereas rigid fixation delayed it until 2 weeks. All defects were radiologically bridged after 3 weeks. Rats were euthanised after 8 weeks and the defects evaluated by a battery of imaging, mechanical and histological tests. All confirmed the superiority of the lowest stiffness fixators.

Based upon these data, I hypothesised that healing would be improved by imposing low stiffness for the first two weeks of healing, followed by high stiffness for the remaining six weeks. The experimental data confirm that this regimen dramatically accelerated callus formation and maturation, and induced faster remodelling of endosteal and periosteal callus. This was associated with higher failure strength, fewer trabeculae, decreased callus size and thicker and more uniform distribution of new cortical bone. Histologically it was not possible to detect cartilage within the defects prior to the appearance of bone, suggesting that healing either does not occur through endochondral ossification, or that this process is very rapid.

These data confirm that the healing of CSDs is highly responsive to the ambient mechanical environment, allowing the rate and quality of healing to be manipulated. This information will help develop more efficient ways to heal CSD clinically.

---

## ABBREVIATIONS

μCT	Micro-Computed Tomography
BA	Bone Area
BA/TA	BoneArea/Total Area – Bone Area Fraction
BMC	Bone Mineral Content
BMP	Bone Morphogenetic Protein
cDNA	Complementary Deoxyribonucleic Acid
CSD	Critical Size Segmental Defect
DBM	Demineralized Bone Matrix
DXA	Dual-Energy X-Ray Absorptiometry
ExFixHigh	Second Generation External Fixator of High stiffness
ExFixLow	Second Generation External Fixator of Low stiffness
ExFixMed	Second Generation External Fixator of Medium stiffness
ExFixOld	First Generation External Fixator
FDA	Food and Drug Administration
IFM	Intrafragmentary Movement
IFS	Intrafragmentary Stain
IGF	Insulin-like Growth Factor
IL-1	Interleukin-1
IL-6	Interleukin-6
IM	Intramedullary Nail
K-Wire	Kirschner Wire
LDPE	Low-Density Polyethylene
MSC	Mesenchymal Stem Cell
NIH	National Institute of Health (USA)
OP-1	Osteogenic Protein-1 (also known as BMP-7)
OPG	Osteoprotegerin
PBS	Phosphate Buffered Saline
PDGF	Platelet-Derived Growth Factor
PEEK	Polyethylethylketone
PMMA	Polymethylmethacrylate
pMOI	Polar Moment of Inertia

RANK	Receptor Activator of Nuclear Factor- $\kappa$ B
RANKL	Receptor Activator of Nuclear Factor- $\kappa$ B Ligand
rhBMP-2	Recombinant Human Bone Morphogenetic Protein-2
rhBMP-7	Recombinant Human Bone Morphogenetic Protein-7 (also known as OP-1)
SMADs	Proteins that are homologs of both the drosophila protein, <i>mothers against decapentaplegic</i> (MAD) and the <i>Caenorhabditis elegans</i> protein smooth muscle actin (SMA). The name is a combination of the two.
TA	Total Area/Callus Area
TGF- $\beta$	Transforming Growth Factor-Beta
Ti	Titanium

# **CHAPTER ONE**

## ***GENERAL INTRODUCTION***

## 1.1 THE STRUCTURE AND FUNCTION OF BONE

The functions of bone are classified as mechanical, mineral storage, and haematopoietic [1]. The mechanical functions of bone include protection for the brain, spinal cord, and chest organs, while providing rigid support for the limbs. The skeletal system provides rigid kinematic links (joints) and muscle attachment sites that facilitate muscle action and bodily movement. Bone is also the principal reservoir for calcium, but additionally stores other ions such as phosphate, sodium and magnesium. Bone also serves as host for the haematopoietic bone marrow. Despite its inert appearance, it is one of the most dynamic and metabolically active tissues in the body.

The mechanical properties of bone are related to its construction and internal architecture. Bone is among the body's hardest tissues, only dentin and enamel in the teeth being harder. Although extremely light, bone has high tensile strength. This combination of strength and light weight is a result of its hollow tubular shape, the layering of bone tissue and the internal support of the matrix.

Because bone is able to remodel and repair, it can adapt its mass, shape, and properties to changes in its mechanical environment and normally endures voluntary physical activity for life without breaking or causing pain.

A typical long bone (e.g. tibia, femur) consists of a central cylindrical shaft, the diaphysis, and two wider and rounded ends, the epiphyses (Figure 1. 1). A metaphysis connects the diaphysis with each epiphysis. In growing mammals, the growth plate, located in between the epiphysis and metaphysis, ensures continuous growth, enlarging the bone while maintaining its shape [1].

The outer surface of bone is covered by the periosteum, a sheet of fibrous connective tissue with an inner cellular or cambium layer of undifferentiated cells. The periosteum has a potential to form bone during growth and fracture healing. The marrow cavity in the diaphysis of cortical and cancellous bone is lined with a thin cellular layer called the endosteum. The endosteum (an internal periosteum) is a membrane of bone surface cells: osteoclasts, osteoblasts and bone lining cells.

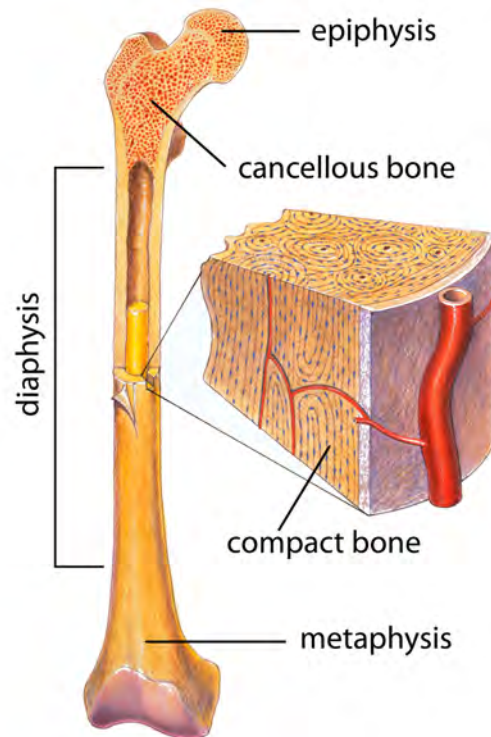


**Figure 1.1** Basic structure of a typical long bone, the femur [2].

Two types of bone can be distinguished in the human skeleton: cortical and cancellous (Figure 1.1). Cortical bone is a dense, solid mass with only microscopic channels. Approximately 80% of the skeletal mass in the adult human skeleton is cortical bone, which forms the outer wall of all bones and is largely responsible for the supportive and protective function of the skeleton. The bulk of cortical bone is in the shaft of long bones in the appendicular skeleton. The remaining 20% of the bone mass is cancellous bone, a lattice of large plates and rods known as trabeculae, found in the inner parts of the bone. Cortical and cancellous bone have a different distribution throughout the skeleton and differ in their development, architecture, function, proximity to the bone marrow, blood supply, rapidity of turnover time, and magnitude of age-dependent changes and fractures. Cortical bone is stiffer than the cancellous bone.

Cancellous bone is found in many places in bone. It is useful to mention five locations: at the ends of long bones, under synovial joints; within short bones; within flat bones; under protuberances to which tendons attach; and in the medullary cavity of some long bones. Short and flat bones are completely filled with cancellous bone.



The mechanical properties of cancellous bone are a function of variation in the material's apparent density and also of the arrangement of the bony trabeculae with respect to the loading direction. The arrangement of trabecular bone is not random, but there is no convincing theory that explains this distribution. One hypothesis is that the distribution of the trabecular bone is mainly related by the direction of the principal stresses arranged so that they will not be subjected to significant bending moments, which minimizes the stress they experience (Wolff's Law). However, a completely different approach suggests that the observed structure is adaptive. This considers cancellous bone structures to be minimum weight braced frameworks. A structure in which load is resisted by changes in length of its members (trabecular struts), rather than by bending, is known as a braced network. They are orthogonal nets and depending on the loading system they may be rectangular or, in systems with concentrated loads, they are developments of equiangular spirals. Furthermore, Hert and his co-workers [3] refuse to believe the idea that trabecular struts in the long bones are organized in the direction of principal stresses. They suggest that the struts are oriented to resist the compressive stresses at the extremes of the joint motion. All in all the architecture of bones is arranged so that they can carry out their functions and yet be as light as possible and of appropriate stiffness.

Bone consists of 65% mineral and 35% organic matrix, cells and water. The bone mineral, which is largely impure hydroxyapatite, is in the form of small crystals deposited between collagen fibers. The organic matrix consists of 90% collagen, predominantly types I, but with small amounts of collagen V and III and about 10% of various noncollagenous proteins, the most abundant ones being osteocalcin, osteonectin, osteopontin and bone sialoprotein [1].

The mechanical properties of bone are dependent on the type of bone, loading direction and the rate of loading. Typical stress-strain curves for uniaxial, monotonic tension and compression loading of cortical bone, both in longitudinal and transverse directions, show that cortical bone is stonger in compression than in tension. For example, the tensile strength in longitudinal loading is aproximately 130(MPa), while in the corresponding compressive strength is 190(MPa). For transvere loading, the tensile strength is very low, 50MPa, while the compressive strength is 130(MPa) and comparable to the tensile strength in longitudinal direction. This suggests that

cortical bone has adapted to a situation where compressive loading is greater than tensile. This is also consistent with the combined bending and axial compressive loads that are acting on the femoral diaphysis during everyday activities such as walking.

The major cellular elements of bone are osteoblasts, osteoclasts, and osteocytes. Osteoblasts are mesenchymal cells that synthesise and mineralize the bone matrix. They are derived from mesenchymal progenitor cells found in marrow, periosteum and certain other tissues; they are often termed Mesenchymal Stem Cells (MSCs). Whether these are true stem cells remains controversial, so they are sometimes termed Mesenchymal Stromal Cells. As a result, while preserving the acronym, the abbreviation MSC is used throughout this thesis to denote a pluripotent, mesenchymal osteoprogenitor cell without taking a position on their stemness. The main stages of osteogenic differentiation are shown in figure 1.2.

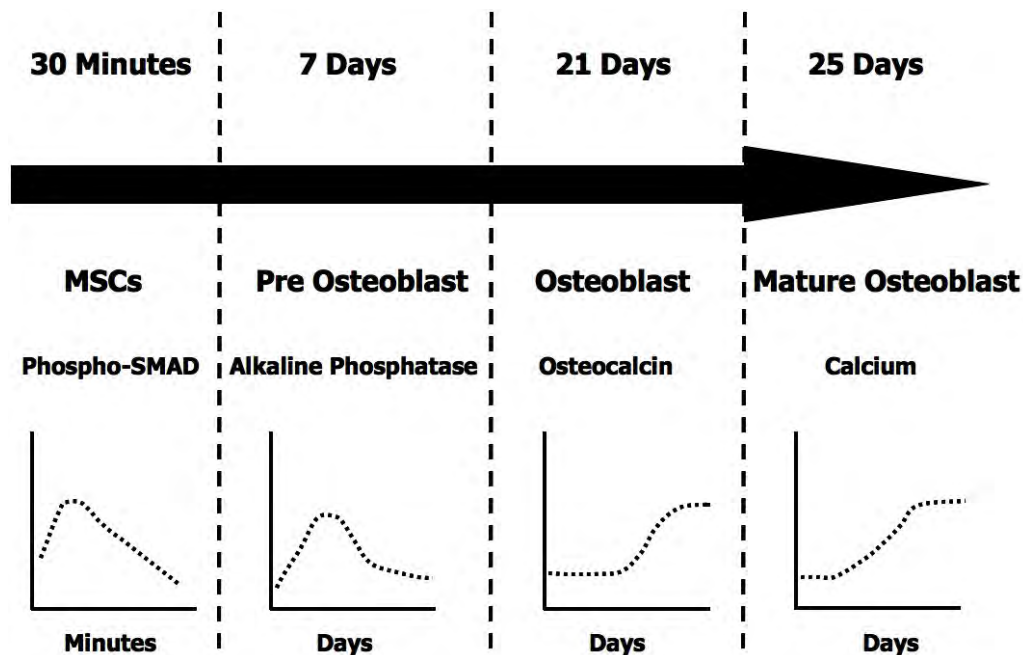


**Figure 1.2** Key stages in the differentiation of MSCs into osteoblasts.

Exposure of MSCs to an osteogenic bone morphogenetic protein (BMP) leads to the rapid phosphorylation of SMADs (Proteins that are homologs of the drosophila protein, *mothers against decapentaplegic* (MAD) and the *Caenorhabditis elegans*

protein SMA. The name is a combination of the two.), which migrate to the nucleus and trigger the expression of a cascade of genes associated with osteogenesis. Alkaline phosphatase is expressed in pre-osteoblasts as an early marker of osteogenesis. Osteocalcin, a late marker, is expressed by osteoblasts with the ability to deposit a mineralized matrix. Under in-vitro conditions, the process of osteogenesis takes about 25 days. (Figure 1.2)

Osteoclasts, which degrade the matrix of bone, are derived from haematopoietic stem cells in the bone marrow. As depicted in figure 1.3, osteoclastogenesis is coupled to osteoblastogenesis through interactions between RANK (Receptor Activator of NF- $\kappa$ B) on the surface of pre-osteoclasts, and RANK ligand (RANKL) on the surface of osteoblasts. This interaction stimulates osteoclastogenesis. A soluble form of RANK known as osteoprotegerin (OPG) inhibits the binding of RANK to RANKL and thus acts to inhibit osteoclastogenesis. During the final stage of osteoclastogenesis, cells fuse to form large multinucleated osteoclasts with the ability to resorb bone.

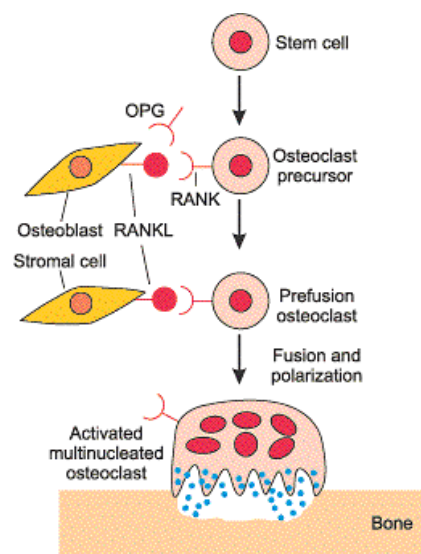


**Figure 1.3** Key steps in the differentiation of haematopoietic stem cells into osteoclasts and its coordinate regulation with osteoblastogenesis via RANK-RANKL interaction [4]

Osteocytes are derived from osteoblasts that became embedded in the matrix that they synthesized, and function as mechanosensors. Each osteocyte occupies a space, or lacuna, within the matrix and extends filopodial processes through canaliculi in

the matrix to contact processes of adjacent cells by means of gap junctions. Because the diffusion of nutrients and metabolites through the mineralized matrix is limited, filopodial connections permit communication between neighbouring osteocytes, internal and external surfaces of bone, and with blood vessels traversing the matrix.

Osteocytes within the mineralized matrix are in direct communication with each other and surface osteoblasts through their cellular processes. The primary function of the osteoblast (or lining cell) - osteocyte continuum is considered to be mechanosensory, to transduce stress signals such as stretching and bending into biological activity [5-7]. The flow of extracellular fluids in response to mechanical forces throughout the canaliculi induces a spectrum of cellular responses in osteocytes. Rapid fluxes of bone calcium across these junctions are thought to facilitate transmission of information between osteoblasts on the bone surface and osteocytes within the structure of bone itself. This mechanism is thought to be involved in the detection of microdamage, and responses to the level and distribution of strain within bone tissue that influences adaptive modelling and remodelling behaviour [8]. At any sites in response to signals which are poorly understood, bone is constantly turning over through the coordinated activities of osteoblasts and osteoclasts (Figure 1.4).

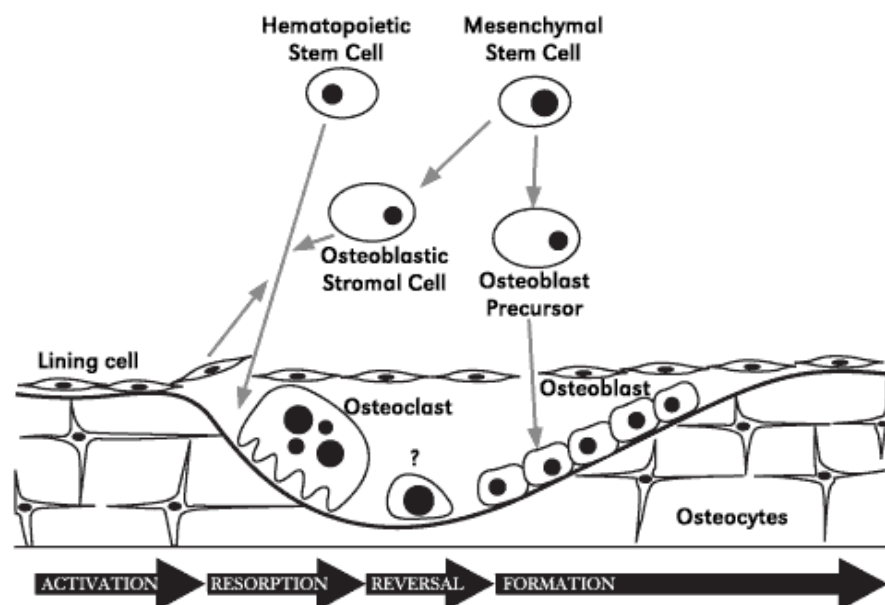


**Figure 1.4** Key events in the remodelling of bone. Bone is constantly remodelling. Osteoclasts adhere to the surface of bone and form a resorption pit. Osteoblasts then enter the site and synthesise new bone. They subsequently become embedded in mineral and differentiate into osteocytes [9].

## 1.2 BONE REGENERATION AND REPAIR

Bone is one of the few organs in the body that heals without scarring. The biology of fracture repair involves a true regeneration of the adult tissue rather than healing and production of a surrogate material. The molecular events that govern fracture healing are a complex network of signals signifying tissue damage, cell death, cell recruitment, cell proliferation, cell differentiation and tissue formation. The phases of fracture healing can be summarized as: hematoma formation (early fracture), inflammation, reparative phase and remodelling phase (Figure 1.5).

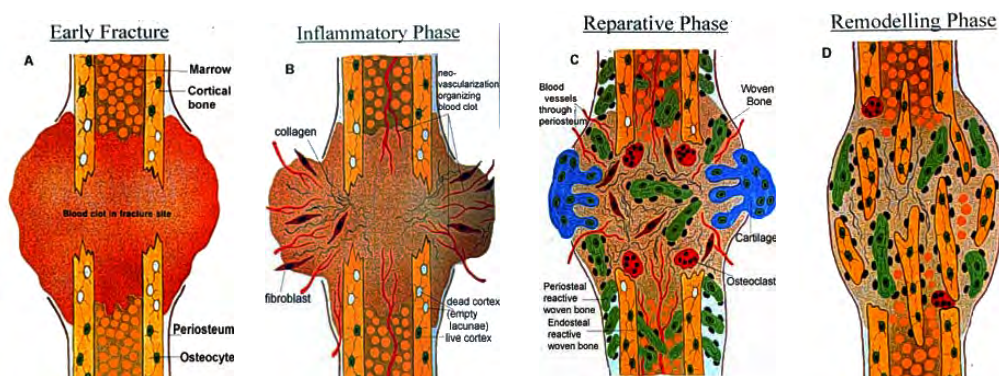


**Figure 1.5** Main phases in fracture healing: A) Early fracture - haematoma phase; B) Inflammatory phase – initiation of fracture healing and the associated cascade of cellular responses; C) Reparative phase - cartilage formation and calcification, calcified cartilaginous tissue replaced with woven bone; D) Remodeling phase - woven bone remodels into mature lamellar bone [10].

These phases involve the coordinated activity of different cell populations that proliferate, differentiate and synthesize extracellular matrix components. During the inflammatory phase, the periosteum of bone lifts, and a haematoma is formed between the bone ends due to the rupture of blood vessels. This haematoma releases a large number of signalling molecules, including inflammatory cytokines such as interleukin-1 (IL-1) and interleukin-6 (IL-6) and growth factors such as platelet-

derived growth factor (PDGF), insulin-like growth factors (IGFs) and members of the transforming growth factor- $\beta$  (TGF- $\beta$ ) superfamily, including BMPs. BMPs are low-molecular-weight homodimeric proteins whose sub-units are linked by a disulfide bond. BMP-2, used throughout the work described in this thesis, has a molecular weight of 26kDa. BMP-2 signals through two types of transmembrane, serine/threonine kinase cell receptors, BMPRI and BMPRII. Binding of BMP-2 to its receptors results in the phosphorylation of BMPRI by BMPRII and, subsequently, Smad-1, Smad-5, and Smad-8 which form a complex with Smad-4 within the cell nucleus. This complex activates the expression of BMP target genes, which ultimately results in cartilage and bone formation. The intracellular process is regulated by the inhibitory function of Smad-6 and Smad-7, which turn off BMP signaling by preventing the phosphorylation of Smad-5. The actions of BMPs are constrained by a number of inhibitory molecules, including noggin, chordin and DAN (Figure 1.6). These factors appear to regulate the initiation of fracture healing and the associated cellular response.

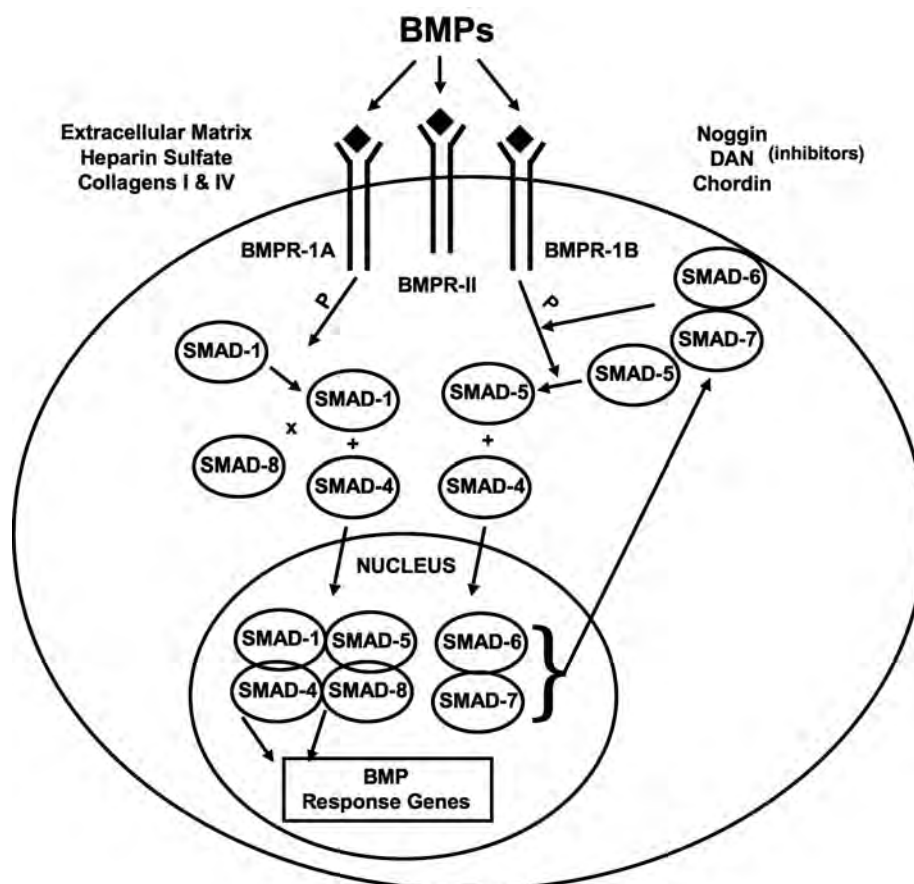


**Figure 1.6** BMP receptor and signalling cascade. BMPs contact with type I and type II BMP receptors (BMPR). BMPR-II phosphorylates BMPR-I, which forms the transducing complex and phosphorylates Smad-1, Smad-5 and Smad-8. Smad-1 and Smad-5 interact with Smad-4 enter the nucleus and initiate the BMP response genes. Smad-6 and Smad-7 inhibit phosphorylation of Smad-5. Noggin, chordin, and DAN are BMP antagonists and prevent receptor binding. (*Adapted from Reddi AH. Bone Morphogenetic Proteins: from basic science to clinical applications. JBJS Am 2001; 83:S1-3*)

MSCs enter the defect to initiate repair. The source of these cells is unclear; possible sources include the inner cambial layer of the periosteum, the endosteum, the bone marrow, the surrounding musculature and the vascular endothelium. In addition, there is recent evidence of circulating osteoprogenitor cells [11]. The MSCs differentiate into chondrocytes and osteoblasts, which will form bone via endochondral and intramembranous ossification, respectively.

Intramembranous ossification forms bone directly from osteoprogenitor cells, according to the schema shown in figure 1.2, without first forming cartilage to create hard callus. Endochondral ossification, in contrast, involves the differentiation of MSCs into chondrocytes, which form a cartilaginous intermediate that becomes calcified and eventually replaced by bone. This type of fracture healing is attributed to the adjacent periosteum and provides an early, bridging, soft callus. Mineralization of the cartilage involves a mechanism similar to long bone growth at the growth plate and requires reestablishment of the vascular and nutrient supply. Chondrocytes hypertrophy and undergo apoptosis, the extracellular matrix calcifies and blood vessels penetrate the matrix. The calcified cartilage is resorbed and replaced by immature, woven bone formed by osteoblasts. In the final healing phase, osteonal remodelling of the newly formed bone tissue and of the fracture ends restores the original shape and mature lamellar structure of the bone. This last phase of bone healing can take from months to years to complete.

### **1.3 CURRENT CLINICAL MANAGEMENT OF LARGE SEGMENTAL DEFECTS**

It is estimated that in the UK alone about 1.6 million bone fractures occur annually, and 10-20% of those fractures result in impaired, delayed or non-unions. This is

associated with economic cost in lost productivity, time off work and morbidity. Although fractures normally heal in the manner described in the previous section, large segmental defects do not. Indeed, once a segmental defect reaches a certain critical size it is too large to heal naturally. While only 5 to 10% of all fractures are critical size defects, they are a serious clinical problem that requires surgical intervention. Most common causes of such defects are related to trauma from car accidents, sports activities etc.; other causes are tumour resection and failed arthroplasty.

Autografting is the method of choice for treating large segmental defects in long bones. In this procedure, autologous bone is surgically recovered from the iliac crest of the patient and transferred to the site of the non-healing osseous lesion. Although successful, this procedure is constrained by the limited amount of autologous material that is available for autografting and by morbidity associated with this invasive procedure. Allografting addresses some of these issues.

Allograft bone is recovered from cadavers and processed to remove pathogens and immunogens. It is readily available in large amounts and, of course, its harvest imposes no morbidity upon the donor. However, it is essentially dead bone. Although, it provides mechanical support and can function as space filler, it cannot undergo remodelling and it has a high failure rate when implanted into load bearing environments.

As an alternative to allograft material, there are a number of synthetic bone substitutes, many of which are based upon calcium phosphate either alone or in conjunction with an organic phase, such as collagen. In general, these are not clinically superior to allograft. Calcium phosphate is available in a variety of forms and products including powders, ceramics and cements. These substitutes are osteoconductive, which means that there is an ingrowth of sprouting capillaries, perivascular mesenchymal tissues, and osteoprogenitor cells from the recipient host bed into the three-dimensional structure of an implant or graft. But they are not osteoinductive, and this is a phenomenon in which there is a mitogenesis of undifferentiated perivascular mesenchymal cells leading to the formation of osteoprogenitor cells with the capacity to form new bone, unless growth factors or



other osteoinductive substances are added to create a composite graft. They do not provide a high level of structural support because they are brittle and have little tensile strength. They increase bone formation by providing osteoconductive matrix for host osteogenic cells. The disadvantages with such materials encountered clinically include: low or unpredictable resorption, difficulty in handling and poor clinical results with occasional inflammatory foreign body reactions.

Distraction osteogenesis provides another option for treating segmental bone defects. Commonly called the Ilizarov technique, it has gained a great deal of popularity since its introduction in the West 20 years ago. Professor Gavril A. Ilizarov [12, 13] invented this procedure in 1951 in Siberia for limb salvaging and lengthening procedures. This is a specialized form of external fixation, also known as ring or circular external fixator (Figure 1.7).



**Figure 1.7** Circular external fixator used for the Ilizarov technique [14].

These devices utilize Ilizarov's theory of controlled distraction histogenesis, whereby bone is fractured, but only involves cortex leaving medullary vessels and periosteum intact, in the metaphyseal region and slowly lengthened. This distraction process allows for bone reconstruction within the segmental defects through the insertion of small Kirschner wires (K-wires) under tension and circumferential ring

supports. As new bone growth occurs in the metaphyseal region, it pushes a segment of healthy bone into the defect. The tension that is created by gradual distraction stimulates the formation of new bone, skin, blood vessels, peripheral nerves and muscle. Bone lengthening can occur at a rate of approximately one centimetre per month.

The advantages of these circular fixators are that they permit stabilization of fractures with minimal operative trauma to soft tissues, while preserving critical blood supply. They allow early use of the limb, including weight bearing. The Ilizarov technique eliminates the need for extensive soft tissue procedures and bone grafting. Angulatory, translation, rotational, and length deformities can be corrected, and union can be obtained simultaneously in many of these difficult situations.

However, there are also disadvantages associated with the use of these devices. The most commonly reported complication is pin-track infections, but most can be prevented with good pin care and local antibiotics. Pain is also common and can be severe to a patient, but is treatable with analgesics. The technique is labor-intensive and requires an extended period of treatment in the device. Due to limited range of movement and cosmetic appearance this technique is not favored by patients. Although for some surgeons it became a method of choice in dealing with large segmental bone defects, the propensity for complications and the length of treatment have limited its universal endorsement.

In recent years, clinicians have been able to use rhBMP-2 (Infuse™) and rhBMP-7 (Osteogenic protein-1; OP-1™) to enhance bone healing. These proteins are surgically implanted on a scaffold into sites requiring an osteogenic stimulus. Infuse is approved by the Food and Drug Administration (FDA) for the use in the specific situation of a single level anterior lumbar spine fusion between L4 and S1 as a substitute for autogenous bone graft in adults with degenerative disc disease who have had at least six months of nonoperative treatment for this condition. It is also approved for the treatment of acute tibial fractures in adults as an adjunct to standard care using open fracture reduction and intramedullary (IM) nail fixation. OP-1 was approved for the treatment of tibial nonunions of at least 9 months duration, secondary to trauma in the skeletally mature patients, in cases where previous

treatment with autograft has failed or use of autograft is unfeasible. Despite this, most use of BMPs in the clinic is “off-label”, which means its not approved by the FDA.

Pre-clinical studies in goat tibia, rabbit ulna and rat femur showed that BMPs were able to accelerate and enhance bone healing by as much as 30-40% in CSDs [15-21]. In contrast to the rich literature concerning animal models of bone healing, there are only a few serious clinical studies in humans that looked at the effects of BMPs on the healing of human long bones, although clinical studies treating spinal fusions with BMPs are more extensive [22-30].

Studies to investigate the effects of BMPs on human long bone healing have concentrated on open tibial fractures, a condition that is known to be associated with complications, particularly non-unions. Govender et al. [31] in a prospective, randomized, controlled, single blinded study evaluated the safety and efficacy of rhBMP-2 in the accelerated healing of open tibial shaft fractures. The study was divided into three groups: 1) intramedullary nail fixation and routine soft tissue management; 2) standard of care and an implant containing 0.75 mg/mL of rhBMP-2; 3) standard of care and an implant containing 1.50 mg/mL of rhBMP-2. The rhBMP-2 was applied to a resorbable collagen sponge and placed over the fracture at the wound closure. The investigators reported that use of rhBMP-2 implant was safe at the dose 1.50 mg/mL and, compared to the standard of care, was associated with accelerated bone healing, a reduction in infection rates, less bone grafting and a reduced frequency of secondary interventions from 46 to 26%. Another study by Swiontkowski et al. [32] reported analysis in a group of patients with severe open tibial fractures treated either with intramedullary nail fixation and routine soft tissue management, or rhBMP-2 1.50 mg/mL absorbed into a resorbable collagen sponge. They found that by adding the rhBMP-2 implant, the frequency of bone-grafting procedures and other secondary interventions was significantly reduced. They also found that patients in the rhBMP-2 group achieved weight bearing an average of thirty-two days sooner than the control group. A study by Jones et al. [33] used rhBMP2/allograft in the treatment of diaphyseal tibial fractures associated with cortical defects. They suggested that rhBMP-2/allograft was a safe and effective alternative to autogenous bone grafting.

Despite these promising findings, most orthopaedic surgeons who use BMP-2 and BMP-7 are of the opinion that, although these molecules are helpful, they provide only incremental improvement over existing methods. It is unclear why their performance in humans is inferior to that in experimental animals. One possibility, which forms the basis of this thesis, is that insufficient attention has been given to the mechanical environment within which these molecules are expected to perform.

#### **1.4 THE INFLUENCE OF MECHANICAL FORCES ON BONE HEALING**

It is well known that the biomechanical environment plays a key role in maintaining, repairing and remodelling bone, thus enabling it to meet its functional demands. Bone adaptation is an important and illustrative example of this. In the 1890s Julius Wolff was one of the pioneers who used his clinical and experimental morphologic observations to develop two concepts, which are today known as Wolff's Law. Wolff stated that skeletal elements are strategically placed to optimize strength in relation to the distribution of applied loading and that the mass of the skeletal elements is directly related to the magnitude of the applied loads. Wolff's Law regards the trabeculae of cancellous bone as embodying the stress trajectories determined from the stress analysis of a homogeneous and continuous elastic object of the same shape as the bone and loaded in the same way. However, stress trajectories and the trabecular architecture cannot be related to one another in the manner suggested by Wolff's Law. For this continuum model it is assumed that bone is linearly elastic, homogeneous and isotropic while it is well known that the real cancellous bone architecture neither homogeneous nor isotropic. This observation is only one of the 20 objections scientists have raised over the years regarding Wolff's Law. Nevertheless the basic tenets of Wolff's Law are generally accepted and scientists today agree that fractures will repair and remodel depending on the loading conditions [8, 34, 35].

After skeletal maturation bone continues to remodel throughout life (Figure 1.4) and to adapt its material properties to meet the mechanical demands placed upon it. The cellular and molecular mechanisms by which bone responds to mechanical stresses

are not well understood. Therefore, it has been a goal of many investigators to understand better the relationship between biomechanical factors and cellular responses involved in normal and impaired bone fracture healing.

Much of our present day understanding about the effects of mechanical forces on tissue differentiation comes from Friedrich Pauwels. Pauwels [36] was one of the first to recognize that physical factors cause stress and deformation of what we now refer to as MSCs, and that such mechanical stimuli could determine the cell differentiation pathway. By using simple experimental models he developed these general concepts and demonstrated how shear stress (also called distortional stress) causes tissues (cells) to change shape, but not volume, whereas hydrostatic stress results in change of volume, but not of shape (Figure 1.8).

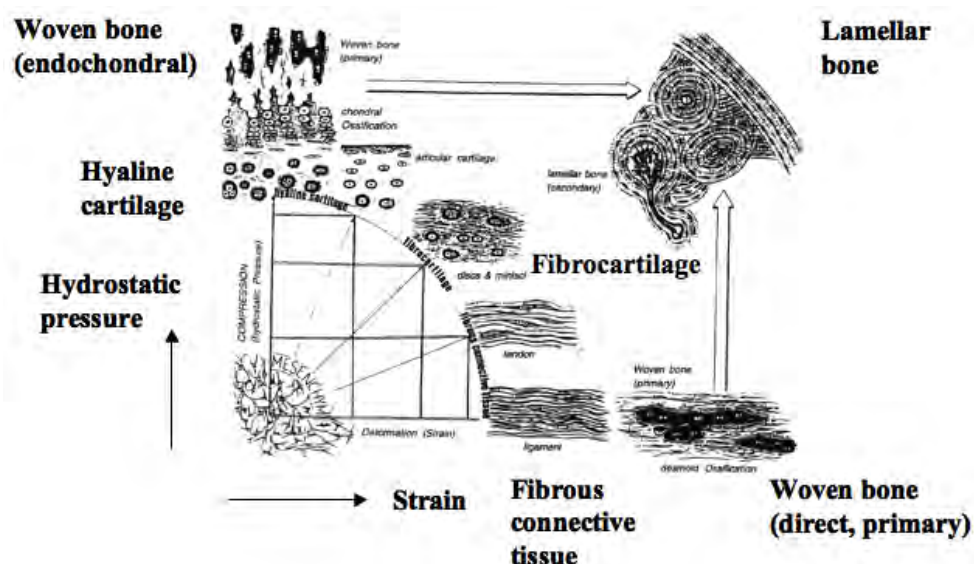


**Figure 1.8** Pauwel's concept of tissue differentiation: a schematic representation of the hypothesized influence of the biophysical stimuli on tissue phenotype. Deformation of shape strain is on the x axis and the hydrostatic compression is on the y axis. A combination of these stimuli will act on the MSCs leading to hyaline cartilage, fibrocartilage, or fibrous connective tissue as shown on the perimeter of quadrant. Depending on the response of the mechanical environment to the presence of these tissues, osteoblast proliferation and ossification can occur. However, bone regeneration occurs only after stabilization of the mechanical environment by the formation of soft tissue. (From Weinans and Predergast, 1996)

Roux [37] was first to explore the relationship between mechanical stimuli on cells and tissue adaptation. He proposed that cells within tissues engage in “a competition for the functional stimulus” and that this competition determines cell survivorship

and therefore tissue phenotype. He hypothesized that the mechanical environment has the following relationship to phenotype: tension forms fibrous connective tissue, shearing forms cartilage, and compression forms bone. He postulated that structural adaptation of tissue to mechanical loads is a direct consequence of competition between the tissue cells. Pauwels [36] compared the mechanical environment on cells in a fracture callus with fracture repair patterns, and proposed that deformation (strain) of shape is a specific stimulus for the formation of collagenous fibrers and hydrostatic compression is the specific stimulus for the formation of cartilaginous tissue. Osteogenesis however requires that the mechanical environment first becomes stabilized by the presence of fibrous tissue, a concept also embraced by Perren. Therefore, Pauwels' hypothesis as shown in the Figure 1.7 is that the ambient mechanical environment determines tissue phenotype. Carter [38] developed this concept as a function of shear and hydrostatic stress called the osteogenic index.

Another important mechanical factor is intrafragmentary strain. When the fractured bone is loaded, the fracture fragments displace relative to each other. This strain produced in the fracture gap is named "Intrafragmentary Strain" (IFS), a concept first introduced by Perren [39]. Although intrafragmentary strain theory is very useful for understanding the relationship between motion and bone healing process, the theory is not a general theory of bone regeneration, because the strain field in the fracture gap is multiaxial and mechanical stimuli vary spatially throughout the fracture callus [39].

Despite this, through observational and to a lesser extent, empirical study, several theories have been developed on the role of mechanical stimuli or intrafragmentary movement in governing the differentiation of MSCs into bone, cartilage, fibrocartilage and fibrous tissue. There are four main factors that influence IFS: the rigidity of the technique used to stabilize the fracture, the surface area of the fracture fragments, gravitational loads and muscular loads. The strain is defined as the relative motion over the surface area at the fracture site. In this way, comminuted fractures can tolerate relatively greater motion, since the strain is applied over a larger surface area of fracture fragments. If IFS exceeds a critical level, the blood supply for healing at the fracture site is subjected to repeated trauma and cannot become established. Moreover, instability prevents the production of stable tissues at

the fracture site. Fibrous tissue is relatively resistant to high stress forces, while cartilage and bone cannot form under conditions of high strain [38, 40]. As long as high strain forces exist at a fracture site (i.e. stability is inadequate), fibrous tissue will remain and stabilizing bony callus will be unable to form. If such conditions continue for long enough, a fibrous non-union will result.

Local tissue stress and strains not only alter the pressure on the bone cells, but also influence cell differentiation [41]. In the mechanically loaded fracture gap after fixation, hydrostatic pressure is relatively low and IFSs are relatively high. However when callus grows the stiffness in the fracture increases. Rising hydrostatic pressure decreases matrix permeability while fracture shear strains decline. In this environment, increasing numbers of chondrocytes are formed and endochondral ossification begins. As more collagen matrix is produced the strain declines further, more osteoblasts accumulate and ossification predominates. It is plausible that MSCs cannot differentiate into bone cells or chondrocytes unless a suitable biophysical environment for tissue differentiation is present. Therefore, for bone healing to occur the fracture environment has to be exposed to the strain rates that elicit bridging callus, increasing collagen synthesis and rising hydrostatic pressures.

## **1.5 CRITICAL SIZE SEGMENTAL DEFECTS**

### **1.5.1. Introduction**

Most of the literature on the biology and biomechanics of bone healing, discussed above, pertains to the behaviour of fractures or osteotomies that are small enough to heal spontaneously. Relatively little attention has been paid to large segmental defects in bone which are unable to heal spontaneously (Figure 1.9).

The concept of a critical size defect (CSD) was introduced by Schmitz and Hollinger [42]. Although it was originally used in the context of craniomandibulofacial nonunions, it is also used for non-healing segmental defects in long bones, and elsewhere. The reason why CSDs do not heal is unknown. Fracture healing has three major requirements: osteoprogenitor cells, a scaffold and an osteogenic stimulus.

Assuming that these requirements also hold true for CSDs, it is possible to speculate that one or more of these are absent from the CSD.

Under natural conditions a CSD fills with a haematoma, a large part of which is a fibrin scaffold. The absence of a scaffold is thus unlikely to account for the inability of CSDs to heal, a conclusion reinforced in the present research, where the implantation of a collagen scaffold into a rat CSD did not result in healing.

The literature contains several reports of healing following the introduction of MSCs into experimental CSDs in laboratory animals [43] and human patients [44]. This suggests a lack of osteoprogenitor cells in CSDs. In laboratory animals, this may reflect the absence of periosteum, which is usually removed during the surgical creation of the defect. In human patients, this may reflect soft tissue damage due to trauma or surgical resection. Experimental CSDs created in laboratory animals usually heal in response to an osteoinductive stimulus, such as BMP-2, suggesting that such factors are also limiting in CSDs.

The data presented in Chapter 5 of this thesis provide further insight and suggest that the reparative cells are derived from periosteum on the cut ends of the bone adjacent to the CSD. BMP-2 seems to have a chemotactic effect, resulting in the migration of cells across the collagen scaffold, and an osteogenic effect, once the cells have traversed the defect. These observations suggest that, at least in this rat model, an untreated CSD fails to heal because osteoprogenitor cells adjacent to the defect are unable to traverse the lesion.

In this thesis, I study the effects of the mechanical environment on the healing of CSDs in rats. It is an attractive topic, because I have been unable to identify any refereed research papers on the influence of the mechanical environment *in-vivo* on the healing of CSDs. The judgment of orthopaedic surgeons, based upon clinical experience, is that rigid fixation favours better healing, but this remains to be demonstrated in controlled studies. Current clinical options for treating large segmental defects were described in section 1.3.





**Figure 1.9** A radiographic image showing critical sized segmental defect in the mid section of human tibia stabilized by an external fixator treated with rhBMP-2 2 weeks post surgery [2].

Therefore, the primary goal of these studies is, using a rat femoral defect model, to investigate the role of the mechanical environment on the healing of CSDs enhanced by rhBMP-2 treatment in long bones.

### **1.5.2. BMP-2 and the healing of critical size defects in the rat femur**

Although rhBMP-2 is used clinically to treat critical sized osseous defects, this is an off-label use for which there is no strong evidential support. Many bone fracture healing studies *in-vivo* illustrate the bone-inducing properties of several different BMPs in laboratory animals. Experiments in animals and humans have confirmed the osteoinductive activity of these proteins by demonstrating new formation of bone in ectopic and orthotopic sites. For example, rhBMP-2 absorbed onto demineralized

bone matrix or a collagen gel and implanted subcutaneously in rats was able to induce bone and cartilage formation [45-47]. Many of the preclinical long bone studies have used CSDs that will not bridge or heal without the addition of an osteoinductive or osteoconductive substances. Implantation of BMP-2 and BMP-7 in a rabbit ulnar model results in bone induction throughout the defects and bony healing as assessed by radiography and histology [48, 49]. Larger animal studies have also supported the ability of BMPs to heal large segmental defects. For example, rhBMP-2 has shown the ability to heal large defects in canine radii and sheep femora [50, 51]. In addition, healing of large segmental defects in a canine long bone ulna model, as well as in the ulnae and the tibiae of African Green monkeys, was accomplished by the application of rhBMP-7 and bone matrix particles [49, 52, 53].

Several studies have investigated bone formation in response to BMPs in the rat femoral defect model, using BMP-2 gene transfer [54-57] or delivery of recombinant BMP-2 [58-61]. In general, these studies confirm the ability of recombinant BMPs to enhance *de novo* bone formation in the critical sized defects. Results from prior studies conducted in this laboratory agree with this general conclusion, but our results have also detected inconsistencies. The new formed bone has poor quality of bone architecture, insufficient mechanical properties and high inter-animal variability. The project reported in this thesis has its origins in our desire to understand the basis of this variability and thereby to provide a remedy.

For the past decade members of our laboratory have studied a rat femoral defect model, originally developed by Einhorn and colleagues [62]. Initially we ascribed the variability of the healing response elicited by BMP-2 to problems associated with its delivery. When BMP-2 is absorbed into a collagen sponge and placed into a defect *in-vivo*, most of the BMP-2 is rapidly released and is essentially gone after a few days. This contrasts with natural bone healing where there is a sustained presence of BMPs. To overcome the delivery problem, we transferred BMP-2 cDNA using a recombinant adenovirus vector. However, gene transfer was no better than rhBMP-2 in repairing the segmental defects, despite providing an endogenous source of BMP-2 for several weeks. With both gene and protein delivery, we found residual cartilage within the defects of many rats, suggesting that healing is not complete by

the end of the 8 week experiment. This conclusion is supported by the results of mechanical testing, which revealed that the torsional strength and stiffness of the newly formed bone reached only approximately 25% of the intact contralateral bone. Moreover, there was high animal to animal variability [54]. This led me to consider more closely the possibility that mechanical factors were involved, especially as we used a very stiff external fixator in this rat model and I observed cortical thinning in the area facing the fixator. For this reason, I designed novel external fixators whose stiffnesses could be adjusted to control the mechanical environment of the segmental defect.

### **1.5.3. Influence of external fixator properties on fracture healing**

Although there are no experimental data on the effects of mechanical forces on the healing of segmental defects, many computational models have been developed to study the effect of the mechanical environment on fracture healing. They all found that the stiffness of external fixation influences fracture healing. Gomez-Benito et al [63] developed a finite element model of a simple transverse mid-diaphyseal fracture of an ovine metatarsus fixed with external bilateral fixators of three different stiffnesses. They found that a lower stiffness (1150N/mm) of the external fixator delays fracture healing and causes a larger callus as compared with 1725 and 2300N/mm external fixator stiffness. Carter et al. [64] examined the importance of cyclic motion and local stresses and strains on bone tissue formation. In this study they confirmed the basic mechanobiologic concepts that bone formation is promoted in the areas of low to moderate tensile strain, fibrous tissue is promoted in the areas of moderate to high tensile strains, and chondrogenesis is promoted in areas of hydrostatic compressive stress (pressure).

Claes et al. [65] in a sheep model investigated the influence of the osteotomy gap size and intrafragmentary motion on fracture healing. They hypothesized that gap size and the amount of strain and hydrostatic pressure along the calcified surface in the fracture gap are the fundamental mechanical factors involved in bone healing. They proposed that intramembranous bone formation would form for strains smaller

than approximately 5% and small hydrostatic pressure of no more than 0.15MPa. On the contrary, strains less than 15% and hydrostatic pressure more than 0.15MPa would stimulate endochondral ossification. They also found that by increasing osteotomy gap size there was a significant decrease in the fracture healing process. Furthermore, they found that 2mm gap size led to greater intrafragmentary movement, bigger periosteal callus and increased amount of connective tissue in the fracture gap. Large, critical sized gaps of 6mm never healed during the period of 9 weeks and they mainly produced fibrous connective tissue in the osteotomy gap regardless of the amount of intrafragmentary motion.

Kenwright and Gardner [66] summarized studies that measured interfragmentary displacement in six degrees of freedom throughout healing in patients with tibial diaphyseal fractures treated by external fixation, and developed a finite element analysis model of healing tibial fractures. The model analysis predicted that tissue damage might occur in the later (hard callus) phase of healing, even while the fixation device is still in place, because of very high stresses and strains. This study also indicates that the mechanical environment should be better controlled to provide amplitudes of movement in the first weeks of healing and the rigidity of fixation should be increased to optimize fracture healing process until the fixator is removed.

Another important factor that helps the healing process is mechanical stimulation. Therefore, it has been a goal of many investigators to find a relationship between mechanical stimulation and cellular responses under normal and defective bone healing. As early as 1955, Yasuda [67] discovered that the energy exerted on bones was transformed into callus formation. Despite his discovery, the ability to manipulate bone and other connective tissue by mechanical energy is still doubted by some, in spite of 52 years of basic science and clinical investigations [68-71]. Rubin et al. [72] discovered that repetitive loading under high frequencies or exercise regimen caused bone hypertrophy. Goodship et al. [73] also investigated strain rate and timing of mechanical stimulation in the fracture healing and hypothesized that an increased rate of deformation will enhance the osteogenic effects with short periods of cyclic micromovement, and that the maximal effect of such stimuli will occur in

the early stages of fracture healing. In this study they found that early application of rapid loading after osteotomy helps rather than hinders bone healing.

There is clear evidence in the literature to confirm that bone cells and their precursors are sensitive to changes in their local mechanical environment and the importance of mechanical stimuli has been confirmed experimentally. However, the mechanisms by which mechanical signals control osteogenesis remain elusive.

BMPs are essential for fracture healing, and genetically modified mice that lack BMP-2 lack all ability to heal fractures [74] Whether the magnitude and type of mechanical loading can enhance or decrease the amount of BMP expression has not been studied extensively. An *in vitro* study by Mitsui et al. examined the expression of BMPs, BMP receptors, BMP antagonists, transcription factors involved in osteogenesis and phosphorylation of Smad1 in cultured osteoblastic cells subjected to mechanical compressive force, and attempted to determine the optimal compressive force to induce osteogenesis. Interestingly, they found that compressive force induced BMP expression and there exist an optimal magnitude for expressing maximal amount of BMPs. However, a different study demonstrated that tension induced BMP-2 and BMP-4, but not BMP-6 and BMP-7, mRNA expression in an *in vivo*. The authors suggested that BMP-6 and BMP-7 genes, unlike BMP-2 and BMP-4, might not have stress response elements [75].

In a different study by Kim et al. [76] investigators looked at osteoprogenitor cell responses to static mechanical stretch through interaction with biochemical components like BMP-2, or other osteogenic cytokines within the distracted tissue mimicking the gradual Distraction Osteogenesis (DO) phase. They found that static stretching force combined with BMP-2 stimulation activates the osteoblastic differentiation of mesenchymal cells and stretch alone increases cell proliferation. Furthermore, they observed that the stretching effect was more apparent at low concentrations of BMP-2 (50 and 100 ng/ml) than at high concentrations (200 ng/ml), which are likely to be saturating.

From the above-mentioned *in vitro* studies it is evident, that not only the type of mechanical loading could maximize BMPs expression, but also the magnitude of the

force. For this reason smaller doses of BMPs in combination with precise mechanical loading conditions could be used to heal fractures more efficiently.

Collectively, the literature suggests that the healing of large segmental defects should be responsive to changes in the mechanical environment treated with rhBMP-2. However, there have been no in-vivo experimental studies to explore this possibility.

## **1.6 HYPOTHESIS**

Based upon the information discussed in this chapter, we postulate that after the initial callus bridging enhanced by rhBMP-2 treatment, CSD healing should take the same or similar pathway as fracture healing. In this case for the optimal CSD healing I suggest that the external fixator should have low rigidity during the early stages of CSD healing so that the early callus formation occurs. The rigidity of fixator should be increased when the cartilaginous callus is formed and beginning of cartilage calcification is seen on the X-rays, which is around 14 days post surgery in the rat femur. This allows angiogenesis to take place, thus removing calcified cartilage and replacing it with woven bone. This suggests that a final period of higher rigidity will enhance bone formation and maturation in the most timely and efficient manner (Figure 1.10). It should be noted that my suggested mechanical regimen differs from standard clinical practice, where initial fixation is highly rigid. It also differs from those who promote dynamization of the fracture site.

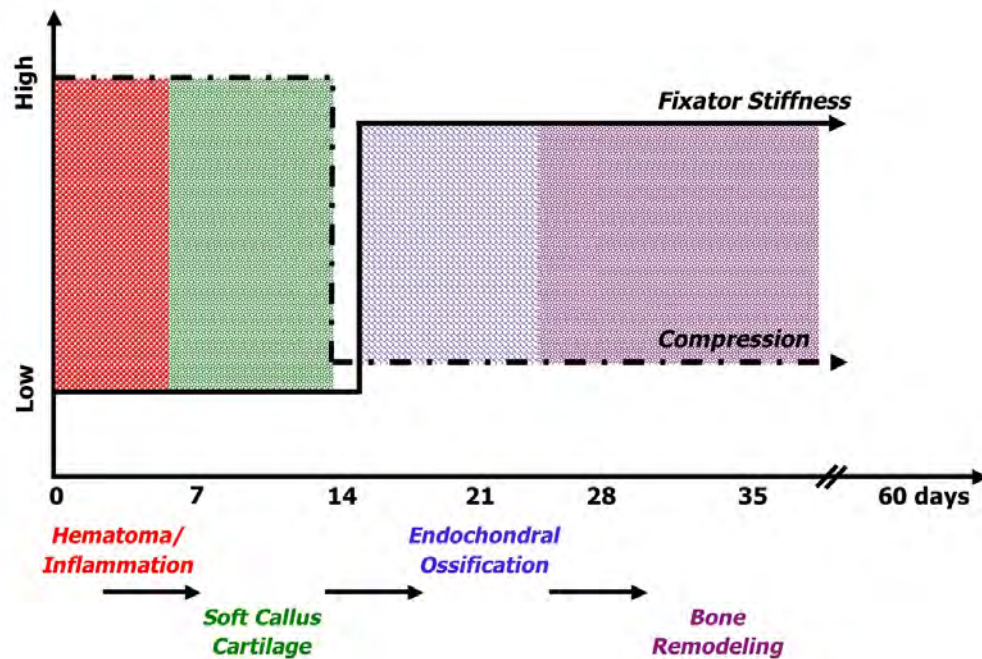


**Figure 1.10** Diagram showing a hypothesis of how fixator stiffness may be modulated to optimize bone healing (solid line - fixator stiffness, dashed l- compression)

Thus my project paid particular attention to development of an external fixator that, in a controlled fashion, would impose the different stiffness environments necessary to test this hypothesis. The aims of this study were:

1. The design and evaluation of a novel external fixator, which allows modulation of the mechanical environment within an experimental, critical-sized, femoral defect in the rat.
2. *In-Vitro* mechanical testing of the fixator to determine its mechanical properties and the mechanical environment it produces within the defect.
3. Investigation of the effect of the mechanical environment on the healing of an experimental, critical sized femoral defect in response to rhBMP-2.
4. The development of a modulated mechanical environment for bone healing in this rat segmental defect mode

## PROJECT AIMS

1. The design and evaluation of a novel external fixator, which allows modulation of the mechanical environment within an experimental, critical-sized, femoral defect in the rat.
2. *In-Vitro* mechanical testing of the fixator to determine its mechanical properties and the mechanical environment it produces within the defect.
3. Investigation of the effect of the mechanical environment on the healing of an experimental, critical sized femoral defect in response to rhBMP-2.
4. The development of a modulated mechanical environment for bone healing in this rat segmental defect model.



## CHAPTER TWO

*The design and evaluation of a novel external fixator, which allows modulation of the mechanical environment within an experimental, critical-sized, femoral defect in the rat*

## 2.1 INTRODUCTION

This chapter describes the design and construction of a novel external fixator for the rat femur that provides precise, standardised stiffnesses, which reliably create a known stress within the defect. The stiffness of external fixator could be modulated by pin offset, pin diameter, pin material, fixator bar length, fixator bar number, fixator bar material and fixator bar thickness. For this study, the fixator design to modulated stiffness was chosen by changing the stability bars. The reason for this was to allow precise modulation of fixator stiffness as bone healing progressed while it is still attached to the animal *in-vivo*. Although, there are two other ways to change stiffness *in-vivo*, one is by changing the offset of stability bar from bone surface, and the other by changing the number of bars. This type of change was avoided to prevent loosening of screws, which secure stability bar to pins. However, changing other design parameters mentioned above was not possible, and in some instances would have required an additional surgery for animals.

The shape and materials for design of the fixator were specifically chosen to mimic one used clinically. The weight and size were also carefully calculated by taking into account animal's body weight. All other related questions in regards to these choices will be further explained in the discussion.

Once designed, the components of the fixator were fabricated by the AO Development Institute (Davos, Switzerland). An extensive literature search failed to identify the prior design and construction of such a device for the critical sized segmental defect (CSD) in a rat model. Moreover, external fixators used previously for the fixation of such defects had not been quantitatively analysed to determine their mechanical parameters *in-vitro* and *in-vivo* in the same study, despite the knowledge that mechanical conditions influence bone healing process in fracture models. We have extensive, prior experience [54, 60] with a previous "first generation" fixator of high stiffness, originally designed by Einhorn and colleagues [62]. To enable comparison with our historical data, the novel "second generation" fixators were designed to give stiffnesses that were theoretically 100%, 70% and 40% of the stiffness of the first generation device stability bar; ExFixHigh, ExFixMed and ExFixLow, respectively.

As well as enabling us to test our hypothesis (Chapter One) concerning the mechanical optimisation of the healing of large segmental defects, the novel fixator could provide the field with a standard instrument for use by other investigators. This would allow for a standardized experimental system to facilitate comparison of data between different groups of researchers. Such commonality is presently lacking, and is a source of confusion.

Therefore, the aim for this study was to design and develop an external fixator with the possibility to adjust the stiffness *in-vivo* to allow optimization of bone healing process in the rat model.

## **2.2 DESIGN OF THE FIXATORS**

### **2.2.1 First Generation Fixator Design and Surgical Implantation**

This fixator was designed for unilateral external fixation in the rat, and consists of rectangular, aluminium stability bar including holes for the application of Kirschner (K)-wires. The stability bar is 30mm in length, 7.5mm in width and 7.5mm in height. There are 4 holes through the stability bar; the distance between the outer and inner pins is 5mm and distance between the two inner pins is 10mm. The arrangement and design of the external fixator stability bar are shown in figure 2.1. Four 1.2 mm diameter K-wires (Figure 2.1 B) are fitted into corresponding holes in the external fixator stability bar (Figure 2.1 A) and fastened with locking screws. To avoid ambiguity, this fixator is referred to as ExFixOld throughout this thesis.

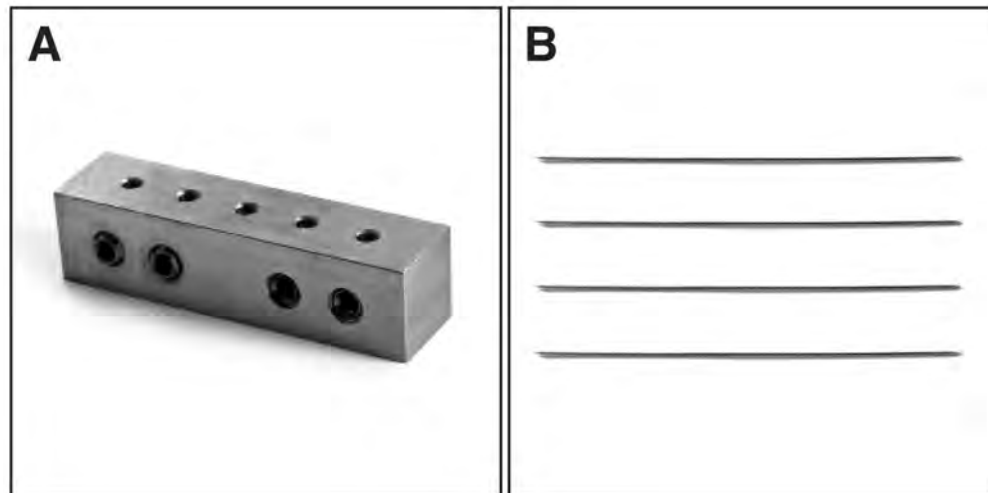


**Figure 2.1** Components of the first generation fixator. The rectangular, aluminium stability bar (A) is fixed to the bone with K-wire (B).

### 2.2.2 Surgical implantation of the First Generation External Fixator

All animal procedures were approved by the ethics committee on animal care and use at Beth Israel Deaconess Medical Center, Boston, MA. Male Sprague-Dawley rats weighing 400-425 g were used for this study. Surgery was performed under sterile conditions and all animals were anesthetized with isoflurane. Before surgery all rats were given antibiotics ceazolin (dose 20mg/kg; 0.5mL) and the analgesic buprenorphine (dose 0.01-0.05 mg/kg) intramuscularly in the left leg. The entire right hind leg of the rat was shaved, cleaned with 70% ethanol and 10% iodine and draped with a sterile towel. An incision was made through the skin running craniolateral on the surface of the right femur (Figure 2.2A). The shaft of the femur was exposed by gentle dissection between the quadriceps and hamstring muscles. The right femur was exposed from the greater trochanter to the supracondylar region of the knee (Figure 2.2B). A template was placed on the craniolateral aspect of the femur to guide the drill and permit reproducible positioning of four drill holes with a diameter of 0.9mm. Irrigation during drilling prevented heat damage to the bone tissue. All four K-wires were driven into each drilled bone hole until their tips reached the outer surface of the cortex. All four K-wires were cannulated through the skin flap and the fixator stability bar was fastened at a preset distance from the bone

surface (Figure 2.2C). Using a dental burr of 4.5 mm diameter, 5mm critical-sized segmental defects were created and measured with callipers to make sure the exact size (Figure 2.2D&E). To minimize tissue damage in the bone, 0.9% saline solution during sawing was applied. The wound was closed in layers, to suture the muscle size 3-0 Vicryl, resorbable sterile suture (Ethicon) was used, and it was sutured underneath the external fixator. To suture the skin, 4-0 Nylon (MONOSOF), monofilament non-absorbable suture was used. (Figure 2.2F). On the first three postoperative days, the rats were given analgesic every 12 hours and antibiotic every 24 hours.

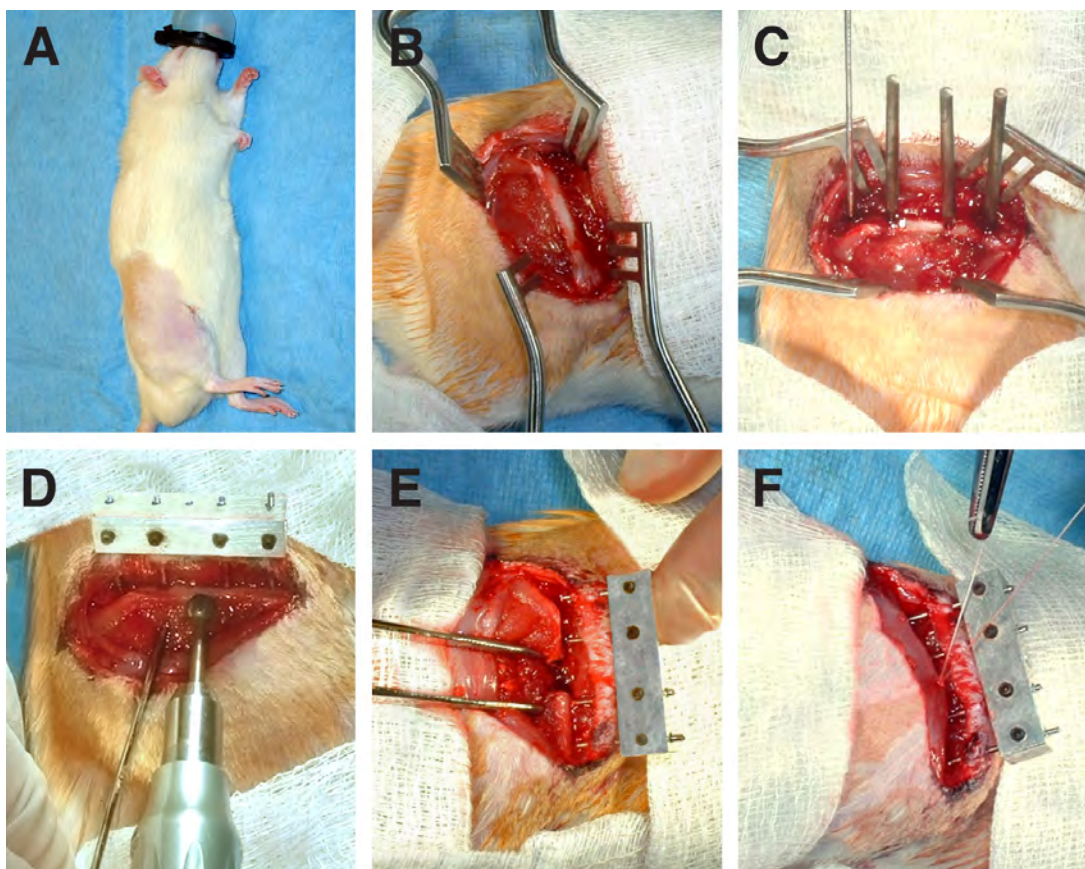


**Figure 2.2A-F** Surgical implantation of first generation fixator (ExFixOld) on the rat femur: A) rat is shaved and disinfected before the surgery; B) the incision is made in tissues until femur is exposed; C) four K-wires are inserted in the craniolateral aspect of the femur; D) the stability bar is secured on the K-wires with screws and the defect is made between two middle K-wires; E) 5mm defect; F) skin and muscle tissues sutured in layers.

## 2.3 NOVEL, SECOND GENERATION FIXATOR DESIGN AND SURGICAL IMPLANTATION

### 2.3.1. Second Generation Fixator design

The external fixator main frame consists of a polyethylene terephthalate (PEEK) body. Each external fixator has two connection elements and two main modules. Three different stiffness connection elements were developed to achieve different fixation stiffnesses equivalent to 40 (1.7mm), 70 (2.1mm) and 100% (2.5mm) of the stiffness of the first generation fixator (Figure 2.3), the absolute values of fixation stiffness will be described in detail in the next chapter. Each main module has two holes where the screws are inserted. The fixator stiffness can be changed while it is still attached to a living animal by changing connection elements with the wire applicator. Titanium (Ti) was used to make the mounting pins shown in the figure 2.3. Four Ti screws are used to secure stability bar to the femur (Figure 2.3).

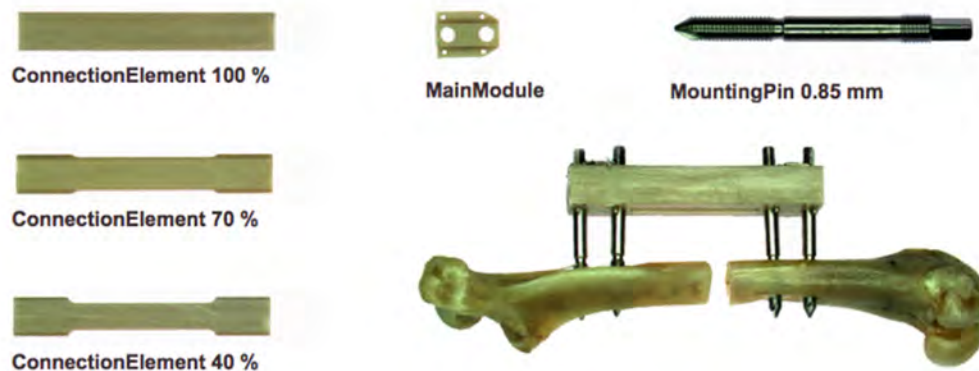


**Figure 2.3** Components of the novel external fixator. Three different stiffness connection elements, main module; titanium mounting pin and external fixator implanted on the femur with the defect.

The second generation external fixator comes in four pieces and needs to be assembled prior to use (Figure 2.4A-F).

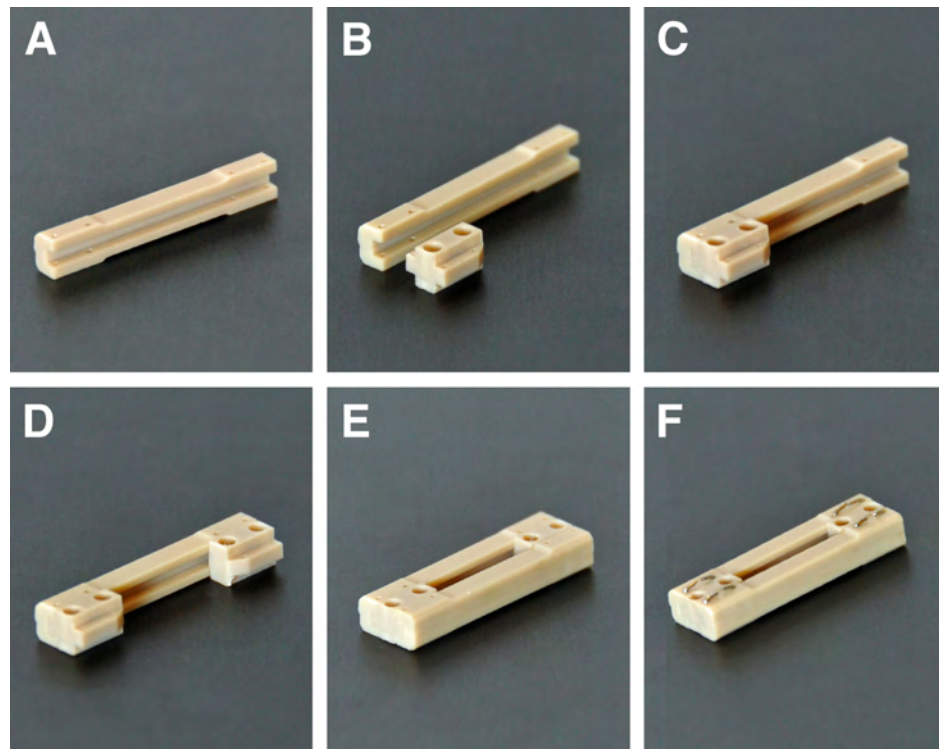


**Figure 2.4A-F** Assembly of the novel external fixator: A) 70% stiffness connection element; B) the connection element and one of the main modules; C) demonstrates how one of the main modules slides inside of the connection element; D) demonstrates how both of the main modules slides inside of the connection element; E) demonstrates both of the main modules and both connection elements in place; F) demonstrates fully assembled stability bar – main modules and connection elements secured with wires.



**Figure 2.5** External fixator with a titanium screw inserted into the main module.

The distance between the outer screws is 4mm and the distance between the middle screws is 11mm. All holes are predrilled using 0.7mm drill bit. The screws are locked in corresponding holes of the main fixator frame, which is parallel to bone surface and set at the distance of 5mm from the bone (Figure 2.5).

To create a 5mm segmental bone defect in the femur the saw guide was developed (Figure 2.6A.). The saw guide helps to create an accurate and precise 5mm defect every time, but also serves as a positioning guide for the installation of the external fixator. The main frame of the external fixator is clipped on to the saw guide and then the whole system is clipped on to the bone as shown in figure 2.6B&C.

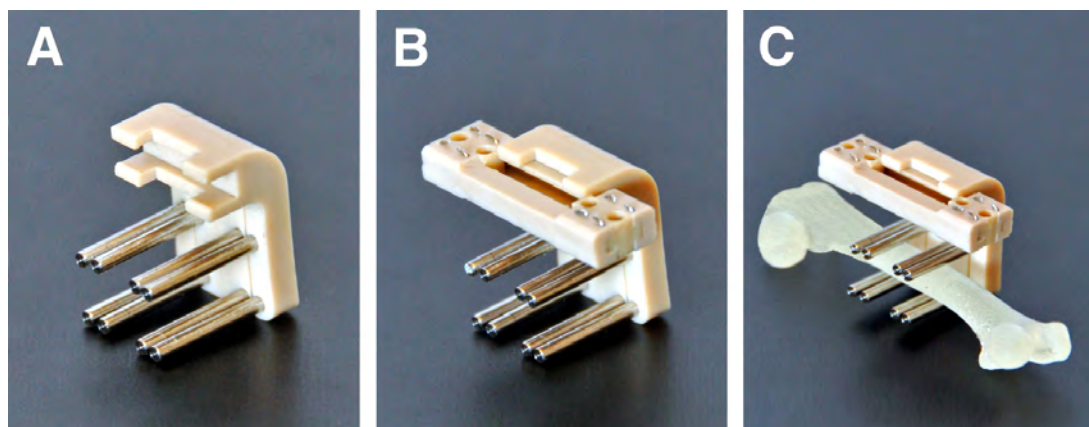


**Figure 2.6** (A) Giggly saw guide; (B) External fixator clipped on the giggly saw guide (C) Giggly saw guide with the external fixator clipped onto femur.

To produce a 5mm transverse defect a micro Gigli saw is used. To minimize a slip-stick effect, two elements of this saw are constructed from wires of different diameter. The thicker wire diameter 0.07mm serves as an axial core and the second wire diameter 0.04mm forms a cutting spiral with adjustable pitch around the core wire. The 5mm gap size was generated by using 0.22mm Gigli saw. Both of these pieces can be autoclaved at 134°C (Figure 2.8E-I).

Due to the miniature size of the external fixator a special set of instruments was designed and acquired for the implantation of this new fixator. A special screwdriver was developed to drive screws into the femur (Figure 2.7A&B). To create holes in



the bone a drill bit with a diameter of 0.75mm was used. When used together with the design of the self cutting tip of the screw radial preload results it was been shown that this prevents loosening due to bone surface resorption at the interface bone-screw. The drill bit is operated by a miniature electrical pen drill producing 2500rpm at a power of 500mW (Figure 2.7C).

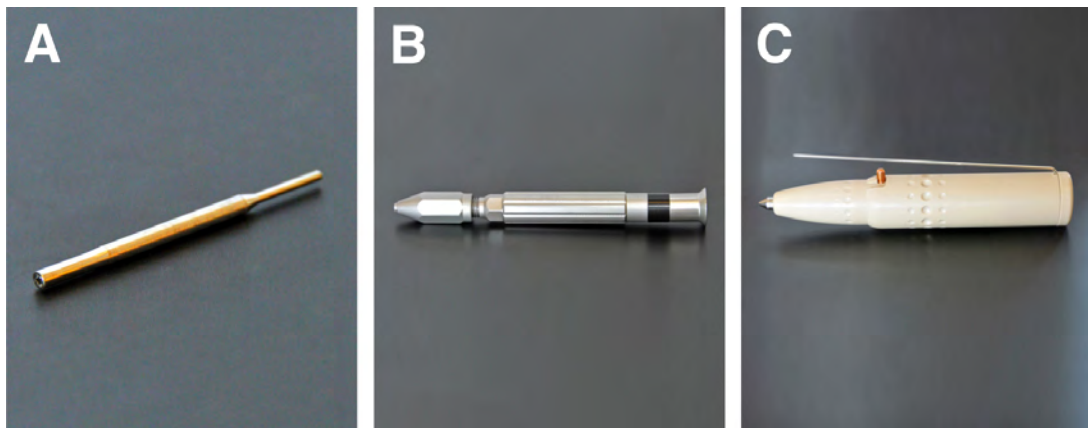


**Figure 2.7** Instruments designed for use with the novel fixator: (A) Screwdriver tip; (B) Screwdriver for the tip attachment; (C) Miniature electrical pen drill used to make holes for insertion of screws.

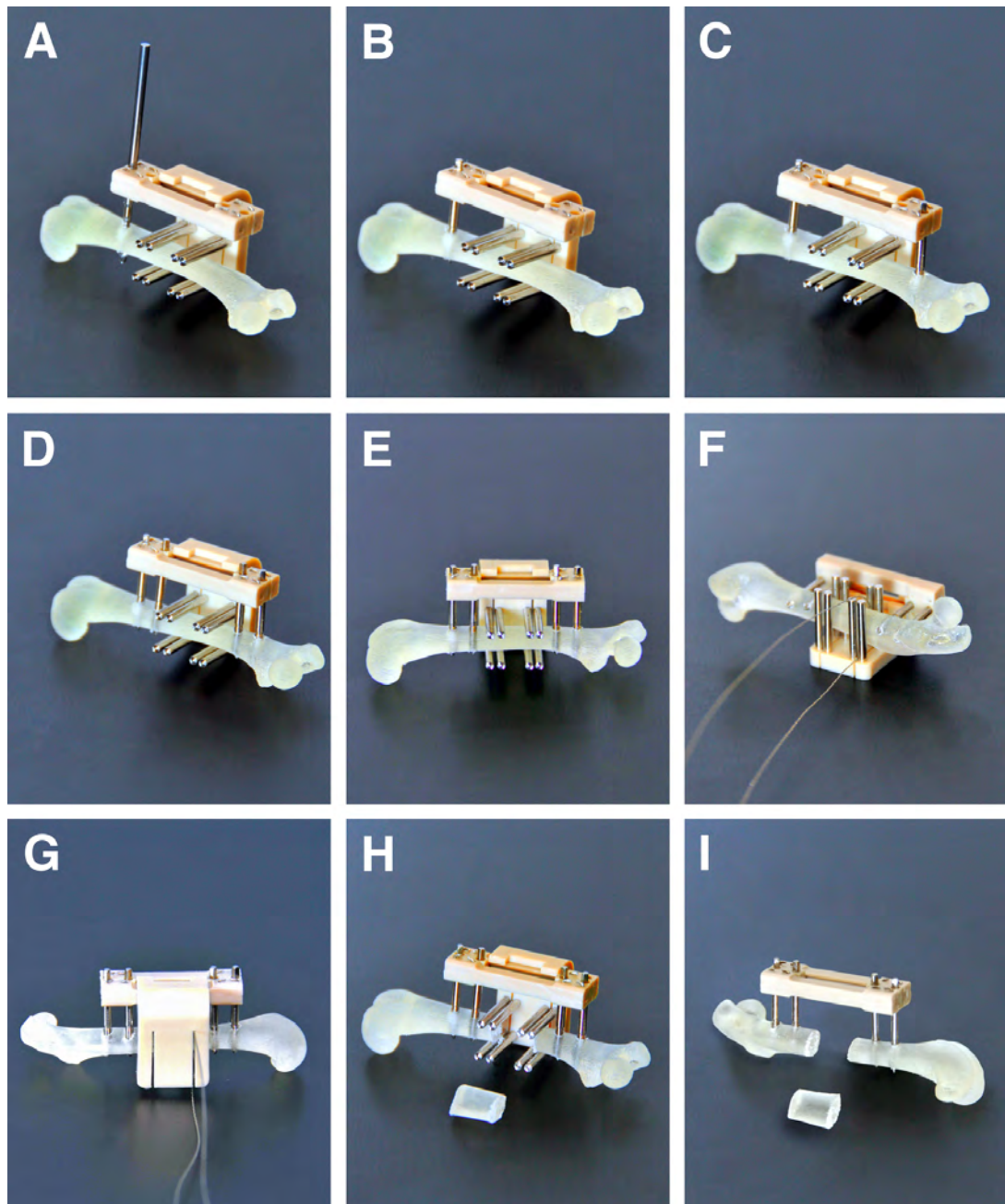


**Figure 2.8A-I** Implantation of second generation external fixator (ExFix): A) ExFix stability bar clipped on the Giggly saw guide, clipped on the femur shows first drilled hole with drill bit in place; B) demonstrates insertion of the first titanium screw in the outer distal part; C) demonstrates insertion of the second titanium screw in the outer proximal part; D) demonstrates insertion of two inner titanium screws (side view); E) demonstrates complete installation of the ExFix from the front; F) demonstrates gigly saw application through the saw guide; G) demonstrates gigly saw pasted through the saw guide grooves; H) demonstrates cut out 5mm defect with saw guide in place; I) demonstrates completion of the procedure without saw guide.

### **2.3.2 Surgical implantation of the Second Generation External Fixator**

Surgery was performed under sterile conditions and the rat was anesthetized with isoflurane (2% at 2 liters/min by air mask). Before surgery the rat was given antibiotic (cefazolin, 20mg/kg; 0.5ml of body weight) and the analgesic buprenorphine (dose 0.08 mg/kg; 0.5ml of body weight) intramuscularly in the left leg. The entire right hind leg of the rat was shaved, cleaned with 70% ethanol and 10% iodine and draped with sterile fenestrated drape so only the right leg was exposed. An incision of approximately 3.5-4cm was made through the skin running craniolateral on the surface of the right femur from the greater trochanter to the supracondylar region of the knee (Figure 2.9A). The shaft of the femur was exposed by gentle dissection between the quadriceps and hamstring muscles (Figure 2.9B).

The external fixator bar was used as a positioning guide, first clipped on to the wire saw guide and then placed on to the craniolateral aspect of the femur to guide the drill and permit reproducible positioning of four drill holes with a diameter of 0.75mm (Figure 2.9C). A “Dremel” saw was used to drill all the holes for the screws one at the time, starting either with the distal or proximal side. It is very important that the first screw is perfectly perpendicular to the craniolateral aspect of the femur and the external fixator bar before drilling. Once the first hole was made the screw was driven into the femur on the distal/proximal side, first through the external fixator bar and then into the bone making sure that it entered perpendicularly into the femur (Figure 2.9D).

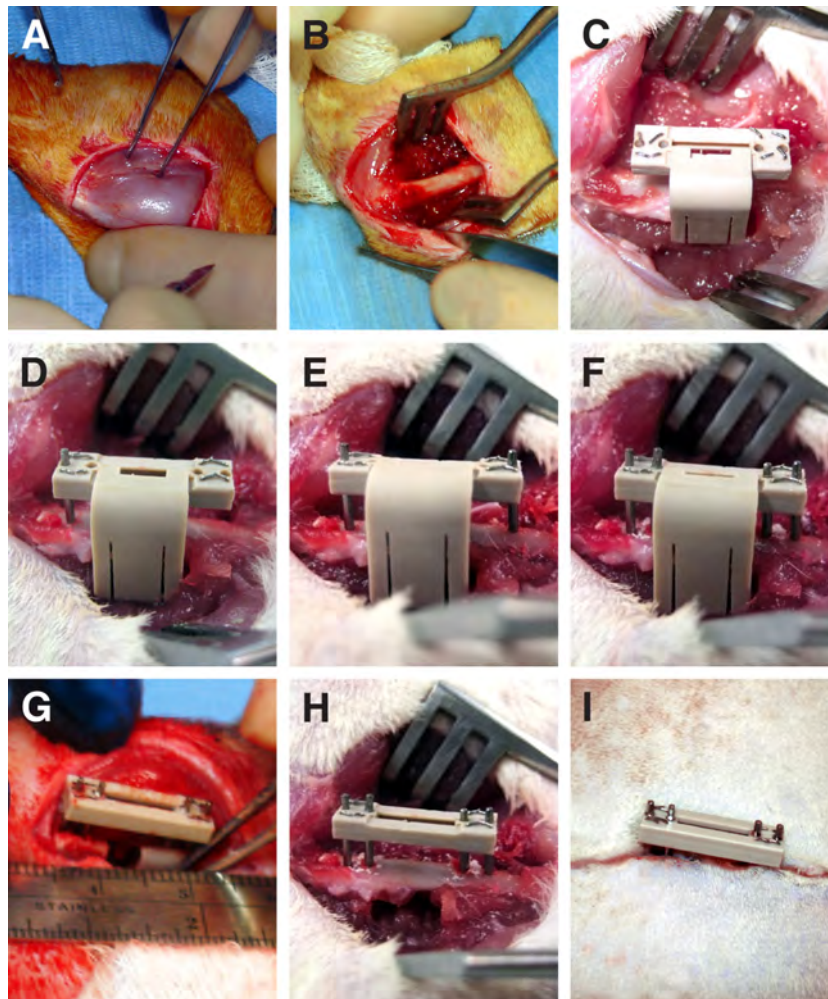


**Figure 2.9A-I** Surgical implantation of the second generation external fixator (ExFix) on the rat femur: A) shows incision made in the skin to expose muscle; B) shows incision made through the muscle to expose femur; C) ExFix stability bar clipped on the saw guide and placed on the femur for the implantation: D) first titanium screw screwed into bone through the distal hole of the stability bar; E) second titanium screw screwed into bone through the proximal hole of the stability bar; F) titanium screws screwed into bone through two inner holes on the stability bar; G) demonstrates created 5mm segmental defect; H) demonstrates completion of the surgical procedure with ExFix in place without the saw guide; I) demonstrates sutured skin with exposed ExFix stability bar.

After the first screw was in place, the most distant hole from the first screw was then drilled, and the second screw was driven into the hole (Figure 2.9E). The implantation order of the two middle screws is not important as long as they are perfectly perpendicular to the craniolateral femoral surface (Figure 2.9F). After the fixator was in place the saw guide was used to make the segmental defect. For this, a 0.22mm wire (Gigly) saw was passed through the 2 grooves underneath the femur to create a 5mm segmental defect by reciprocal motion back and forth (Figure 2.9G).

After the defect was created, the saw guide was removed and any treatment (e.g. rhBMP-2) added to the defect area. The wound was closed in layers, the muscle first and then the skin (Figure 2.9H). On the first three postoperative days, the rat was given analgesic every 12 hours and antibiotic every 24 hours.



**Figure 2.10.** Novel fixator in place across a rat, femoral 5mm defect. The stability bar of first generation, ExFixOld, is shown below for comparison.

## 2.4 DISCUSSION

As described here, a novel external fixator was designed and a prototype manufactured. The primary innovation of this fixator was the ability to exchange the stability bar connective modules to select different, standardized stiffnesses. Because the stability bar's connective elements can be exchanged while the device is attached to the animal, the stiffness can be adjusted at different stages during the healing process. This is important for the studies described in the Chapter 5. Although three different stiffnesses were generated for the present work, additional stiffnesses could be achieved by fabricating additional connective elements of different thicknesses for the stability bar.

The screws and main frame were made from Ti and PEEK, respectively, because these materials are already used for orthopaedic implants in humans and their

biocompatibility is well established. These materials also allow *in-vivo* imaging in the early stages of fracture repair with a minimal distortion, and reduce the incidence of infections.

As an additional design feature, the fixator was made so that it has preset offset of 6mm from the bone surface to the stability bar no matter which stiffness connection elements are used. This has an advantage over ExFixOld where offset was predetermined by measuring the distance on the K-wire and making a mark with a marker pen, and then sliding the stability bar on the marks before securing with the screws. This method was not very reproducible and this could be one of the reasons why this animal model had high variability.

Another big advantage over alternative designs described in the literature [62, 77] including the one we have used in the past, is that the new external fixator was designed to have a minimal mass to avoid uncontrolled loading due to inertia. The new fixators were made taking into account rat body weight and the size of femur and this relationship was scaled accordingly as is done with human fixation devices.

To keep the surgical trauma low, conventional and rotating saws were not considered as tools for creating 5mm critical size defects. Such saws either cut into adjacent tissue or strip off the periosteum when the tissues are retracted. In the past we have used a 4.5mm dental burr saw to create 5mm defects and found that it was impossible to create exact and reproducibly sized defects with parallel ends. To avoid all these problems we took an advantage of the Gigli saw. A conventional Gigli saw has substantially different static and kinetic friction and two intertwined diamond cords create very minimal damage to the bone while cutting. The saw guide was developed for creating precise defects with the parallel ends every time.

The *in-vivo* pilot experiment was performed with the new external fixator prototype to make sure that it meets all proposed demands before it is manufactured in larger quantities. The results of the first evaluation of the *in-vivo* performance at the time of surgery showed that the distance between the bone and the stability bar, needed to be increased by 3mm to avoid impinging the skin immediately after surgery due to

tissue swelling. This was achieved by changing the screw length, a modification that resulted in minimal change in the overall stiffness of the construct.

In conclusion, in this study I was able to develop a standardized method for bone fixation in this CSD rat model, which produced a controlled mechanical environment. Furthermore, the first *in-vivo* pilot data demonstrate that it is a highly reliable and reproducible method to study bone repair of long bones in the rat model.

Having successfully designed this device and demonstrated the merits of a prototype, the fixator was subject to further, detailed, quantitative analysis to determine its precise mechanical properties and the mechanical environment it generates within a segmental defect *in-vitro* and *in-vivo*. These studies are described in the following two chapters.

## **CHAPTER THREE**

*Determination of the in vitro mechanical properties of first and second generation external fixators*



### 3.1 INTRODUCTION

A number of studies have improved our understanding of the biologic mechanisms involved in bone tissue repair [62, 78-82]. The effects of mechanical conditions on bone repair such as axial, shear and IFM have been studied extensively [40, 83-91]. On the contrary, the *in-vivo* mechanical environment generated by fixation is rarely investigated in detail.

Data on compliance, stiffness, torsional rigidity and IFMs are rarely tested *in-vitro* and described in detail in existing models of fracture fixation to determine fixation mechanical properties prior to *in-vivo* experiments. Fixation device mechanical properties are even more important when studying bony healing of CSDs to establish fixation that provides not only a constant gap size throughout the experiment period of full weight bearing, but also a perfect mechanical environment for the healing bone.

The choice of fixation device is very important and should be carefully selected depending on the study design, and other factors such as gap size and the type of fracture. Different types of intramedullary nails, internal plates and external fixators have been used in the experimental studies as well as in the clinical practise to stabilize the fragments of broken bones. Several studies examined the influence of fixation stiffness in the rat femoral fracture model by comparing different types of nails [92-94] or comparing intramedullary nails made from different materials [95-98]. Yet, only half of them reported *in-vitro* evaluation for their nail devices such as axial and torsional stiffness [93, 94, 96, 97] prior to *in-vivo* studies. External fixation devices used for distraction osteogenesis [75, 82, 99-105], fracture fixation [77, 106-111] and large defect models [54, 112-115] allow controlled and reproducible mechanical environment in the rat femoral fracture model.

The mechanical characteristic of a specific external fixator are major factors in determining the biomechanical environment at a fracture, osteotomy and most importantly at the segmental defect site, hence, it has an effect on the healing process. Although the optimal biomechanical environment for healing of a fracture or an osteotomy is unknown, a specific range of interfragmentary motion (IFMs)

exists which promotes healing. It is therefore desirable that the mechanics of an external fixator can be manipulated to enable control of the range of IFM. The characteristics of an external fixator are defined and can be modulated by a large number of variables, which include: pin offset (distance between the pins), pin diameter, pin material, the amount of pins used, fixator bar length, fixator bar number, fixator bar material, fixator bar thickness and distance from the bone surface to the fixator bar, or so the called offset. Therefore, to gain control over the degree of IFM and gain a clear understanding of the effect of each variable and how it interacts with the others is to determine the overall characteristics of the device required. In the past several years only a few studies investigated the effect of individual components and whole frame configurations and how this effects system stiffness used in the experimental small animal models [77, 106, 107, 116].

An *in-vitro* study by Mark et al. [77] found that the distance between the bone surface and the fixator (offset) was linearly related to the stiffness in axial loading of rat bone and brass rod constructs. Furthermore, a 0.2mm decrease in pin diameter changed the axial stiffness of rat bone by about 50%. They also found that if the bone fragments touched, the axial stiffness increased almost 10 times as compared to a gap size of 2mm.

Harrison et al. [106] reported no difference in axial stiffness when different materials such as aluminium and titanium were used for the stability bar *in-vitro*, and increasing the osteotomy gap from 1 to 3mm decreased the mean axial stiffness by only by 6% for the three fixator frames tested. In the *in-vivo* study they showed that while using the same fixation conditions and changing the gap size from 0.5 to 3mm the pattern and progression of repair process were very different. In the group with 0.5mm gap bone, union was attained by around 5 weeks and the torsional strength of intact femur was reached by week 9 post-surgery. In contrast, a consistent pattern of atrophic fibrous pseudoarthrosis was seen in the group with the 3mm gap due to larger IFMs.

Study by Willie et al. [116] found that the contribution to the total stiffness of the fixation construct was dominated by the flexibility of the pins in relation to their offset, diameter and material properties. For example, titanium pins resulted in

significantly lower axial stiffness compared to stainless steel pins of the same design.

It is evident that external fixators are commonly used in fracture and segmental defect healing experimental models because they have an advantage over other fixation devices. The main advantage of the external fixators are that they allow the change of mechanical environment at the defect site *in-vivo*, which can be achieved by changing or adjusting the stability bar of the device during the course of the experiment as the bone healing progresses. Moreover, it permits the application of specific local mechanical stimulation to enhance the repair of bone, and also provides the potential to measure stiffness of callus tissue *in-vivo*. Although the devices have also a few disadvantages that include: irritation of soft tissue, infections and breakage of pins.

The studies mentioned above mechanically characterized the *in-vitro* fixation stiffness and its effect on different modes of loading by changing gap size, material of the stability bar, pin diameter and offset in different models. The difficulty in assessing the importance of these studies arises from the uncertainty as to whether the experimental conditions were realistic. This raises the question of whether the observed behaviour in these studies is representative of real fractures and provide an increasing constraint to movement throughout the healing process. Moreover, in the natural environment of fracture healing, different amounts of loads such as axial, bending and shear arise not only from fixation device stability, but also from weight bearing, muscle forces, tendon and ligament activity. While this type of loading is very complex and would be hard to model experimentally, a more realistic approach is needed so that the influence of the mechanical environment on healing fractures are better understood and interpreted. Most of the *in-vitro* models with fixation devices found in the literature are tested with different gap sizes. Although this explains the mechanical conditions to some extent, in reality fracture gaps have various types of tissue within them, depending on the healing phase. Therefore, to determine “true” local mechanical environment for the healing fracture is not really possible using existing methods. In particular, the contribution of the repair tissue with the lesion to overall stability has been ignored.

In the literature I found only one *in-vitro* study [117] that looked not only at the local mechanical environment provided by five different types of clinical external fixators, both dynamized and non-dynamized, but also at the effect of the resistance to axial IFM created by four different stiffness materials simulating the main stages of the healing process. Using fixators implanted on glass fibre tubing in axial compression to simulate weight bearing, Gardner et al. [117] found that if there is no material present in the fracture gap, which simulates the conditions immediately post-surgery, the fixator frame provided complete stability at the fracture site, and there was no contribution from the gap (fibre glass tube) to support the fracture site. On the contrary, when they interposed material with the lowest stiffness, which represents early stages of fracture healing, they found that the mechanical properties of the fixator were as important as those of the fracture material in influencing axial IFM at around two to four weeks post fixation. Furthermore, the five clinical external fixators tested contributed differently depending on their stiffness. In contrast, using three stiffer intra-fracture materials, simulating all but the initial stage of fracture healing, axial movement was influenced only by the stiffness of these materials and only slightly influenced by the contribution of the fixation devices. Nevertheless, angular, transverse and torsional shear movements were enhanced, depending on the type of the fixator. These motions were also enhanced by unlocking the fixator to initiate fixator looseness.

The studies of Gardner et al. [117] demonstrate the importance of including contributions by the intra-defect tissue when analyzing the overall mechanical environment created by an individual fixation device, but, to my knowledge, no study to date has extensively investigated this interaction. Thus, in the next stage of my studies, I undertook a series of *in-vitro* mechanical studies to determine the stiffness created by each of the fixators when a standard material of known mechanical properties was inserted into the defect. Each of the inserts represented a different tissue that would be present in the defect during healing process. The hypothesis for this part of the experiment is that the mechanical boundary conditions and the external fixator stability are the most important at the initial phase of CSD healing and will determine the success of it. The aim for this part of the study was to determine mechanical properties of the external fixators described in the previous

chapter and to estimate how they influence the mechanical properties of a rat segmental, femoral defect during the main stages of healing. For the first objective three point bending measurements were used to determine the mechanical properties of the stability bars; and for the second objective fixators were then attached to intact rat femur and to femur with a 5mm segmental defect. To simulate three of the main stages of healing, rubber, low-density polyethylene or wood was inserted into the defects. In each case, axial compression testing, simulating weight bearing, was used to determine mechanical properties of the construct.

Data from this study provide a better understanding of mechanical conditions needed at the different stages of osseous repair for rapid and most efficient healing under the weight bearing.

## **3.2 MATERIALS AND METHODS**

### **3.2.1 MATERIALS: External Fixators**

In this experiment all external fixators ExFixOld, and newly designed external fixators with ExFixLow, Medium and High (see earlier comment about nomenclature) were tested empirically by *in-vitro* mechanical testing to determine detailed mechanical characteristics. The dimensions and materials of all external fixators are described in chapter two.

### **3.2.2 METHODS**

#### **3.2.2.1 3-Point-Bending of Stability Bars**

Non-destructive 3-point-bending mechanical tests with 6 samples per group were used to determine the mechanical properties of the stability bars for all external fixators. Because of its size difference the ExFixOld was tested with different mechanical parameters.

For the ExFixOld fixator, load was applied midway between two supports that were 25.94mm apart; the diameter of the supports was 4mm (Figure 3.1A). Load-displacement curves were recorded at a crosshead speed of 1mm/min to a 2% strain rate or a maximum force of 250N using Mechanical Testing System Synergie 200. The force/displacement data was acquired at 100Hz. The bending stiffness was calculated from the linear region of the load-deflection curve.

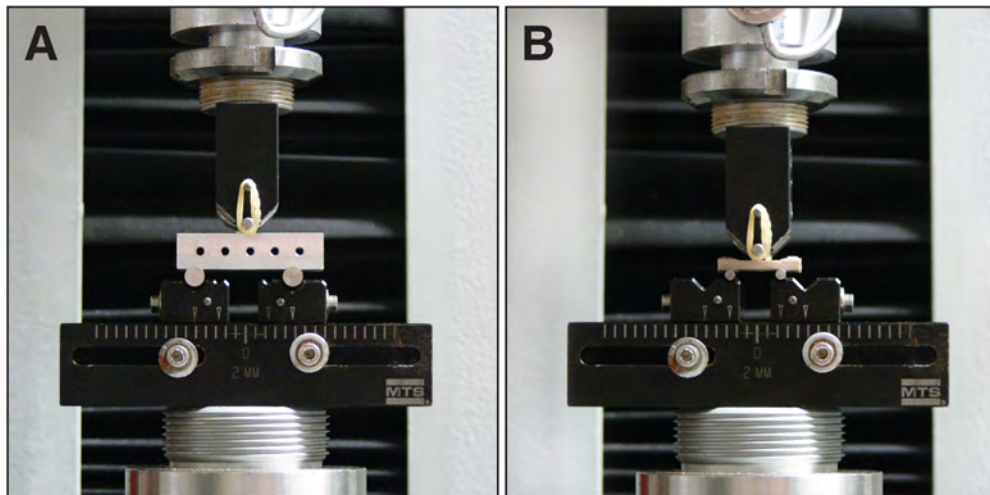


**Figure 3.1** Images illustrating 3-point-bending rig for testing of the external fixator stability bars: (A) ExFixOLD aluminium stability bar; (B) ExFixLow PEEK stability bar.

Because the ExFixLow, Medium and High fixators were much smaller in size than the ExFixOld the load was applied midway between two supports that were 14.09mm apart; the diameter of supports was 1.95mm (Figure 3.1B). Load-displacement curves were recorded at a crosshead speed of 1mm/min to a 2% strain rate or a maximum force of 250N using Mechanical Testing System Synergie 200. Samples were preloaded  $\sim 8$ N before each test. The force/displacement curves were acquired at 100Hz rate. The bending stiffness was calculated from the linear region of the load-deflection curve (Figure 3.2). Three point bending test was chosen only to test if in fact there was 30% differences between each stiffness fixators. The main advantage of a three point bending test is the ease of the specimen preparation and testing. While this method has also some disadvantages like the results of testing method are sensitive to specimen and loading geometry and strain rate. Since the shape and heterogeneity of fixator materials were uniform this test was appropriate to determine difference in stiffness between them.

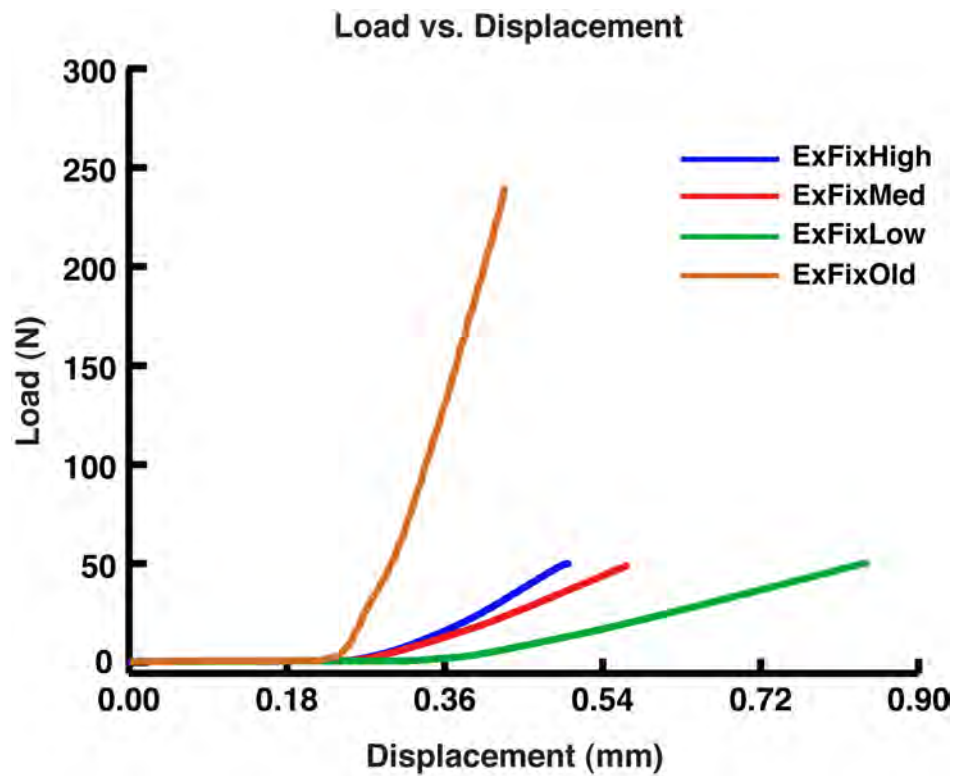


**Figure 3.2** Data from one representative sample shows an example of load-displacement curves from 3-point-bending test of stability bars for different stiffness external fixators: ExFixOld, ExFixLow, Medium and High with 8N preload.

### 3.2.2.2 Axial Compression Validation Test of Materials

In this test four materials were chosen to simulate the different types of tissue at the various stages of the bone healing process. Their selection was based upon the mechanical data of Morgan et al. [118] (Table 3.1). A rubber insert was chosen to simulate the early stage of healing, at the time when the haematoma within the defect is being replaced by cartilage. According to the literature, at this stage of healing the tissue elastic modulus is about 0.01-0.1GPa [118], which is in the same range as rubber. For the subsequent stage, at which calcified cartilage is being replaced by woven bone, low-density polyethylene (LDPE) was chosen to simulate tissue stiffness, which has been reported to be in the range of 0.2-0.9 GPa [118]. For the final stage of bone healing, during which woven bone is maturing into lamellar bone, two different woods were evaluated as to their proximity to physiological stiffness.

Cortical bone elastic modulus at this stage has been reported in the range of 10GPa; therefore maple and oak were the appropriate choice [118].

Tissue Type			
	Granulation Tissue n=10	Chondroid tissue n=18	Woven bone n=41
Mean (MPa)	0.99	3.10	201.16
Median (MPa)	0.99	2.89	132.00
SD (MPa)	0.20	1.30	200.85
Max (MPa)	1.27	4.42	1010.00
Min (MPa)	0.61	1.39	26.92

**Table 3.1** Indentation moduli for three tissue types in an unstabilized fracture (SD - standard deviation) from *Leong, P.L. and Morgan, E.F. "Measurement of fracture callus material properties via nanoindentation", Acta Biomater. 2008 September; 4(5): 1569–1575 [119].*

Axial compression testing was performed to confirm that their stiffnesses, as measured under our experimental circumstances, corresponded to those reported in the literature. Rubber and LDPE were purchased in a sheet of 12×12 inches with 6.35mm in thickness. Rubber was cut into 25×25mm squares with length of 6.35mm and LDPE was cut into 5×5mm with length of 15mm for testing. Maple and oak were purchased as rods 36 inches long and 9.54 mm in diameter and cut into 5.5 mm thickness samples for the testing. Six samples per group were used to determine the Young's moduli of these materials in axial compression testing with an Instron 8550 mechanical testing system. Load-displacement curves were recorded at a crosshead speed of 0.5mm/min to a 5% strain rate using a 2224N load cell. The force/displacement curves were acquired at 100Hz (Figure 3.3).



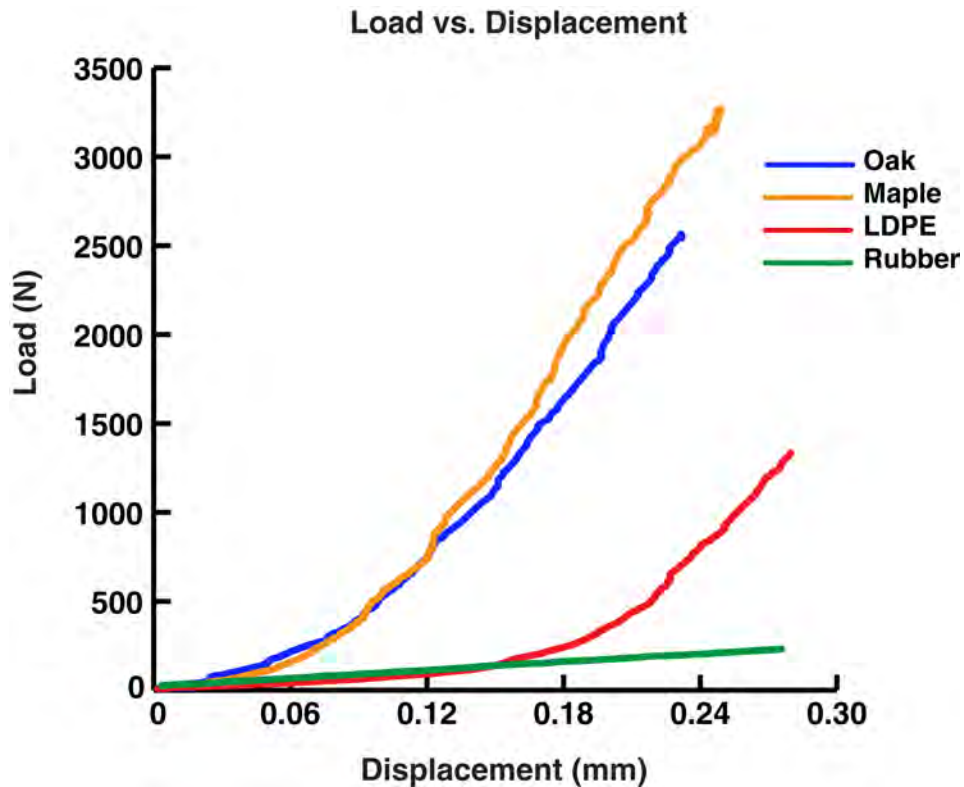
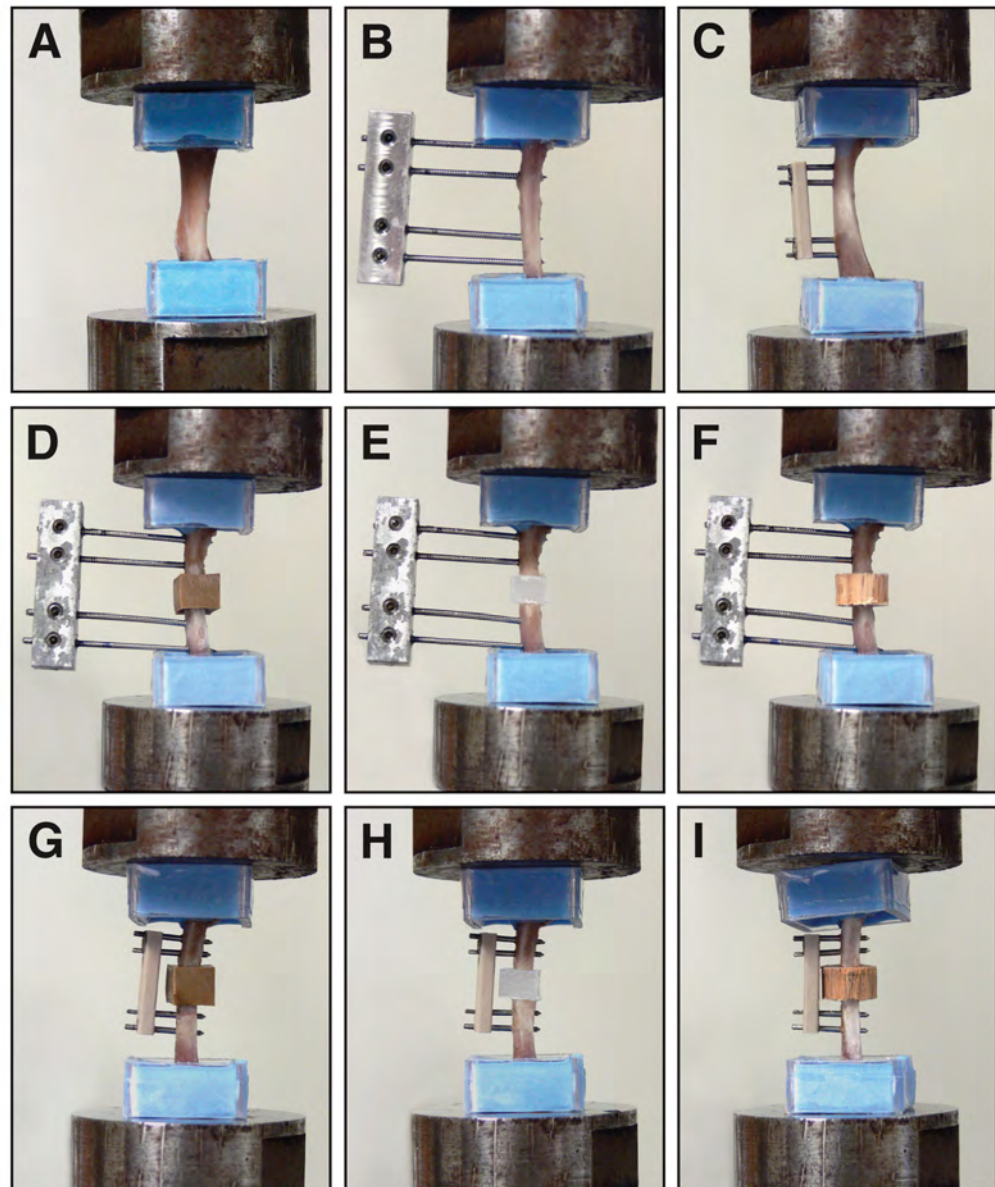


**Figure 3.3** Data from one representative sample shows an example of load-displacement curves of materials: rubber, LDPE, maple and oak tested in an axial compression mode.

### 3.2.2.3 Axial Compression Testing

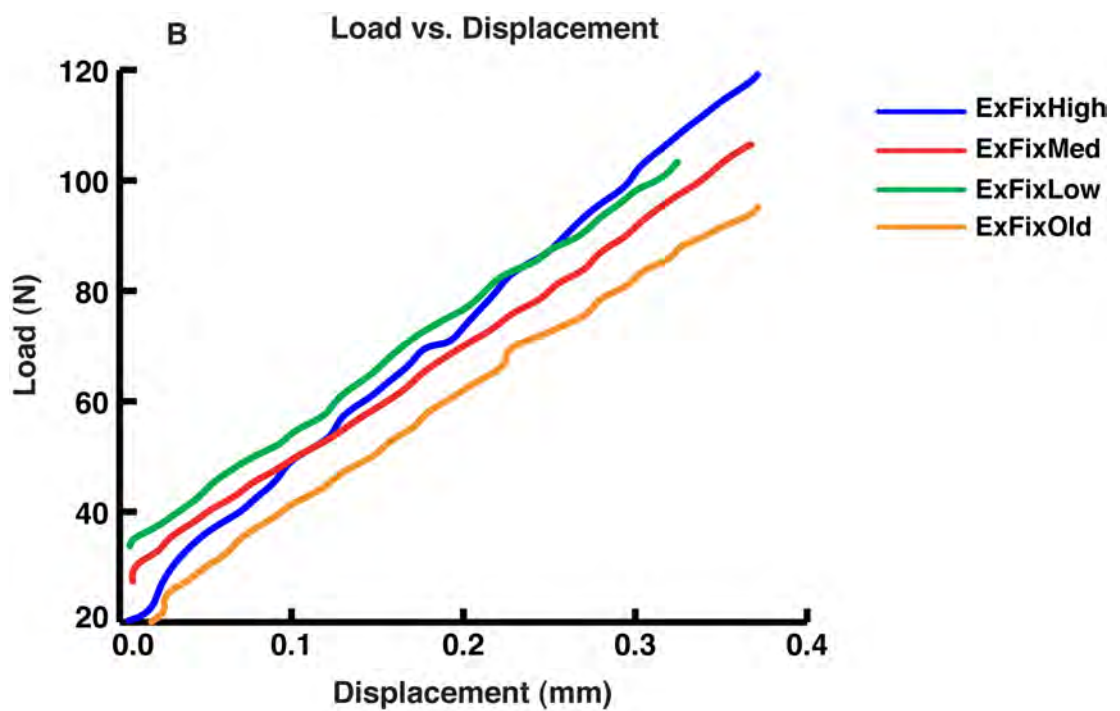
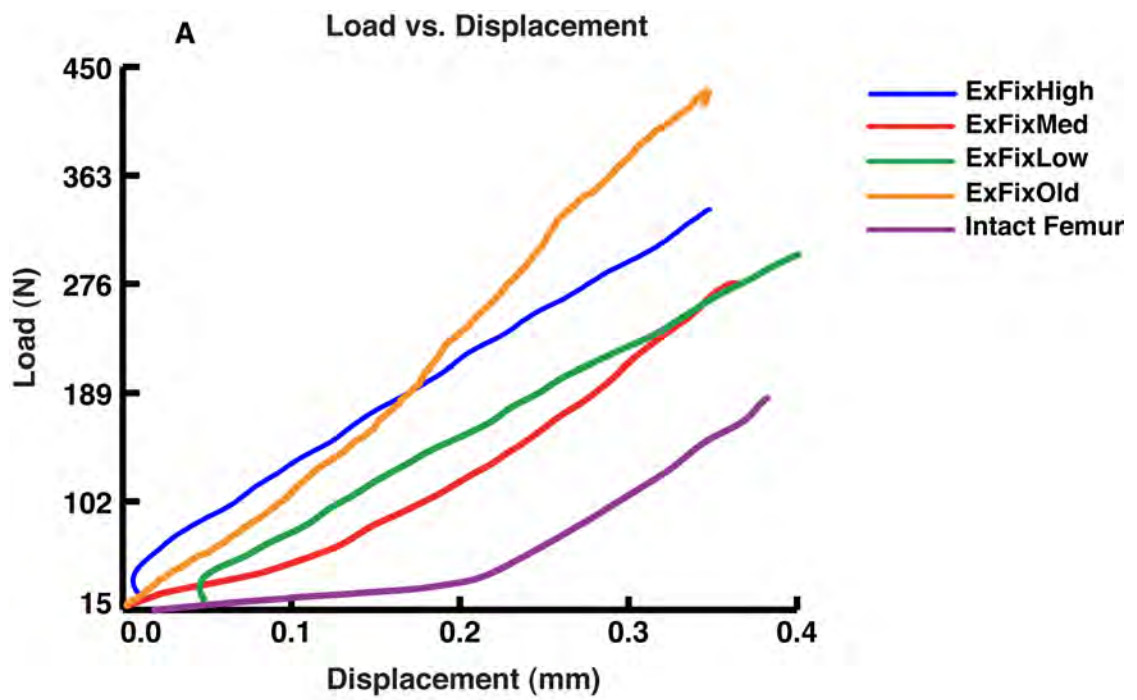
After stability bar and material testing was completed, axial compression testing was used to determine the mechanical environment created when the 4 different stiffness external fixators were fixed onto rat femora with and without the defect. For this experiment the external fixators ExFixOld, ExFixLow, Med, and High (see earlier comment about nomenclature) were fixed in position on the right femur of a total of eight Sprague-Dawley rats, with 2 rats per group. After the external fixators were in place the 5mm segmental defect was created in one of the femurs in each group and then the femurs were excised from the body. The procedure was performed in this manner to avoid drying out and cracking of the bones during the procedure. Also, 6 intact contralateral femurs were used as controls. Both ends of each specimen were

embedded in polymethylmethacrylate (PMMA) to provide a reproducible, flat interface with the testing fixture. The four different test materials were put into defects to simulate different stages of fracture healing. The thickness of all materials was cut to 5.5mm to fit the defect tightly; the diameter for the wood was 9.54mm, rubber and LDPE was cut into 6 by 6mm squares. Since the specimens were tested in compression the area of the material inserts in the defect had no effect on mechanical properties. Six samples from each material were placed in the segmental defect for each of the different fixators to determine the mechanical environment (Figure 3.4). After each test constructs from all groups were taken out from mechanical fixture, then one of the material samples were inserted into the defect and repositioned in the mechanical testing machine.



**Figure 3.4** Representative examples of femur constructs tested in axial compression with various stiffness fixators and different materials in the defect gap: (A) Intact femur; (B) ExFixOld no defect; (C) ExFixHigh no defect; (D) ExFixOld rubber insert; (E) ExFixOld LDPE insert; (F) ExFixOld maple insert; (G) ExFixHigh rubber insert; (H) ExFixHigh LDPE insert; (I) ExFixHigh maple insert.

Load-displacement curves were recorded at a crosshead speed of 0.5mm/min to a 1.5% strain using an Instron 8550 mechanical testing system. The force/displacement curves were acquired at 100Hz rate. The stiffness of the construct was automatically calculated from the linear region of the load-deflection curve (Figure 3.5).



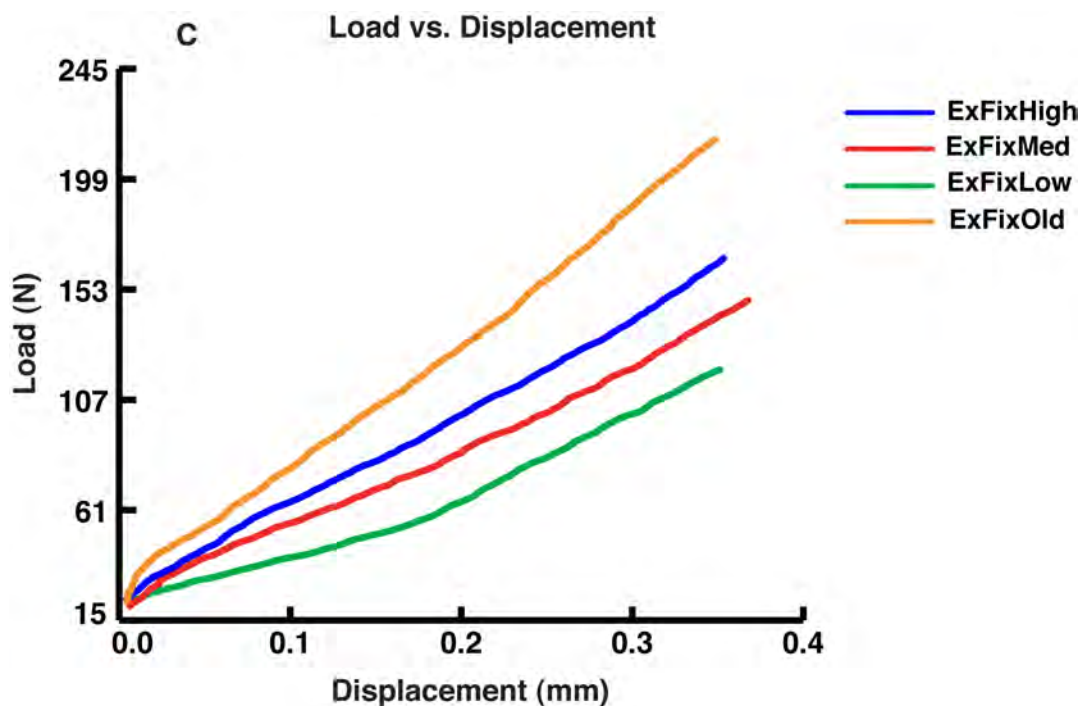


**Figure 3.5** Data from one representative sample shows an example of load-displacement curves from axial compression test of femur constructs with various stiffness fixators: ExFixOld, ExFixLow, Medium and High, and different materials in the defect gap: (A) No Defect; (B) LDPE; (C) Maple.

### 3.2.2.4 Statistical Analysis

For the stability bar and the material mechanical testing, comparisons of continuous variables between the groups were performed using analysis of variance (One Way-ANOVA). If the difference between the ExFixOld and other groups was significant, a posthoc test (Tukey) was performed. A post-hoc test was performed because of the limitation of the results from a One-Way ANOVA, this statistical test does not show how the means differ, and only shows that the means are not equal to each other. Therefore, to see how the means differ from each other post-hoc tests were used. A post-hoc test is conducted always after determining if there is a difference among the means being compared. To compare tested materials (rubber, LDPE, maple and oak) an unpaired t-test was performed, with differences considered significant at  $p < 0.05$ . For the axial compression test statistical analyses were performed using either analysis of variance (Two Way-ANOVA) or a two-tailed t-test to determine if there

was a significant correlation between the stiffnesses of the different fixators and the materials used.

A power analysis after the study was calculated to determine if we had sufficient numbers of samples per group to detect a significant difference. The power level for all the data was found to be from 0.9 to 1. Thus the number of samples per group used in these studies are enough to determine a 5% difference between the test groups. All tests were two-tailed, with differences considered significant at  $p < 0.05$ . Data are presented as mean  $\pm$  SE, unless otherwise noted.

### **3.3 RESULTS**

#### **3.3.1 Three Point Bending of Stability Bars**

Three point bending tests performed on the  $x$  axis or anterior lateral of stability bar revealed that ExFixOld, with the large aluminium bar, had six times higher stiffness than the ExFixHigh, the stiffest of newly designed fixators. The stiffness for the ExFixOld was 1487 N/mm and for the ExFixHigh was 254 N/mm and this was statistically significant,  $p < 0.0001$ . Statistically significant differences were seen between the stiffnesses of all fixators tested,  $p < 0.0001$  (Figure 3.6).

Three newly designed fixators were tested to determine actual stiffness and also to confirm that they indeed have 30% difference from each other, as intended. Mechanical testing showed that the stiffness for ExFixLow, Med and High was 114, 185 and 254 N/mm respectively and they were significantly different from each other,  $p < 0.001$ . Calculated percent differences showed that the ExFixHigh was 27% stiffer than the ExFixMed and this difference was significantly different,  $p < 0.0011$ . The difference between the ExFixMed and ExFixLow was 38% and this difference was also statistically significant,  $p < 0.0008$  (Figure 3.6).

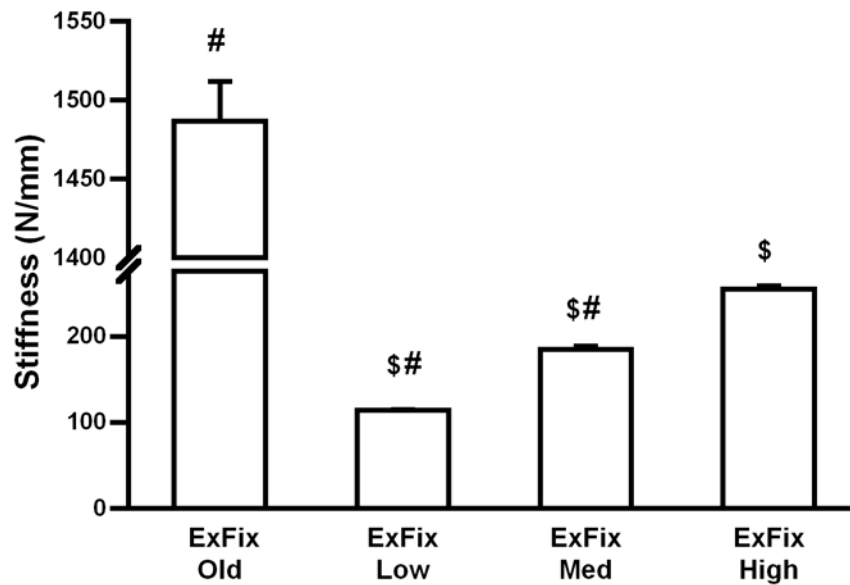


**Figure 3.6** Stability bar stiffness in 3-point-bending for four different stability bars: ExFixOld, ExFixLow, Med and High. Values given are means  $\pm$  SEM; Dollar signs indicate statistical significant difference from ExFixOld, and hash signs indicate significant difference from ExFixHigh ( $p < 0.05$ ,  $n=6$  per group).

### 3.3.2 Axial Compression Validation Testing

Axial compression testing was performed to confirm Young's modulus for rubber, LDPE, maple and oak as cited in the literature. Young's modulus is a measure of stiffness of an isotropic elastic material. It is defined as a ratio of the uniaxial stress over the uniaxial strain in the range of stress. These tests showed that Young's modulus for all four materials falls within the range reported in the literature (Table 3.2).

Materials	Young's modulus(GPa) (Wikipedia)	Young's modulus(GPa) Axial Compression Test Data
Rubber	0.01-0.1	0.074
LDPE	0.2	0.197
Maple	9-10	9.8
Oak	11	10.6

**Table 3.2** Young's modulus values for materials: rubber, LDPE, maple and oak reported in the literature and compared to the axial compression test performed in the laboratory.

Axial compression test revealed that there was no significant difference between maple and oak. Therefore, for further *in-vitro* testing maple was chosen due to its smaller inter - sample variability.

There was a statistically significant difference when rubber was compared to LDPE and both woods,  $p < 0.0001$ . The significant difference was also seen when LDPE was compared to all the materials tested,  $p < 0.0001$  (Figure 3.7).

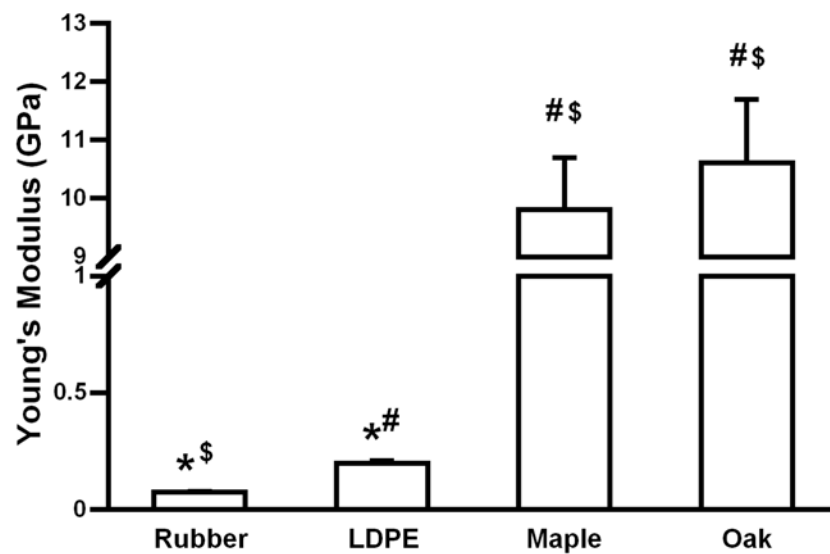


**Figure 3.7** Young's Moduli calculated from axial compression of four different materials: rubber, low-density polyethylene (LDPE), maple and oak. Values given are means  $\pm$  SEM; Dollar signs indicate statistical significant difference from LDPE, hash signs indicate significant difference from rubber and asterisks signs indicate significant difference from oak ( $p < 0.05$ ,  $n=6$  per group).

### 3.3.3 Axial Compression Testing

Axial compression mechanical testing was used to determine the local mechanical properties within the critical size defects imposed by the four different stiffness fixators. First, the influence of the fixators on the stiffness of intact rat femur was determined, then the three different materials validated in the previous section were each inserted in turn into defects in the rat femur.



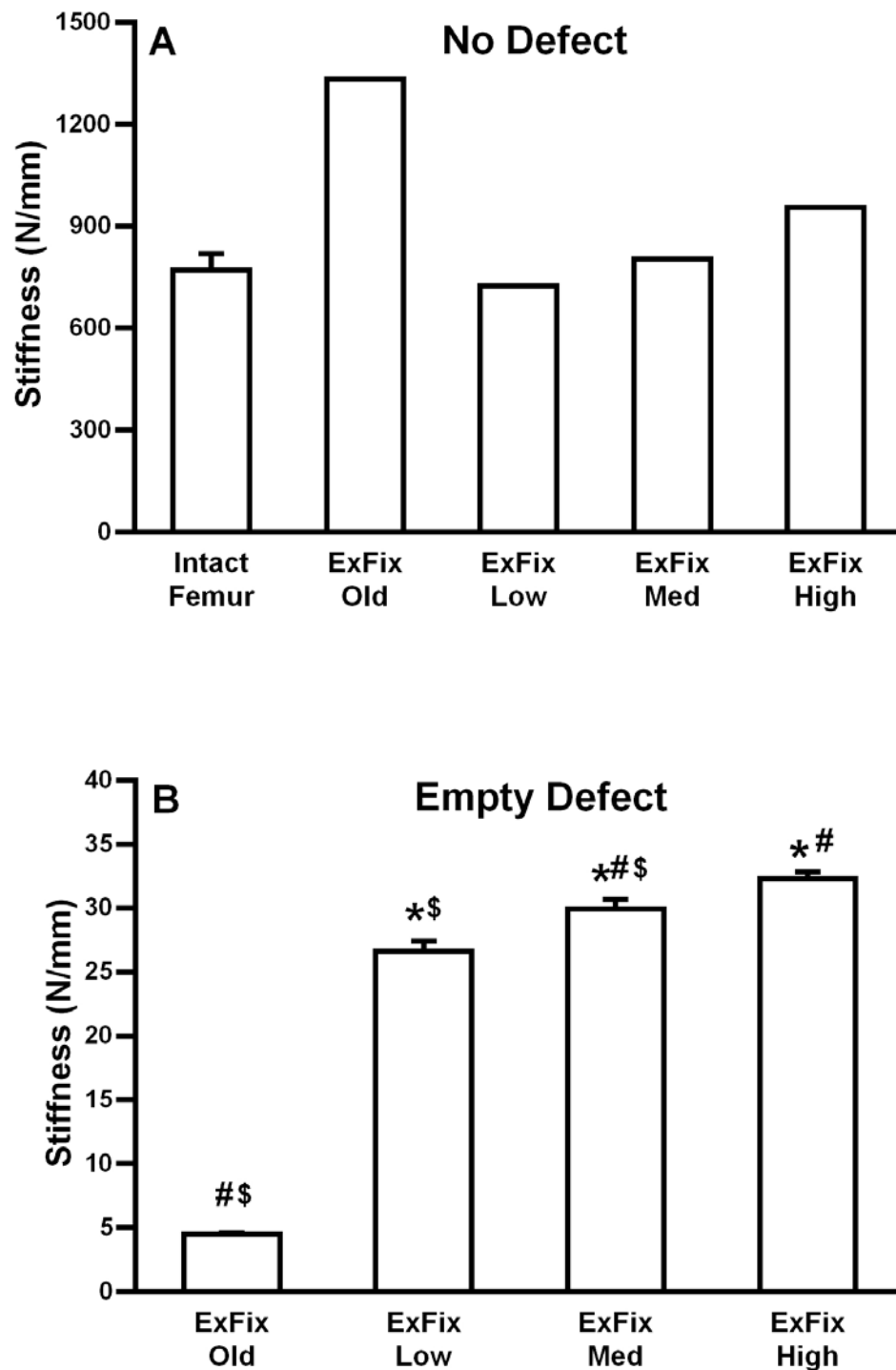
Using intact femur, axial compression testing revealed that the highest stiffness was achieved in the group with ExFixOld (Figure 3.8A). Indeed, placement of the fixator increased the stiffness of the intact femur by approximately 48%. The other external fixators, in contrast, had only minor effects on the stiffness of the intact femur: for example, with the ExFixLow the construct stiffness increased only by 5% as compared to the intact femur, for ExFixMed and High the stiffness increased by 15% and 20% respectively (Figure 3.8A). When ExFixOld construct was compared to the ExFixLow, Med, High external fixators, this difference was 45, 40 and 28% respectively.

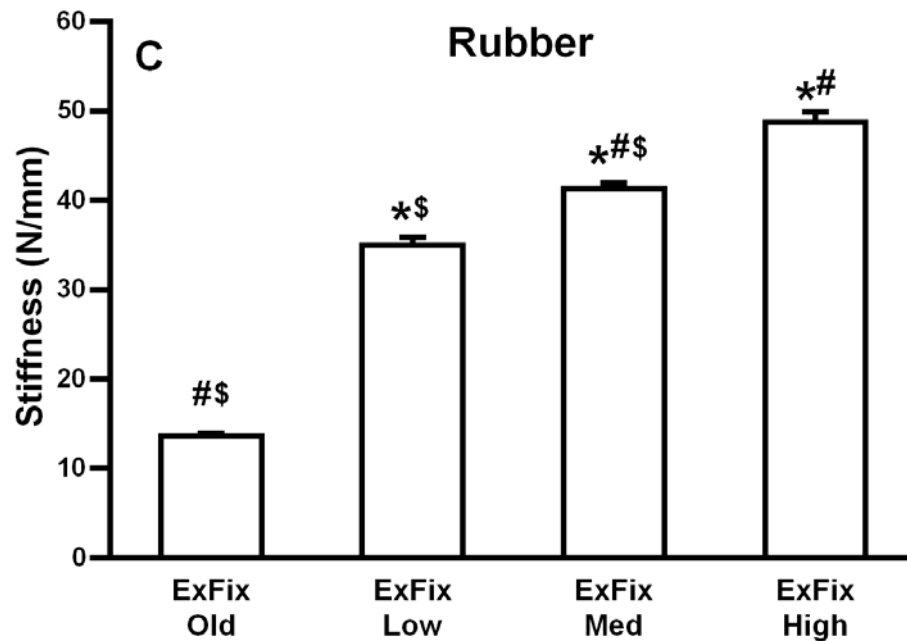
Having tested intact bone, 5mm defects were created in the femur and tested without any inserts to see stability of constructs (Figure 3.8B, Table 5.3). The constructs with empty defects with four different stiffness fixators were tested to determine construct stability without any material inserts. The results showed that the construct that had ExFixOld fixator had lowest stiffness when compared to ExFixLow, Medium and High and this was significantly different. There was also significant difference between Low, Medium and High external fixator. The results using a rubber insert to simulate early stages of healing showed that the construct with the ExFixOld had at least 3 fold *lower* stiffness as compared to all three of the new ExFixs and this was significantly different from all other external fixators,  $p < 0.0001$ . Significant differences were also seen when ExFixHigh was compared to ExFixLow and Med,  $p < 0.001$ . Furthermore, the ExFixLow construct was less stiff than ExFixMed and this was also significantly different,  $p < 0.0001$  (Figure 3.8C, Table 5.3).

In the third test low density polyethylene (LDPE) was used to simulate a later stage of fracture healing at which cartilage is being replaced by woven bone (Figure 3.10). The results revealed that significant differences were seen when the ExFixHigh construct was compared to the other three external fixators, ( $p < 0.001$ ). However, the difference was small compared to that seen at other simulated stages of healing; indeed the ExFixOld, ExFixLow and Med showed no difference when they were compared to each other (Figure 3.9D, Table 5.3).

Finally, to simulate the third stage of fracture healing, when woven bone is maturing into lamellar bone, maple was inserted into the defect for each construct (Figure 3.9E, Table 5.3 & 3.10). The highest construct stiffness was observed with the

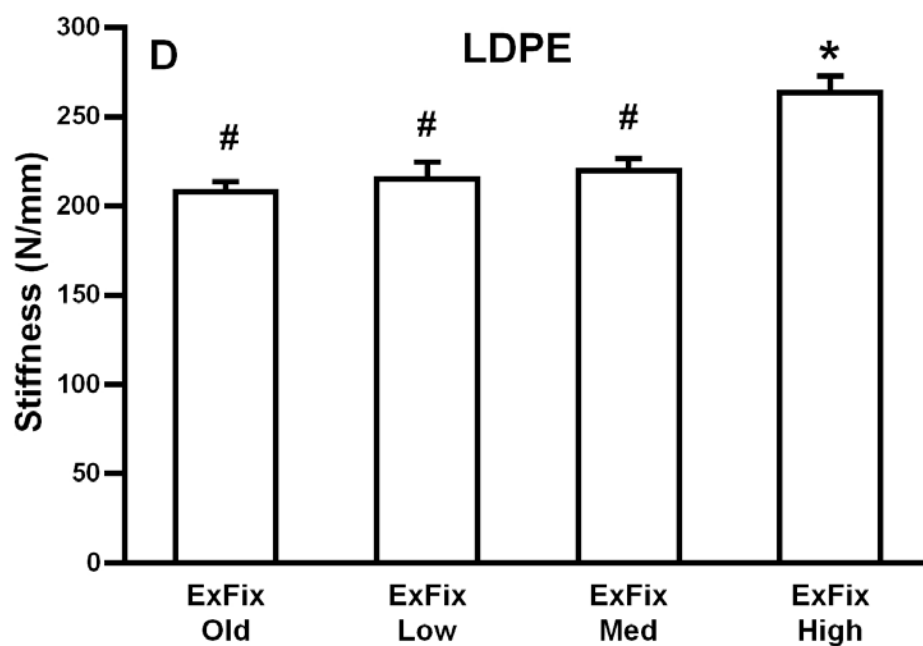
external fixator ExFixOld and this was significantly different from the other three external fixators, ( $p < 0.0001$ ). Interestingly, there was no difference between the ExFixLow, Med and High constructs when maple was used in the defect (Figure 3.9E, Table 5.3). Overall, Two Way Anova statistical test revealed that there is significant interaction between the materials and external fixators used ( $p < 0.0001$ ).





**Figure 3.8** Stiffnesses created by the different fixators applied to rat femur.

ExFixOld, and ExFixLow, Med, High were placed upon isolated rat femora. (A) Intact femora and (B) femora with 5mm empty defect without an insert were tested in an axial compression mode (C) femora with 5mm empty defects containing rubber were tested in an axial compression mode. Values given are means  $\pm$  SEM; Asterisks indicate statistical significance from ExFixOld, dollar signs indicate statistical significant difference from ExFixHigh, and hash signs indicate significant difference from ExFixLow ( $p < 0.05$ ,  $n=6$  per group).



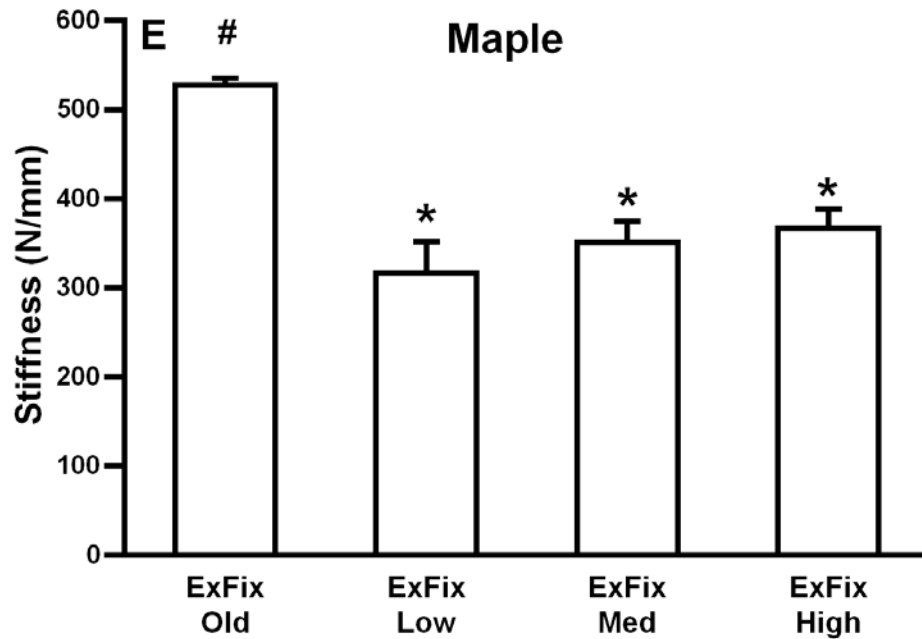


**Figure 3.9** Stiffnesses created by the different fixators applied to rat femur.

ExFixOld, and ExFixLow, Med, High were placed upon isolated rat femora. (D) Femora with 5mm defects containing low density polyethylene (LDPE) and (E) maple were tested in an axial compression mode. Values given are means  $\pm$  SEM; Asterisks indicate statistical significance from ExFixOld, dollar signs indicate statistical significant difference from ExFixHigh, and hash signs indicate significant difference from ExFixLow ( $p < 0.05$ ,  $n = 6$  per group).

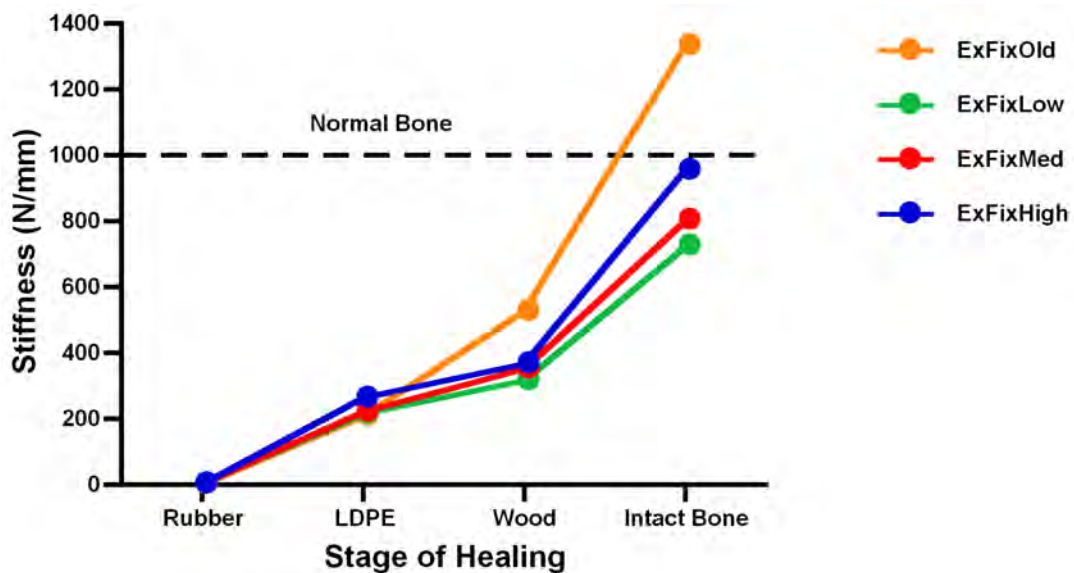


**Figure 3.10** Stiffnesses created by different fixators: ExFixOld, ExFixLow, Medium and High, with various inserts: rubber, LDPE, wood and intact bone in the CSD simulating stages of bone healing, tested in axial compression,  $n = 6$  per group.

### 3.4 DISCUSSION

These data confirm that the design of an external fixator has a major influence on the mechanical environment experienced by a healing segmental defect, as reflected in the stiffness of the system. Although the stiffness of the stability bar is an important determinant of this property, it is also influenced by the nature, diameter, position and quantity of the pins, preset offset from the bone surface to the stability bar and, to a surprising degree, by the mechanical properties of the material within the segmental defect.

Knowledge of the mechanical properties of the fixation device is very important because its stiffness determines mechanical environment of the healing bone and the healing pathway that it is going to undertake. Given this state of affairs, it is remarkable that there is little in the literature on the *in vitro* mechanical characterization of devices used for *in-vivo* animal studies.

Although the stability bar of the ExFixOld was approximately 3-fold higher than those of the new fixators, it provided only 30-40% of the stiffness of the new fixators when placed across a 5mm defect with a rubber insert to simulate an early stage of healing. This dramatic decline in stability is presumably due to the greater distance of the ExFixOld stability bar from the bone and the diameter of the pins. For our old generation fixator we used 1.2mm diameter stainless steel K-wires with the offset of 25mm from tip of the pin, with our new generation external fixators we used 1mm diameter titanium pins with the offset of 11mm. The importance of pin diameter and offset have previously been noted by Willie et al. [116], who found that the contribution to the total stiffness of the fixation device was dominated by the flexibility of pins in the relation to the offset, diameter and material properties. In agreement with this, a study by Mark et al. [77] also found that axial and torsional stiffness was significantly increased depending on the diameter and material of pins used. Titanium pins led to about 40% lower axial stiffness and 30% lower torsional stiffness than the stainless steel pins. Furthermore, this finding is also in the agreement with a study by Gardner et al. [117] where they observed that during initial stages of healing there is very little tissue solidity at the fracture site and it is then that the degree of support from the interposing fragments is very critical and

mainly depends on the fixation stability. This period might be prolonged or delayed in the case of poorly supported fractures. In this regard it is noteworthy to mention that all of the fixators, provided sufficient strength to a femur with a 5mm defect to allow testing to be performed, however the ExFixOld has the least amount of stability as compared to the other stiffness fixators. It is possible that under *in-vivo* conditions, the surrounding soft tissue provides sufficient stability to initiate a healing response.

When the simulated intra-lesional healing tissue progressed from haematoma-cartilage (rubber insert) to calcified cartilage-bone (low density polyethylene insert), the ExFixOld provided greater stability, approximately equal to that of the new more rigid fixators. Similar phenomenon was also observed in the study by Gardner et al. [117] where they found that the amount of axial movement was largely controlled by the material in the fracture gap rather than by the fixator stiffness. Which in part explains the findings in the current study, it appears that in the ExFixOld group stiffer material in the gap was able to take over and support most of the load and the low stiffness fixator device had minimum effect.

At the stage of immature-mature bone (wood insert), the ExFixOld provided much greater stiffness than any of the new fixators, equal to about 80% of the native femur. When placed on an intact femur, the ExFixOld approximately doubled the stiffness of the system, unlike the new fixators that had relatively little effect. This observation in the ExFixOld construct group could be related to the other loading conditions such as torsional or transverse shear. It seems that when the defect material is at the maximum stiffness and the fixation device is loose, the system is subjected to enhanced shear loads [117], which have been shown to be detrimental to bone healing. On the other hand, because the new generation external fixators are more rigid shear loads are very minimal and hardly contributes to the overall stiffness of the system; similar results were also observed by Gardner et al. [117].

The results from this study thus confirm that the fixators used in this project provide an experimental range of mechanical environments that can be used to investigate the role of this environment on healing. This is important because through observational and to the lesser extent empirical study, several theories have been

developed on the role of the certain mechanical stimuli governing differentiation of pluripotent mesenchymal tissue into fibrous tissue, fibrocartilage, cartilage and bone [38, 41, 65, 120, 121]. In nearly all fracture treatments require the use of the artificial support to stabilize bone fragments; therefore the major determining factor of mechanical environment at the fracture site and the subsequent pattern of healing is the fixation device stiffness. Testing the effects of mechanical environment on fracture healing requires measuring the distribution of mechanical stimulus in the fracture callus. This is a very complicated task, because at the tissue level mechanical stimuli are determined not only by the types of applied loads such as axial, transverse and bending to the healing bone, but also by the geometry, fracture gap and mechanical properties of the callus tissues. This is why many investigators tackle this by using computational models where they can control and use different mechanical parameters to simulate different stages of fracture repair. Mine is one of the few studies to make empirical measurements of these parameters.

In conclusion, it appears from this study that mechanical conditions experienced at the site of a segmental defect are highly sensitive to the material properties and design of fixators, and these are further modulated by the material properties of the tissues present in the gap. This suggests the potential for interesting and important mechanical and biological interactions between the fixator stiffness and the tissue type being formed. From these data, it appears that these interactions will vary considerably during healing, in accordance with our hypothesis that healing can be manipulated by altering the mechanical properties of the fixator after healing has begun.

In the next chapter I test this hypothesis more directly by investigating the effects of the mechanical environment upon healing critical size segmental femoral defects in response to rhBMP-2 in the in-vivo rat model using new generation external fixators with different stiffnesses.

## **CHAPTER FOUR**

*Investigation of the effect of the mechanical environment on the healing of an experimental, critical sized femoral defect in response to rhBMP-2.*



## 4.1 INTRODUCTION

The design, construction and thorough *in-vitro* mechanical characterization of the new, novel external fixators, were described in the previous two Chapters. These novel external fixators were tested in an *in-vivo* experimental femoral CSD rat model, where healing was initiated by rhBMP-2 treatment. The outcomes were compared with “first generation” ExFixOld fixator used in our laboratory for various previous *in-vivo* experimental studies, and for which we have considerable historical data.

BMP-2 protein was chosen to enhance healing process because of the wide use in animal experimental studies and several clinical trials where has been shown that BMP-2 and BMP-7 was able to repair segmental defects, non-unions and delayed unions. Furthermore, a study by Tsuji et al. [74] reported that BMP-2 is a necessary component of the signalling cascade for initiating fracture healing. They found that mice lacking to produce BMP-2 protein in the limb bone have spontaneous fractures that do not heal at any time point. In fact, the absence of BMP-2 in bone seems to block the earliest steps in fracture healing. Although, other osteogenic stimuli such as BMP-4 and 7 were still present in a limb of BMP-2 deficient mice, they could not compensate for the absence of BMP-2. In addition, this protein has been clinically approved for the treatment of acute tibial fractures in adults as an adjunct to standard care (see more details in Chapter One, section: Current Clinical Management of Large Segmental Defects).

As mentioned in the general introduction, in our laboratory, rat CSDs healed inconsistently and did not provide optimal healing in response to BMP-2, whether delivered as a protein or a gene (cDNA). As noted in the previous Chapter, ExFix Old stability bar is very stiff and in many rats, bone mineralization failed to occur on the cortical surface facing the fixator even as bone was accumulating on the opposite surface. Figure 4.1 shows that there is variability in the pattern of bone defect healing in the group treated with rhBMP-2 [60].

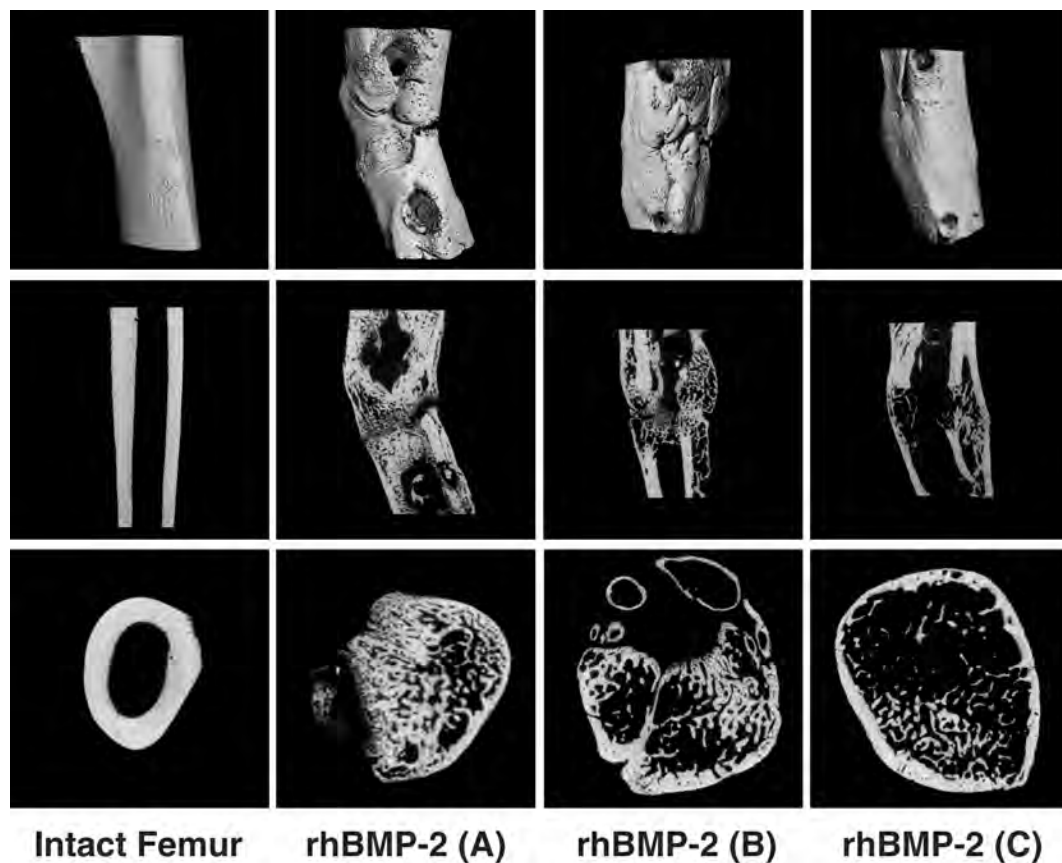


**Figure 4.1** Representative 3D (top row) and 2D (second row) longitudinal and transverse (third row)  $\mu$ CT images of femur after 8 weeks of treatment with rhBMP-2 with an external fixator (ExFixOld) and contralateral, intact femur.

While one of the images (Figure 4.1, rhBMP-2 C) show complete healing of the defect with defined cortical and trabecular bone after 8 weeks of treatment, the other two defects have incomplete healing, including the presence of soft tissue (Figure 4.1, rhBMP-2 A&B) and one of them developed pseudoarthrosis or so called “fake joint” (Figure 4.1, rhBMP-2 A). This variability is probably due to the increased IFM caused by insufficient stability provided by the old external fixator in the initial phase of bone repair. In chapter three I described the mechanical environment created by this external fixator *in-vitro* in axial compression, which is a simulation of weight bearing. Interestingly, while the old external fixator implanted on the rat femur *in-vitro* was very stable and rigid on the intact rat femur, as soon as the defect was created the construct became very unstable, probably due to the large 25mm offset from stability bar to the bone surface, which might have made defect site unstable. In addition, K-wires were used to stabilize CSD they are not very rigid and

this might have caused rotational instability. Molster et al [93] and other investigators [92, 122, 123] have shown that great rotational instability or shearing movements were detrimental to the process of fracture healing and prolonged the maturation of external callus.

Collectively, these observations led to the hypothesis that healing of a critical-sized segmental defect under the influence of rhBMP-2 is exquisitely sensitive to the local mechanical environment; as noted, this hypothesis forms the basis of the current project. Therefore, a primary goal for this part of the study is to understand better the role of the mechanical environment in the induced healing of critical-sized segmental bone defects in long bones with various stiffness external fixator *in-vivo*. To test this hypothesis I investigated bone healing using my newly developed external fixators, in conjunction with a 5 mm segmental bone defect in the rat femur. Healing was initiated with rhBMP-2 to determine the effects of different stiffnesses on healing and compared to the data from the ExFixOld fixator used in our laboratory.

## 4.2 MATERIALS AND METHODS

### 4.2.1 *In-Vivo Studies* - Study design

A 5 mm, critical sized mid-diaphyseal femoral defect was created in the right hind limb of each of 45 male Sprague-Dawley rats (weight 325-360 g) and stabilized by an external fixator [54] with one of the three stiffnesses described in Chapter 2. The rats were assigned to one of four groups.

Group one: Empty Control (n=3) ExFixHigh

Group two: Empty Control (n=3) ExFixMed

Group three: Empty Control (n=3) ExFixLow

Group four: rhBMP-2 (11  $\mu$ g) ExFixHigh (n=12)

Group five: rhBMP-2 (11  $\mu$ g) ExFixMed (n=12)

Group six: rhBMP-2 (11  $\mu$ g) ExFixLow (n=12)

The number of control animals in groups 1-3 was low because of extensive historical data confirming that these defects do not heal spontaneously [54, 62]. The numbers

of animals in the treatment groups were based upon historical data confirming sufficient statistical power [54]. The concentration of BMP-2 we used is based upon the data of Yasko et al. [61] and our previous experience in using rhBMP-2 in this model [60]. BMP-2 was delivered on absorbable collagen sponges that form part of the system, “Infuse” (Medtronic).

In all groups, treated femora were compared to the intact, contralateral femur. Healing was monitored by weekly radiologic evaluation. Eight weeks after surgery, final X-rays were taken and animals euthanized. The amount and quality of healed bone defects were evaluated by dual-energy X-ray absorptiometry (DXA), micro-computed tomography ( $\mu$ CT), histology and torsional mechanical testing. All specimens were subjected to the non-destructive analyses, DXA and  $\mu$ CT. Subsequently, 2-3 femora per group were randomly selected and fixed for histology in 4 % ice cold paraformaldehyde. The remaining specimens were wrapped in the gauze, soaked with 0.9% saline solution and frozen at -20°C for mechanical testing.

#### **4.2.2 Surgical Procedure**

Animal care and experimental protocols were followed in accordance with NIH guidelines and approved by the Beth Israel Deaconess Medical Center Institutional Animal Care and Use Committee. Following a minimum 48-hour acclimatization period, the animals were transported to a dedicated surgical procedure room. All the animal surgeries were performed as described in chapter two, section 2.3.2 page 48.

#### **4.2.3 Implants**

Recombinant, human BMP-2 was delivered on absorbable collagen sponges, Infuse, obtained from Medtronic (Minneapolis, MN, USA). These were cut under sterile conditions to a length of 1.0 cm to produce a dry implant volume of 0.33 ml. The rhBMP-2 at a dose of 11  $\mu$ g (Medtronic) was applied to the collagen sponge, in a total volume of 200  $\mu$ l PBS and allowed to soak into the sponge for at least 15

minutes, prior to implantation. Only PBS was delivered on absorbable collagen sponge in a total volume of 200  $\mu$ l for the empty control group.

#### **4.2.4 External Fixators**

Novel, external fixators of stiffnesses  $114\pm 1.14$  (ExFixLow),  $185\pm 6.14$  (ExFixMed) and  $254\pm 9.54$  N/mm (ExFixHigh), described in Chapter 2, were used for this set of experiments. Characteristics of the “first generation” external fixator, ExFixOld, are also described in chapter 2. More detailed *in-vitro* mechanical characterization of these external fixators is described in chapter three.

#### **4.2.5 Radiographic Evaluation**

Bone healing was evaluated by radiography once per week for 8 weeks using a digital dental X-ray unit (Heliodont DS, Sirona, Germany). While under general anesthesia, the rats were placed in a ventral position and the hind limb was laterally rotated so that the external fixator was not in the path of the X-ray source. While I didn't have a jig for standard positioning of hind limb for weekly X-rays, I was careful to take weekly X-rays in exact orientation as in the previous week. Each radiograph were examined by me in a “semi-blinded” way, which means that I did know the ID number for each animal, but didn't know in which experimental group they belonged and gave a score depending on the amount of bone that had formed. All femurs were evaluated for radiographic evidence of healing, using a graded scoring system (0, minimal to no evidence of new bone formation; 1, evidence of bone formation, complete healing questionable; 2, solid-appearing bone, complete healing) [54, 124]. The defect was considered united when the osseous continuity of the femur was restored across more than 25 per cent of the cross-sectional diameter of the defect, as determined radiographically. There are of course the limitations of not having an independent observer reading the radiographs. Since I was the one who took weekly X-rays I might have been biased in the scoring process.

#### **4.2.6 Dual-Energy X-Ray Absorptiometry (DXA)**

We assessed the bone mineral content (BMC g) of the defect region by dual-energy X-ray absorptiometry (PIXImus 2, GE-Lunar, Madison, WI). Specimens were placed on a lucite block during scanning to simulate soft tissue. The scans were acquired using small animal high-resolution mode. All excised femurs were evaluated after 8 weeks of treatment in the area corresponding to the region of the critical-sized segmental bone defect. The DXA machine is calibrated yearly by the manufacturer.

#### **4.2.7 Micro-Computed Tomography ( $\mu$ CT)**

All femurs were scanned using a desktop micro-tomographic imaging system ( $\mu$ CT40, Scanco Medical AG, Bassersdorf, Switzerland) equipped with a 10 mm focal spot microfocus X-ray tube. Femora were scanned using a 20 $\mu$ m isotropic voxel size, at 55keV energy, 200ms integration time, with approximately 720  $\mu$ CT slices per specimen. Evaluation was done only in the 4mm (200 slices) central defect region to ensure that no pre-existing cortical bone was included in the analyses (Figure 4.2). This was standardized by excluding 10 slices from proximal and distal sides at the cortical edge of created defects. To evaluate the region of interest we assessed the following variables: total cross-sectional area or the callus size of the defect (TA, mm<sup>2</sup>), bone area (BA, mm<sup>2</sup>) and bone area over total area (BA/TA, mm<sup>2</sup>). Polar moment of inertia (pMOI, mm<sup>4</sup>) was also calculated from  $\mu$ CT images. Images were thresholded using an adaptive-iterative algorithm and morphometric variables were computed from the binarized images using direct, 3D techniques that do not rely on any prior assumptions about the underlying structure [125-127].

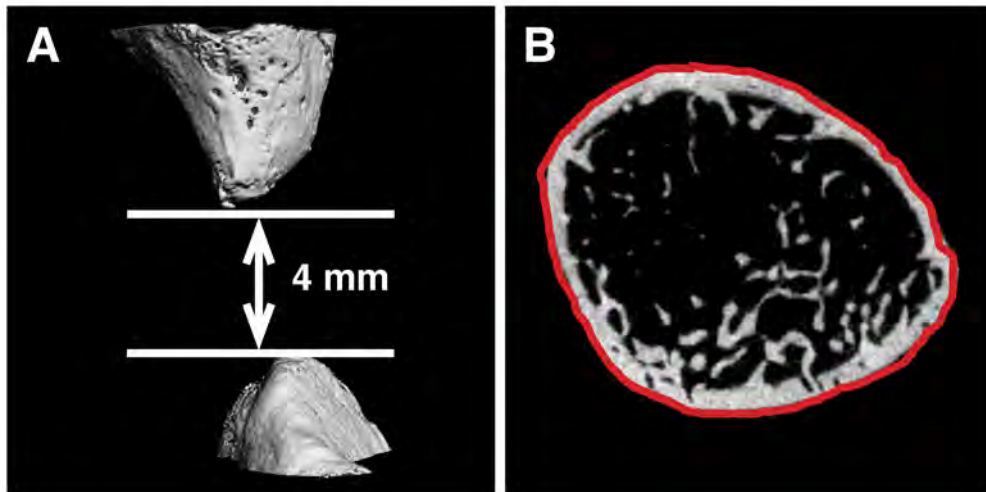


**Figure 4.2** Micro-computed tomography images showing evaluation of central defect after 8 weeks of treatment: (A) longitudinal 3D view of sample of non-healed defect from the Empty Defect group shows region of interest analyzed between the two white lines; (B) Red line represents contour around external callus from 2D transverse section, in the middle of the healed defect from one of the sample treated with rhBMP-2. All the data presented were calculated within the red line.

#### 4.2.8 Histology

After evaluation by  $\mu$ CT and DXA the specimens were decalcified 6-8 hr in RDO Rapid decalcifier (Apex Engineering, Aurora, IL), testing with a needle as the decalcification proceeded.

Fixed and decalcified tissues were dehydrated in graded ethanols up to 100%, transferred to xylene, and embedded in paraffin. Five-micron paraffin sections were placed on poly L-lysine coated slides, dried overnight and evaluated immediately or stored at 4°C. Sections were stained with hematoxylin-eosin to determine general morphology and safranin orange-fast green to detect cartilage. Safranin O is a nuclear stain, which produces red nuclei and used as a counter stain.

#### **4.2.9 *Ex-Vivo* Torsion Testing**

After all noninvasive imaging was completed, 7-8 specimens per group were tested to failure in torsion to determine the mechanical properties of the healed defect in shear. Before the test both ends of each specimen were embedded in polymethylmethacrylate (PMMA) to provide a reproducible gripping interface with the testing fixture. All femora were tested to failure under regular deformation control and at the constant deformation rate of 5 rad/min. Angular deformation and applied load data were acquired at 10Hz. The torque and rotation data were used to calculate the torsional stiffness and strength of the healed defect.

Before the actual bone testing was executed, a validation test was performed to make sure that the mechanical test system was calibrated. Plexiglas rods were used for the calibration. This material was chosen because it has similar behavior to bone tissue and therefore is suitable for this purpose. The material properties for this material was obtained from the supplier (McMaster-Carr, NJ, USA). The Plexiglas rods used for the validation test were embedded using the same procedure as the bone specimens. The same test parameters were used for the torsion test. The strain rate was chosen at 5 rad/min, which resulted in the material workstation crosshead speed of 75mm/min. The results from the test were very close to the values that were provided by the manufacture. Therefore, it was determined that the system is functional and accurate for bone testing.

#### **4.2.10 Statistical Analysis**

Comparisons of continuous variables between two treatment groups were performed using a two-tailed t-test, and between three groups by analysis of variance (One Way-ANOVA). If the difference between the contralateral femur and the treatment groups was significant, a posthoc test (Tukey) was performed. A power analysis after the study was calculated to determine if we had sufficient animals per group for significant difference. The power level for all the data was found to be from 0.8 to 1. Thus the numbers of animals per group used in these studies is enough to determine



a 5% difference between the test groups. All tests were two-tailed, with differences considered significant at  $p < 0.05$ . Data are presented as mean $\pm$ SE, unless otherwise noted.

## **4.3 RESULTS**

### **4.3.1 Radiographic Evaluation**

Weekly X-rays revealed that bone callus size was biggest in the group with the lowest stiffness fixator. Furthermore, early mineralization of the callus was seen in this group and in the medium stiffness group after 9 days of treatment. However, the group with the highest stiffness external fixator had no callus formation at this time; indeed callus formation was delayed until after two weeks of treatment. By the third week defects were bridged regardless of the fixation methods, with the biggest callus being in the groups with low and medium stiffness fixators and the smallest callus in the group with the highest stiffness (Figure 4.3A&B). No bone formation was seen by X-ray at any time point in any of the animals lacking rhBMP-2.

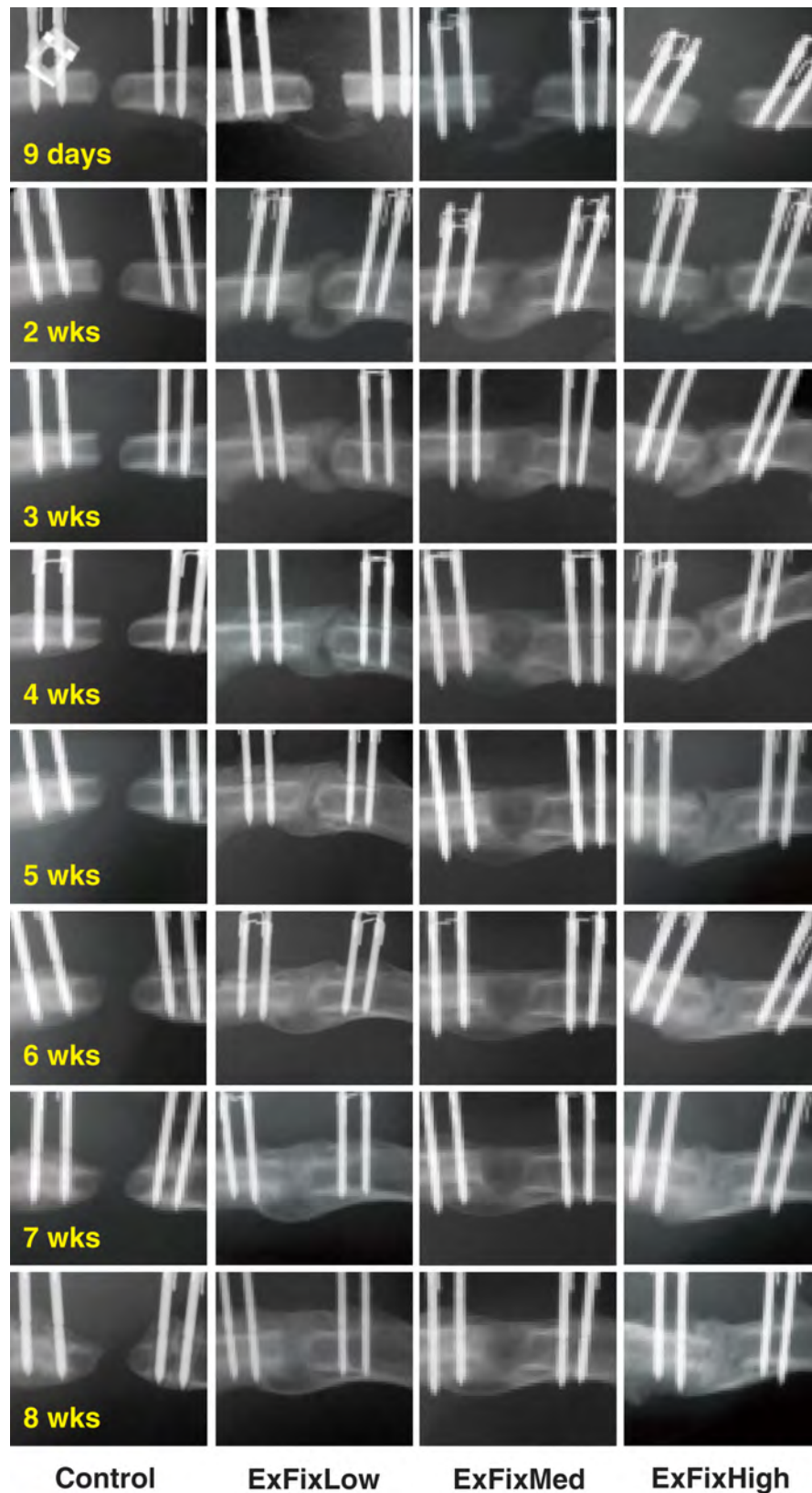


**Figure 4.3A** First set of representative radiographic images with low, medium and high stiffness external fixators after 9 days, and 2, 3, 4, 5, 6, 7 and 8 weeks of treatment with rhBMP-2. Defects without rhBMP-2 (Control Group with ExFix40%) did not heal no matter what stiffness fixator was used.

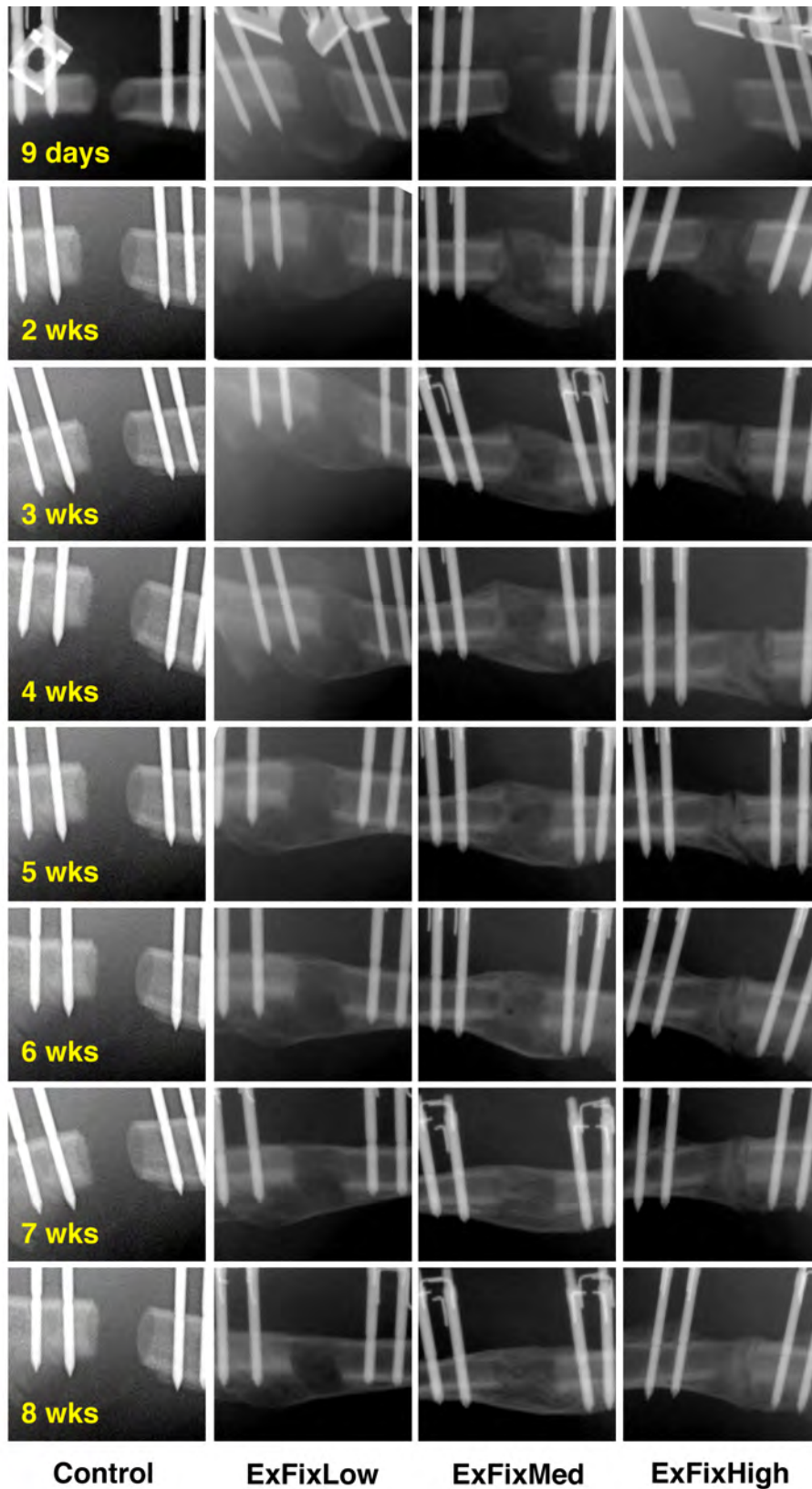


**Figure 4.3B** Second set of representative radiographic images with low, medium and high stiffness external fixators after 9 days, and 2, 3, 4, 5, 6, 7 and 8 weeks of treatment with rhBMP-2. Defects without rhBMP-2 (Control Group with ExFix40%) did not heal no matter what stiffness fixator was used.

### 4.3.2 Dual-Energy X-Ray Absorptiometry (DXA)

After 8 weeks of treatment bone mineral content (BMC, g) was highest with ExFixLow as compared with all the other groups, exceeding that of the contralateral femur. This was statistically significant when compared to the contralateral femur and ExFixOld, but there was no statistically significant difference between ExFixLow and ExFixMed and ExFixHigh, although there was a trend downward with the two higher stiffness fixators. Also, there was no difference between intact contralateral femur and ExFixOld. (Figure 4.4 and table 4.1 and 5.3).

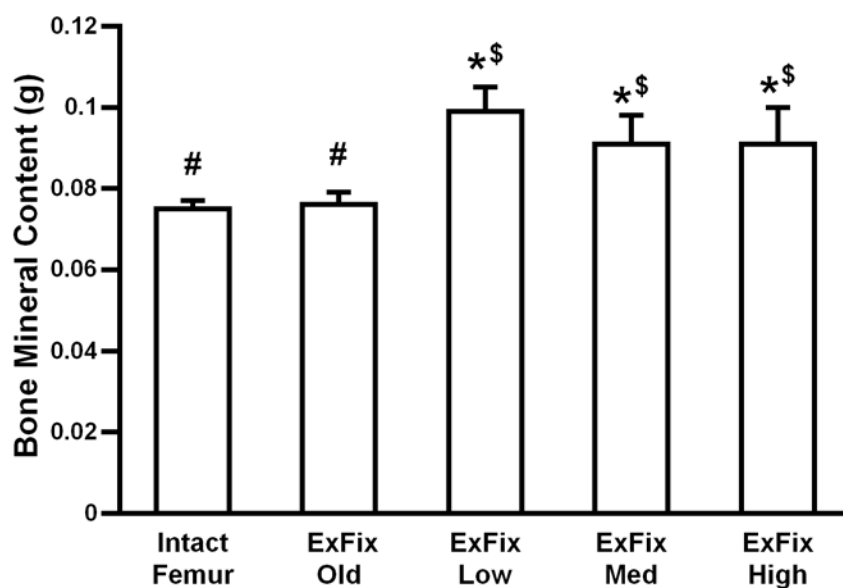


**Figure 4.4** Bone mineral content (BMC, g) in the segmental defect region after 8 weeks of treatment with rhBMP-2 as measured by DXA. Values given are means  $\pm$  SEM; Asterisks indicate statistically significant from intact, contralateral femur, dollar signs indicate statistical significant difference from ExFixOld, and pound signs indicate significant difference from ExFixHigh ( $p < 0.05$ ,  $n=9-10$  per group).

Variables	Intact Femur (n=10)	ExFixOld (n=10)	ExFixLow (n=10)	ExFixMed (n=9)	ExFixHigh (n=9)
BMC (g)	0.075 $\pm$ 0.01 <sup>#</sup>	0.076 $\pm$ 0.01 <sup>#</sup>	0.099 $\pm$ 0.02 <sup>*\$</sup>	0.091 $\pm$ 0.02 <sup>*\$</sup>	0.091 $\pm$ 0.03 <sup>*\$</sup>

**Table 4.1** Bone mineral content segmental healing characteristic of intact femur, ExFixOld, ExFixLow, ExFixMed and ExFixHigh treated with rhBMP-2 as measured by MicroCT (mean  $\pm$  SD). Asterisks indicate statistical significance from intact, contralateral femur,

dollar signs indicate statistical significant difference from ExFixOld, and pound signs indicate significant difference from ExFixHigh ( $p < 0.05$ ,  $n=9-10$  per group).

### 4.3.3 Micro-Computed Tomography ( $\mu$ CT)

Quantitative analysis of the  $\mu$ CT data confirmed the radiographic images. The total cross-sectional area (TA,  $\text{mm}^2$ ) or callus size in the ExFixOld group was three times bigger than the intact contralateral femurs, ( $p < 0.0001$ ) (Figure. 4.5, Table 4.2 and 5.3). The intact contralateral femur was also significantly lower in cross-sectional area when compared to ExFixLow, ExFixMed and ExFixHigh; this difference was 57, 48 and 41% respectively, ( $p < 0.0001$ ). Furthermore, there was a gradual decrease in cross sectional area from the ExFixOld group when compared to the other ExFix groups, and this difference was statistically significant, ( $p < 0.0001$ ) as shown in the figure 4.5. Defects in groups lacking rhBMP-2 had no callus formation and were significantly different from the other groups and the contralateral femur, ( $p < 0.0001$ ), (data not shown).

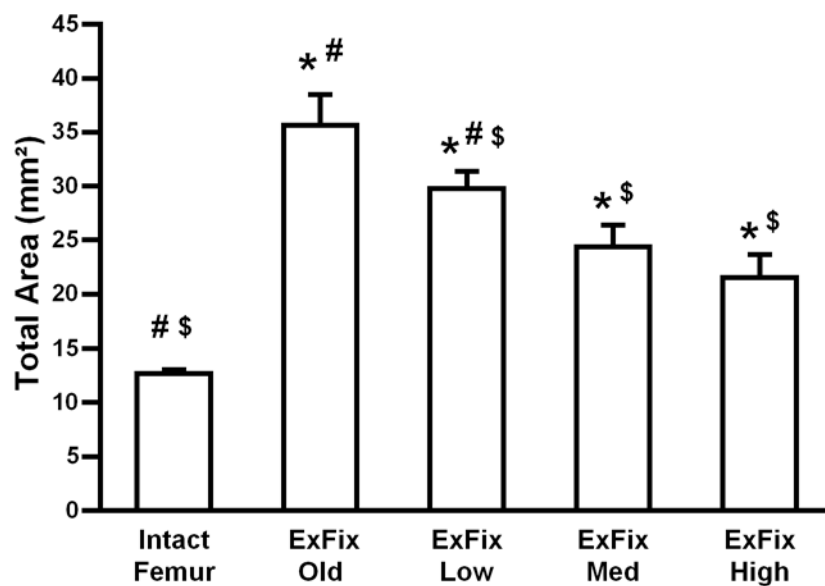


**Figure 4.5** MicroCT was used to measure Total Area/callus ( $\text{mm}^2$ ) with four different stiffness fixators (mean  $\pm$  SEM). Asterisks indicate statistical significance from intact, contralateral femur, dollar signs indicate statistical significant difference from ExFixOld, and pound signs indicate significant difference from ExFixHigh ( $p < 0.05$ ,  $n=9-10$  per group).

Bone area (BA, mm<sup>2</sup>) in the defect region in all the groups was at least 30% higher than in the intact contralateral femurs, ( $p < 0.003$ ). The smallest amount of bone was seen in the ExFixOld group; however, a statistically significant difference was only seen when compared with ExFixLow fixator ( $p < 0.004$ , Figure 4.6, Table 4.2 and 5.3). Interestingly, the same group had the highest amount of bone and this difference was at least 12%.

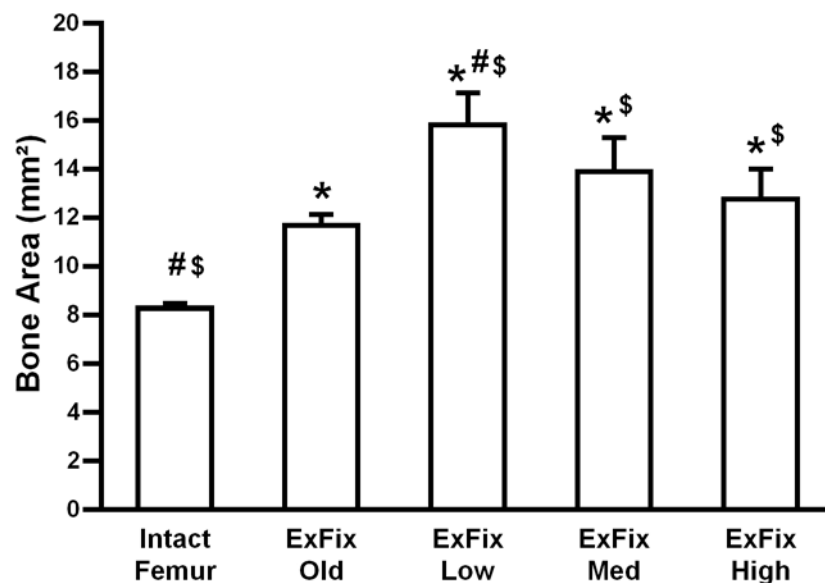


**Figure 4.6** MicroCT was used to measure Bone Area (mm<sup>2</sup>) following healing in the presence of rhBMP-2 under the influence of fixators with four different stiffnesses (mean  $\pm$  SEM). Asterisks indicate statistical significance from intact, contralateral femur, dollar signs indicate statistical significant difference from ExFixOld, and pound signs indicate significant difference from ExFixHigh ( $p < 0.05$ ,  $n=9-10$  per group).

Bone area/Total Area (BA/TA, %) the so called bone area fraction, which reflects callus size in the defect region was lower in all different stiffness external fixator groups compared to the intact contralateral femurs, ( $p < 0.008$ ). The lowest BA/TA was seen in the ExFixOld group and it was significantly different from all other groups ( $p < 0.006$ , Figure 4.7, Table 4.2 and 5.3). Interestingly, the ExFixMed and ExFixHigh groups had almost the same amount of bone as intact contralateral femur.

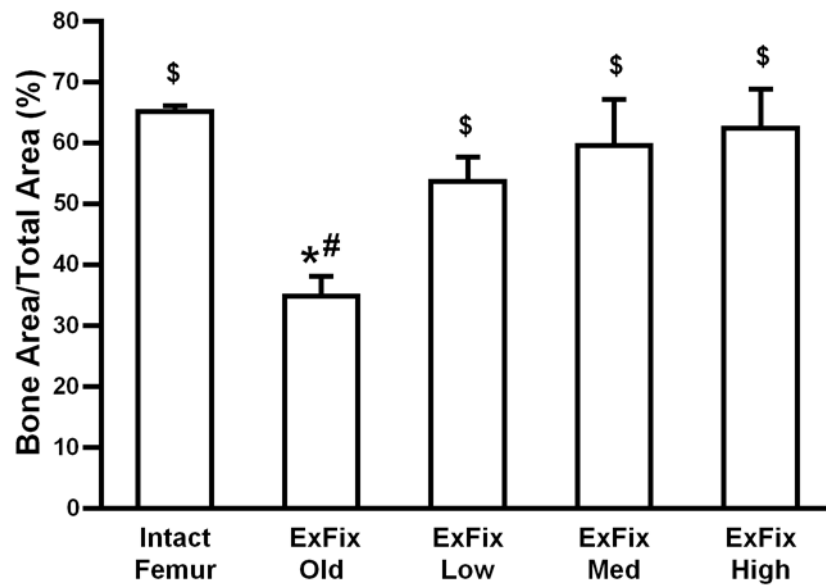


**Figure 4.7** MicroCT was used to measure Bone Area/Total Area (%) with four different stiffness fixators across defects treated with treated with rhBMP-2 (mean  $\pm$  SEM). Asterisks indicate statistically significant differences from intact, contralateral femur. Dollar signs indicate statistical significant difference from ExFixOld, and hash signs indicate significant difference from ExFixHigh ( $p < 0.05$ ,  $n=9-10$  per group).

The polar moment of inertia (pMOI,  $\text{mm}^4$ ) is a quantity used to predict an object's ability to resist torsion. The larger the pMOI, the less the beam will twist, when subjected to a given torque. The polar moment of inertia (pMOI,  $\text{mm}^4$ ) was at least twice as big in all the groups when compared to the intact contralateral femurs, ( $p < 0.0001$ ) (Figure. 4.8, Table 4.2 and 5.3). The ExFixOld created the biggest pMOI when compared with other external fixators, with a gradual downward decrease as the stiffness of the fixator increased. The pMOI was not statistically different from the ExFixOld compared to ExFixLow, but it was statistically significant from ExFixMed and ExFixHigh. The ExFixMed and ExFixHigh were not statistically different from each other.

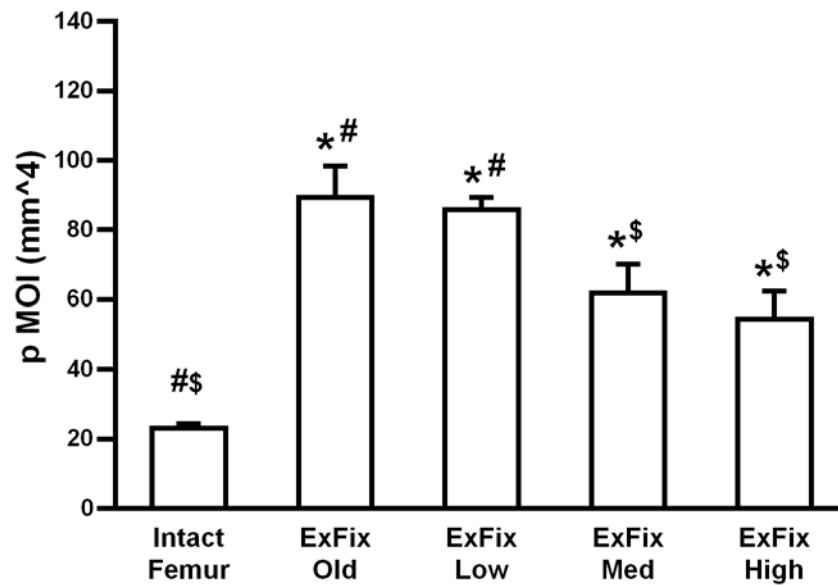


**Figure 4.8** MicroCT was used to measure polar moment of inertia (pMOI, mm<sup>4</sup>) with four different stiffness fixators treated with rhBMP-2 (mean ± SEM). Asterisks indicate statistical significance from intact, contralateral femur, dollar signs indicate statistical significant difference from ExFixOld, and hash signs indicate significant difference from ExFixHigh ( $p < 0.05$ ,  $n=9-10$  per group).

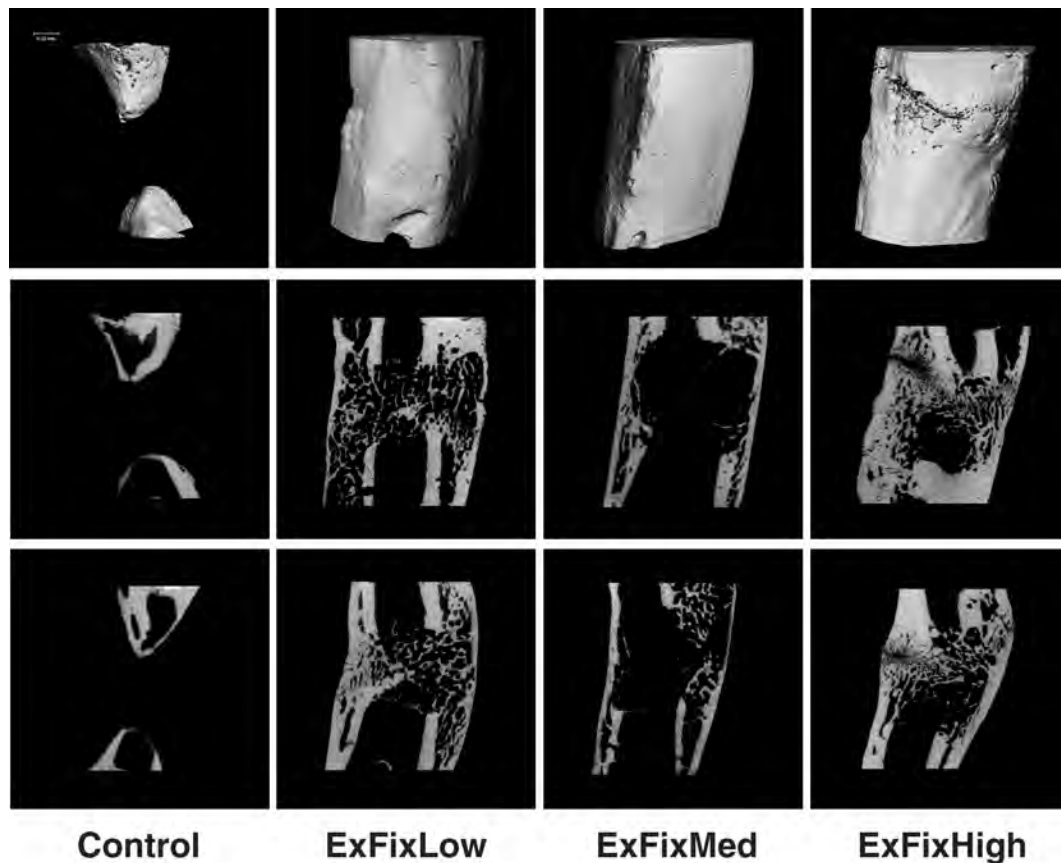
The results of the physical testing are collated in Table 4.2

<i>Variables</i>	Intact Femur (n=10)	ExFixOld (n=10)	ExFixLow (n=10)	ExFixMed (n=9)	ExFixHigh (n=9)
TA (mm <sup>2</sup> )	12.7±0.3 <sup>#</sup> \$	35.6±2.8 <sup>*#</sup>	29.8±1.5 <sup>*#</sup> \$	24.4±2.0 <sup>*\$</sup>	21.5±2.1 <sup>*\$</sup>
BA (mm <sup>2</sup> )	8.3±0.2 <sup>#</sup> \$	11.7±0.5 <sup>*</sup>	15.8 ± 1.3 <sup>*#</sup> \$	13.8 ± 1.4 <sup>*\$</sup>	12.8 ± 1.2 <sup>*\$</sup>
BA/TA (%)	65.1±0.9 <sup>\$</sup>	34.8±3.2 <sup>*#</sup>	53.6±4.1 <sup>\$</sup>	59.6±7.6 <sup>\$</sup>	62.4±6.4 <sup>\$</sup>
pMOI (mm <sup>4</sup> )	23.1±1.2 <sup>#</sup> \$	89.2±9.0 <sup>*#</sup>	85.9±3.5 <sup>*#</sup>	61.8±8.2 <sup>*\$</sup>	54.4±8.1 <sup>*\$</sup>

**Table 4.2** Segmental healing characteristics of Intact femur, ExFixOld, ExFixLow, ExFixMed and ExFixHigh treated with rhBMP-2 as measured by MicroCT (mean ± SEM). Asterisks indicate statistical significance from intact, contralateral femur, dollar signs indicate statistical significant difference from ExFixOld, and hash signs indicate significant difference from ExFixHigh ( $p < 0.05$ ,  $n=9-10$  per group).



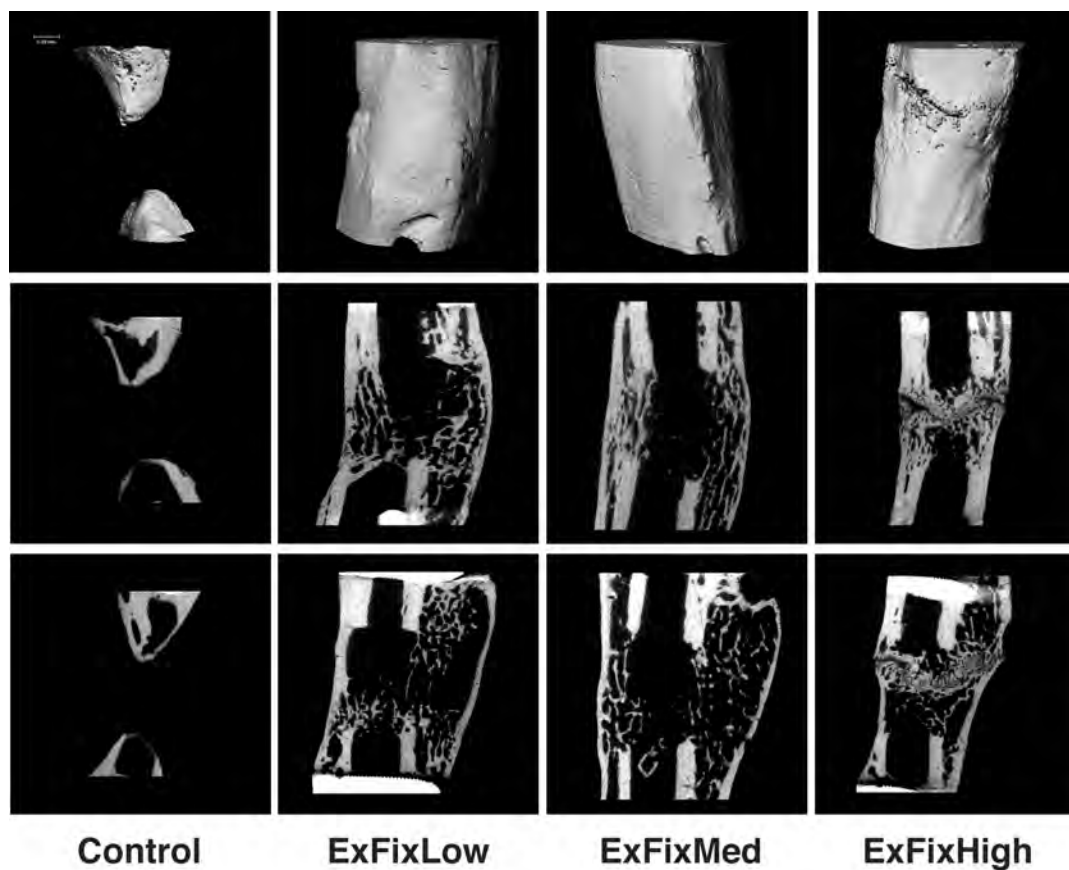
The bone architecture of three different stiffness fixator groups differed from that of the intact, contralateral femur, at 8-weeks treated with rhBMP-2. Figure 4.9A&B shows representative longitudinal images from the  $\mu$ CT analysis. These confirm healing of the defects in the presence, but not the absence, of rhBMP-2 no matter what stiffness fixator was used. There was no evidence of healing in the untreated defects.



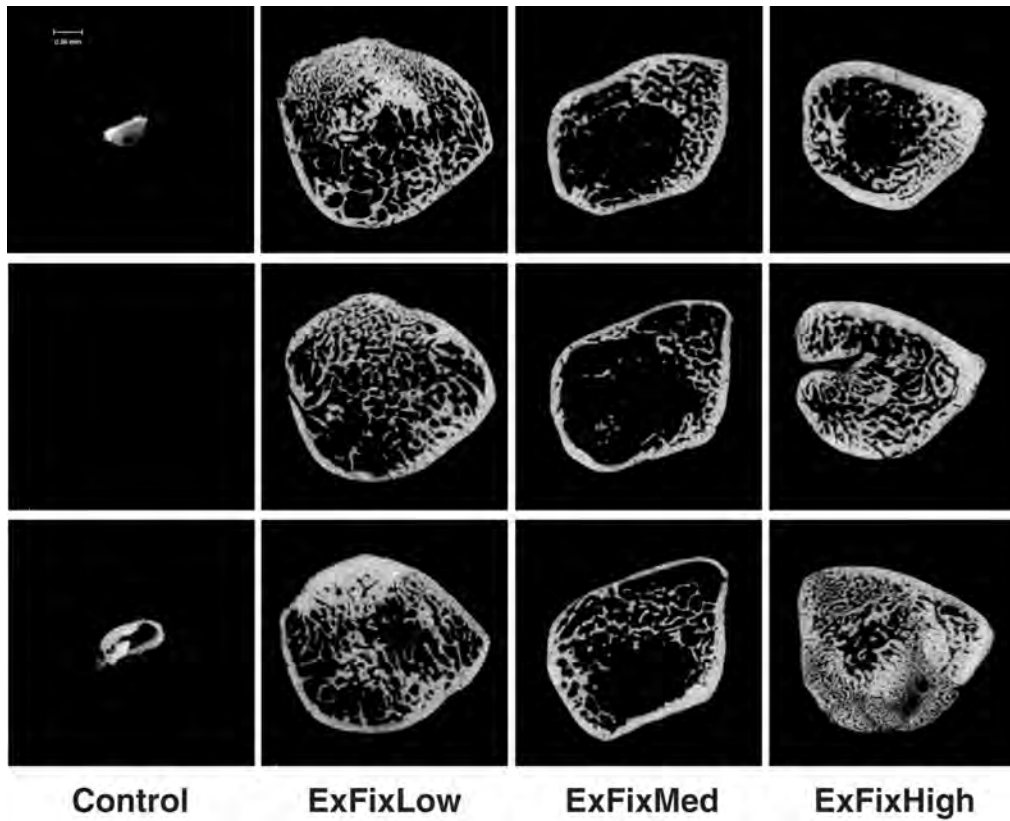
**Figure 4.9A** First set of representative (each sample was selected as an overall mean from each group) 3D (top row) and 2D (second and third rows) longitudinal  $\mu$ CT images of femora after 8 weeks of treatment with rhBMP-2 and three different stiffness fixators.

Figure 4.10A&B shows representative transverse images that confirm the presence of an intact cortex in the healed bones, and the presence of trabecular bone within the marrow of bones when treated with rhBMP-2 despite the type of external fixator used. It also shows a different pattern of bone healing in the defect region produced by the three different stiffness fixators. Interestingly, the thickest cortex and the

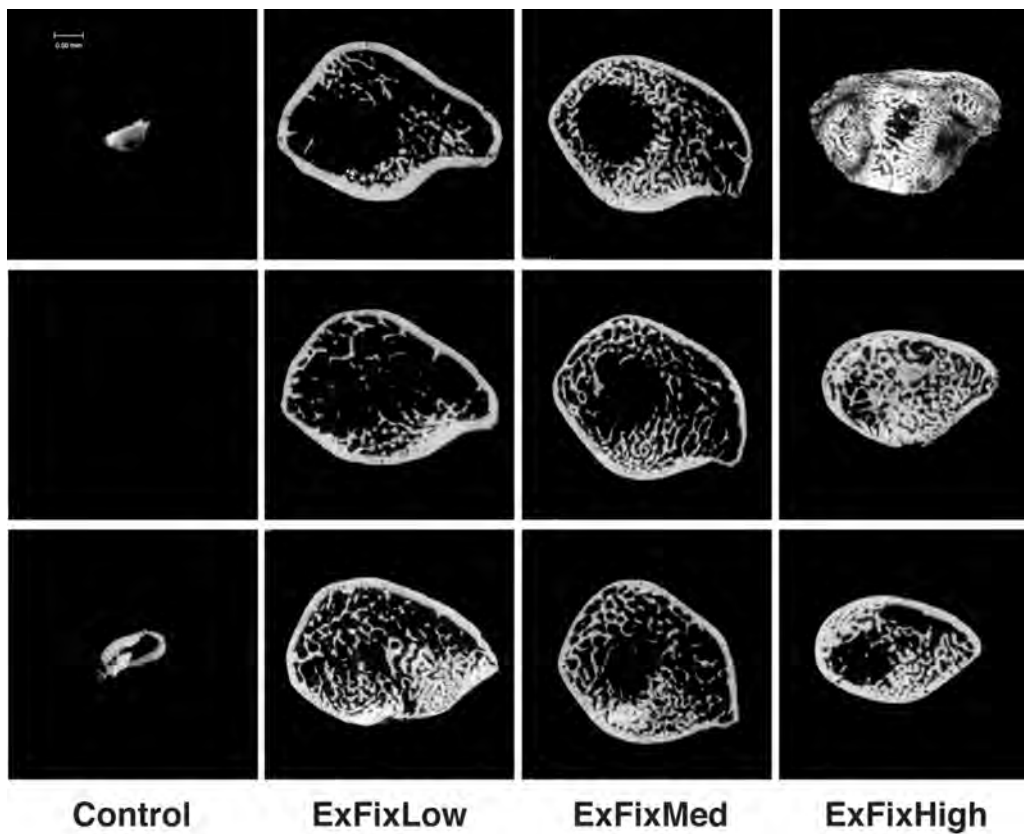
biggest amount of trabecular bone formed was observed with the most rigid external fixator (ExFixHigh), yet this group had the smallest callus size. As mentioned earlier the biggest callus was formed with the most flexible external fixator (ExFixLow), but this group had the thinnest cortex, but not the smallest amount of bone. The middle stiffness fixator group had the least amount of trabecular bone, but the thickness of cortical bone formed was intermediate.



**Figure 4.9B** Second set of representative (each sample was selected as an overall mean from each group) 3D (top row) and 2D (second and third rows) longitudinal  $\mu$ CT images of femora after 8 weeks of treatment with rhBMP-2 and three different stiffness fixators.



**Figure 4.10A** First set of representative transverse 2D  $\mu$ CT images of femur after 8 weeks of treatment with rhBMP-2 and three different stiffness fixators: top row-distal part of the defect; middle row-middle of the defect; bottom row-proximal part of the defect.



---

**Figure 4.10B** Second set of representative transverse 2D  $\mu$ CT images of femur after 8 weeks of treatment with rhBMP-2 and three different stiffness fixators: top row-distal part of the defect; middle row-middle of the defect; bottom row-proximal part of the defect.

#### 4.3.4 Histology

The histological findings (Figure.4.10) were consistent with the imaging data. There was no evidence of bone formation in the groups without rhBMP-2 and a complete transverse separation of the diaphysis in the defect region no matter which stiffness fixator was used. Moreover, the defect region was filled with layer of fibrous connective tissue continuous with the periosteum lining the cortices on the outer surface adjacent to the defect (images not shown).

There was periosteal and medullary bone formation in the defect region in the groups treated with rhBMP-2 regardless of the fixator stiffness. In these groups the entire defect was filled with well-differentiated islands of bone. Furthermore, there were mild to moderate zones of woven bone along the cortices proximal and distal to the segmental defect region, but with no obvious differences qualitatively between the treatment groups. The defects treated with ExFixLow had the biggest callus as compared to the ExFixMed and ExFixHigh, which supports the imaging data. Interestingly, ExFixMed and ExFixHigh groups had persistence of cartilage as shown by safranin orange staining, which could not be seen in the x-ray and  $\mu$ CT images. The group with the ExFixLow had no residual cartilage (Figure 4.11, bottom row).

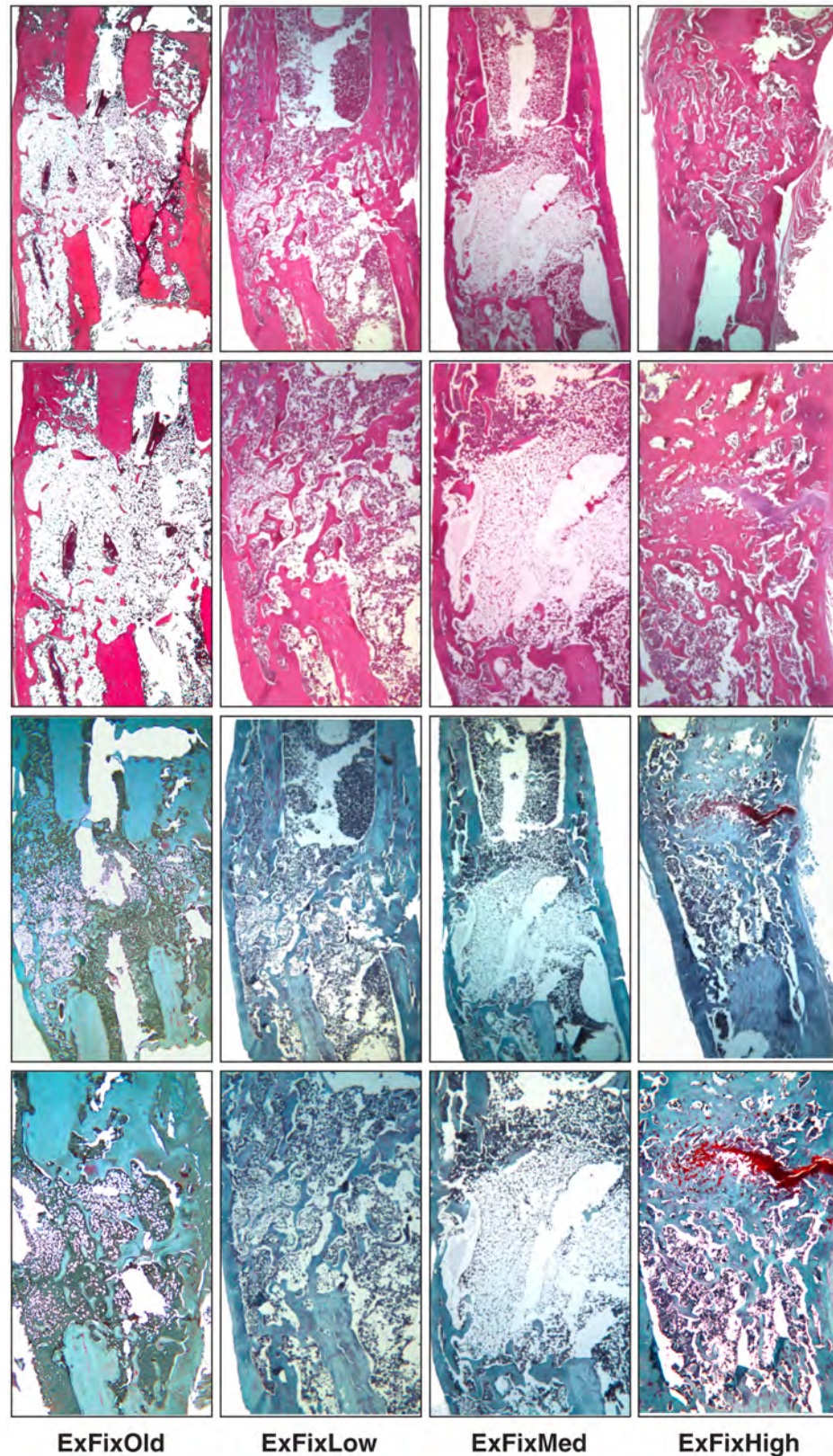


**Figure 4.11** Representative longitudinal histological sections of femoral segmental defects after 8 weeks of treatment with rhBMP-2 with three different stiffness fixators. Paraffin embedded sections were stained with Hematoxylin & Eosin (rows one and two) and Safranin Orange-Fast Green (rows three and four). Magnification for rows one and three is 16x, and rows two and four 25x).

### 4.3.5 Ex-Vivo Torsion Testing

Torsional testing was used to determine the mechanical properties of critical sized segmental defects treated with rhBMP-2 using four various stiffness external fixators: ExFixOld, ExFixLow, ExFixMed and ExFixHigh groups and compared to those of the intact contralateral femur. Torsional stiffness measurements revealed that ExFixLow produced a statistically significant increase in stiffness compared to intact contralateral femur, ExFixOld and ExFixHigh, this increase was 29%, 24%, 24%, respectively  $p < 0.047$  (Figure 4.12 and Table 5.3). The difference between the stiffnesses generated by ExFixLow and ExFixMed was not statistically significant  $p < 0.07$ .

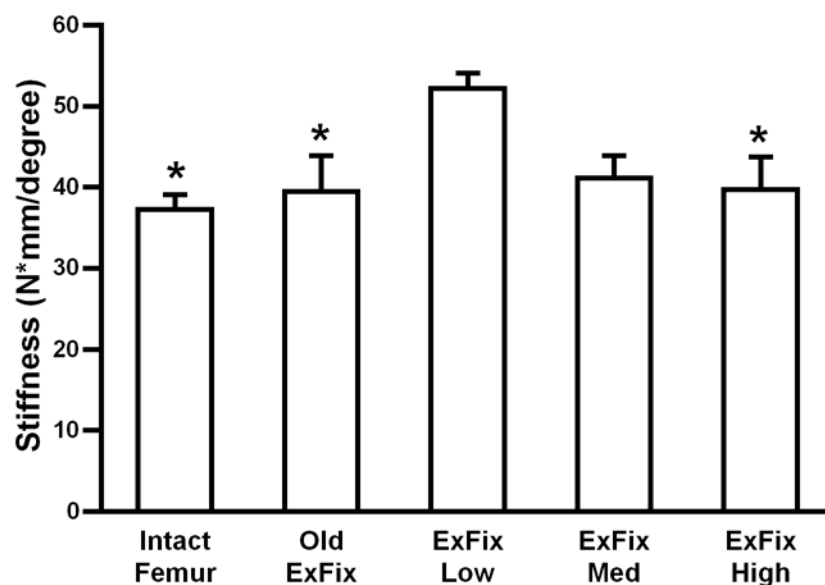


**Figure 4.12** Torsional stiffness of femurs treated with rhBMP-2 with four different stiffness fixators treated with rhBMP-2 after 8 weeks (mean  $\pm$  SEM). Asterisks indicate statistical significance from ExFixLow ( $p < 0.05$ ,  $n=7-8$  per group).

Interestingly, the maximum torque was not different between the groups. However, there was a trend reflecting the torsional stiffness data, where defects healed in the presence of ExFixLow needed the most force to fail (Figure 4.13 and Table 5.3).

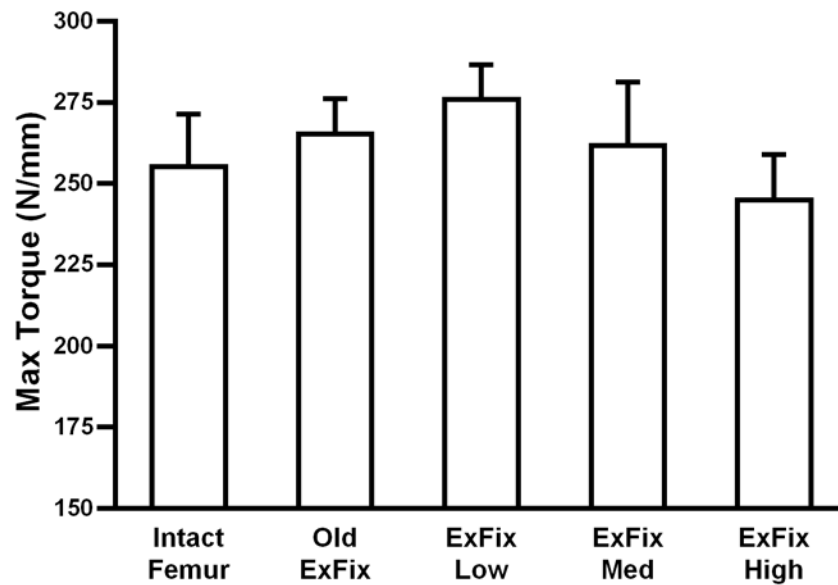


**Figure 4.13** Maximum Torque to failure of femurs treated with rhBMP-2 with four different stiffness fixators treated with rhBMP-2 after 8 weeks (mean  $\pm$  SEM,  $p < 0.05$ ,  $n=7-8$  per group).

### 4.3 DISCUSSION

This study and others have shown that rhBMP-2 promotes bone formation and the healing of CSDs in animal models [17, 58-61, 112, 128-130]. However, many studies show that the healing of segmental CSD under these conditions is subject to variability and the new bone has poor quality compared to normal bone. For reasons discussed earlier in this thesis, this is likely to be related to the stability of CSD fixation. In addition other factors such as weight bearing of the animal, muscle loads will also influence healing of defects, however this was not addressed in this thesis.

The radiographic data obtained in this study demonstrate that the stiffness of the external fixator can have a marked effect on healing, especially at early time points. Indeed, a difference in the femoral defect repair pattern was already evident nine days post-surgery, at which time defects fixed with the two least rigid external fixators showed evidence of bridging mineralization. Interestingly, this always occurred initially on the side of the defect that was opposite the fixator. Neither the

fixator (ExFixHigh) imposing the highest rigidity at early time points, nor the fixator (ExFixOld) imposing the lowest rigidity at early time points produced a radioopaque line at this time. This finding is consistent with the hypothesis that mesenchymal cells commit to either a chondrogenic or an osteogenic lineage during the first few days of healing depending on the mechanical environment [131].

By the week two there were signs of new bone formation and bony bridging in all defects, regardless of the stiffness of the fixators. However, the most rigid fixator produced a smaller callus than the other two lower stiffness fixators, which supports existing data in the literature. Furthermore, the radioopaque line was still seen by the third week post surgery, but by week four all groups had complete bone defect bridging as assessed by X-ray. At the end of the eight week experiment all defects had complete healing no matter which stiffness fixator was used, although the defects stabilized with the most rigid fixator had smaller callus than those stabilized with lower stiffness fixators.

The radiographic observations were supported by additional imaging analyses. Dual-energy X-ray absorptiometry, for example, showed that bone mineral content was significantly different from the intact contralateral femur no matter which stiffness external fixator was used. Furthermore, this significant difference was also seen when the ExFixOld was compared to the new fixators, but it was not different from the intact contralateral femur. In addition mCT revealed that the biggest callus and the greatest amount of new bone was formed with the lowest stiffness, ExFixLow, fixator. Furthermore, the ExFixMed and ExFixHigh showed no difference when compared to each other. Not surprisingly, ExFixOld produced the biggest amount of callus, but the amount of new bone formed within the callus was only comparable to the new most rigid fixator, ExFixHigh. This is probably related to the higher axial intrafragmentary movement related to the poor stability of ExFixOld in the early stages of defect healing and supports my findings from the axial compression in-vitro test where it showed that after 5mm defect was created in the constructs with ExFixOld, they became unstable, which would have increased the IFMs in an in-vivo setting. On the contrary, after the harder material was used which simulated final stages of healing, the ExFixOld became rigid again, which in turn would have decreased the IFMs in the in-vivo situation. This finding partially explains



comparable amounts of healed bone in the callus between ExFixOld and ExFixHigh, because after the IFMs have decreased, the callus tissue began to remodel by resorbing trabecular bone formed as part of the process in the regeneration of bone tissue.

These observations support a number reports in the literature that have shown that the healing of long bone fractures and callus size is sensitive to the axial intrafragmentary movement or the axial fixation stability [65, 73, 132, 133]. Furthermore, the  $\mu$ CT images of longitudinal and transverse sections showed the presence of soft tissue in the healed defect when the most rigid fixator, ExFixHigh, was used (Figure 4.9A&B and 4.10A&B). These data are supported by the histological images, which demonstrated persistent cartilage 8 weeks post-surgery using ExFixMed and ExFixHigh. This is contradictory to the reported influence of mechanical conditions on fracture healing, where less stable fixation has been shown to have cartilage that persists longer before ossifying, and illustrates the need for caution when extrapolating from concepts derived from studies of fractures that spontaneously heal to CSDs, which do not. Nevertheless, the larger callus seen with ExFixLow is in agreement with previous observations that less stable fixation produces greater amount of cartilage leading to a larger soft callus [41, 81, 88, 92, 106, 108, 120, 134-136]. In addition, the histological findings from the present study suggest that segmental defects treated with rhBMP-2 and stabilized with ExFixMed and ExFixHigh heal through endochondral ossification. This process appears to be influenced by the fixation stability, although the exact mechanism is not clear and requires further study.

Biomechanical torsional testing of femora at 8 weeks revealed significantly higher stiffness with ExFixLow when compared to the intact contralateral femurs and all other stiffness fixators. This finding compliments the study by Epari et al. [136] where they examined the interaction between the axial and shear components of the fixation stiffness in the osteotomy sheep model. They found that axial stiffness together with high shear stiffness provides excellent healing. Furthermore, if axial stiffness is either increased or decreased from the moderate range, the strength and stiffness of the callus is reduced despite only a marginal change in the shear stiffness, as in cases of rigid and semi-rigid fixators.

The maximum torque at which femurs broke under torsion followed the same pattern as the stiffness, but there was no significant difference between the different fixators. It is possible that the healed defects converged on a common strength by various combinations of callus size and bone area. For example, when ExFixOld was used the healing defects formed the biggest callus, but had the least amount of new bone. The new external fixators produced smaller calluses but larger amounts of new bone.

These findings are consistent with those of other investigations who found that fixation stability and applied loads determines intrafragmentary movements, which influence the pattern of bone healing [41, 65, 66, 71, 81, 91, 98, 135-145]. Insufficient shear stability has been shown to delay fracture healing by disrupting the blood supply [146]. This may partially explain the bigger callus and the smaller amount of new bone formed with the old external fixator stabilized with K-wires. This also was shown in an *in-vitro* axial compression test where the rubber material was inserted into the critical-sized segmental defect. This construct had the lowest stiffness, probably due to rotational instability caused by high shear intrafragmentary movements. Furthermore, it has been shown that in the segmental CSDs, K-wires do not provide sufficient stability and particularly almost no rotational stability is achieved [59, 92]. The exact mechanism cannot be explained by this study.

In Conclusion, this is the first study to confirm the importance of the mechanical environment on the healing of critical sized segmental defects treated with rhBMP-2, therefore a careful consideration is needed when selecting the fixation device. Some of the data suggest that the mechanical influence on the healing of CSDs differs from its influence on fracture healing, indicating the need for separate investigation of the two. This realisation could help to define the mechanical environment for healing CSDs using BMPs in the most efficient and timely manner. By carefully selecting the fixator stiffness, optimizing the fixator stiffness and determining the optimal time point to change the stiffness of the fixator *in-vivo* as the healing progresses. These factors might reduce the requirement for high doses of BMPs, which are currently used. Studies towards achieving this aim will be described in the next chapter.

## CHAPTER FIVE

*The development of a modulated mechanical environment for bone healing in the rat segmental defect model*

## 5.1 INTRODUCTION

Bone repair involves interactions of cells within local mechanical environments that generate a cascade of molecular events resulting in the repaired and remodelled bone tissue at the fracture site [38, 147, 148]. It has been long recognized that the formation of cartilage and bone, as well as the architecture of the bone laid down during bone healing in response to normal activity such as weight-bearing, is influenced by the local mechanical environment. If there is excess motion at the injury site, the principal mechanism of bone regeneration is through secondary or endochondral ossification, or the formation of cartilaginous callus, which is gradually replaced by new bone. The majority of clinical fractures heal by secondary union or endochondral ossification where a certain amount of micromotion at the fracture site is necessary to stimulate the formation of callus.

The data from the previous chapter suggest that there is not one set of mechanical circumstances that suits all stages of healing, and that healing might be improved by changing the stiffness of the fixator as healing progresses. Previous investigators have attempted to achieve this by the dynamization of operatively stabilized fractures [35, 83, 98, 139, 140, 142, 149-152]. Dynamization is a word used when the IFM is increased by changing from rigid fixation to a more flexible fixation. It is also used when an implant allows axial shortening of a bone through a telescoping mechanism incorporated into the fixation device. In this study I use dynamization in the first sense.

Although several fracture fixation devices have been developed that allow dynamization in the clinical treatment of fractures, it remains unclear at which time during the healing process the dynamization should be applied and whether it helps fractures to repair more efficiently. Unfortunately, few clinical studies have attempted to determine the optimal axial IFM or the effect of dynamization at the various stages of fracture repair, and it is unclear whether this accelerates bone repair in a more efficient and timely manner [152-154]. There are no studies to my knowledge that have attempted to determine the effects of dynamization on the healing of CSDs.

The results of animal studies on the effects of dynamization on fracture healing are inconsistent. A study by Larsson et al [151] investigated the effect of early axial dynamization on tibial bone healing in a canine model. They used a rigid external fixator to stabilize 2mm transverse osteotomy on both tibiae in each dog to allow paired comparison of the results. One week after the surgery, the telescoping mechanism of one randomly selected fixator on each dog was unlocked to allow free axial movement whereas the other side was kept rigidly fixed throughout the study. Animals were sacrificed at 1, 3, 5, 8 and 11 weeks after dynamization. They found that early dynamization resulted in accelerated callus formation, maturation and increased remodelling of endosteal and periosteal callus tissue. Moreover, the dynamized side showed significantly higher torsional stiffness after 5 weeks of treatment than did the controls. In addition, a study by Aro et al. [83] also investigated bone healing pattern affected by loading, fracture fragment stability, fracture type and fracture compression in a canine osteotomy model. This study had three different groups; they looked at transverse and oblique fractures fixed with a rigid unilateral external fixator with the cut ends of the bone separated by a distance of 1 or 2mm, or in a contact. Dynamization of uniform axial loading and motion was performed at two or four weeks. They found that, at the given rigidity of external fixation, the amount of physiologic stresses and the presence of a significant gap proved to be the most significant factors in determining the pattern of fracture repair. Motion with loading tended to promote external callus maturation in secondary bone healing.

On the contrary, two studies in a rat model found that neither early nor late fracture dynamization was beneficial to fracture healing. Although they used different fixation devices such as a rigid nail [98] and an external fixator [149] and initiated dynamization either at the later or earlier healing phase, both groups found that dynamization increased callus formation, but the quality of healed bone was reduced. These findings are not really surprising knowing that the evidence in the literature shows that increased IFM resulting from the flexible fixation device leads to bigger callus formation, prolonged chondral phase and delayed bone healing by disrupting the vascular supply needed for bone tissue to repair and remodel (Rand et al, Ozaki et al). In fact, a study by Culinane et al. [139] tried to regenerate a complete joint by

precisely controlled motion using a custom made external fixator and introducing IFM bending strain and comparing this to the rigidly fixed segmental defect. The results of the study showed that although joint development was incomplete, they were able to direct formation of cartilage and bone during fracture repair by inducing controlled motion. They also have demonstrated, that the spatial organization of the molecular components within the newly formed tissue is influenced by the local mechanical environment and if the IFM is too high, bone does not form.

Augat et al (1996) confirmed that increased flexibility at the fracture site results in enhanced callus proliferation and that increased callus volume was not necessarily associated with increased mechanical quality of the healed bone. They found that an extension in diameter of callus increased the flexural rigidity of the fracture only if the quality of tissue remained the same. In addition, in the previous chapter I showed that earlier and bigger callus was formed with more flexible external fixators and that these produced bone with a higher bone mineral content. This is probably due to a delayed remodelling process, which could make the tissue of bone more brittle. On the contrary, a more rigid fixation device had later callus formation with less mineralized bone tissue at the end of 8 weeks treatment. This leads to a postulation that the cartilage in the callus is calcified and remodelled into bone tissue only after reduction of local strains or so called axial IFM at the surface of new bone formation.

Knowing this, I hypothesize that the fixation device should be flexible, but not too flexible, in the early stages of healing, in order to promote rapid callus formation. The stiffness of the fixation device should be increased after there is evidence from the X-Ray images that sufficient callus is formed and the cartilage calcification process has begun. This should promote osteochondral ossification by allowing better vascularisation of soft calcified tissues, as well as more rapid repair and remodelling of the newly formed bone. Nevertheless, it is very important to make sure that stiffness of the fixation device is not too rigid, because excessively rigid fixation has a reputation for contributing to fracture healing problems. Major concerns are the possible inhibition of external callus formation, maintenance of a fracture gap aggravated by bone end resorption, and the excessive protection of the healing bone from normal stresses (stress shielding) producing adverse remodelling.

Therefore, the specific aim for this chapter was to improve the mechanical environment for bone healing induced by rhBMP-2 in the femoral rat segmental defect model, by altering the stiffness of the fixator during the healing process. According to my hypothesis, healing would be accelerated by first applying a flexible fixator to encourage rapid cartilage formation and then imposing rigid fixation to promote endochondral ossification. First, it was necessary to determine a suitable initial fixator and a suitable time for switching from loose to stiff fixation. This was accomplished by a pilot histological study to determine when the cartilaginous callus began to mineralize.

The main hypothesis for this project was to modulate the mechanical environment in the rat segmental defect model enhanced by rhBMP-2 treatment. For this, low external fixator was used at the time of surgery and 2 weeks later changed to high stiffness external fixator.

## **5.2 MATERIALS AND METHODS**

### **5.2.1 *In-Vivo* Study Design**

#### **5.2.1.1 Histological Study**

The first part of the study determined the degree of early callus formation produced in response to each fixator, and the appropriate time point at which to increase the stiffness of the fixator. A 5 mm, critical sized mid-femoral defect was created in the right hind limb of each of 27 male Sprague-Dawley rats (weight 325-360 g), treated with 11 $\mu$ g rhBMP-2 and stabilized by one of the external fixators described previously ExFixLow, ExFixMed, ExFixHigh. The rats were assigned to one of 3 groups with 3 animals per group and sacrificed 6, 9 and 14 days post surgery. In all groups, after the rats were euthanized femurs were harvested and fixed for histology in 4 % ice cold paraformaldehyde.

### 5.2.1.2 Healing Study

Once the histological data had provided information on which fixator provided the best callus formation and early mineralization, as well as an appropriate time to change to a stiffer fixator, a full healing study was performed. For the second part of the experiment, a 5 mm critical sized defect was created in the right hind limb of each of 12 male Sprague-Dawley rats (weight 325-360 g) treated with rhBMP-2 (11 µg) and stabilized by the ExFixLow. Two weeks after surgery all 12 rats were anesthetized with isoflurane (2% at 2 l/min by air mask). Before the procedure the rats were given one dose of analgesic buprenorphine (dose 0.08 mg/kg) intramuscularly in the left leg to prevent any pain or discomfort. The connection modules of the ExFixLow were then removed and replaced with ExFixHigh connective modules to increase rigidity in the healing femur for the remaining 6 weeks of treatment; this group will be referred to as Modulated group. All rats were sacrificed at the end of treatment and treated femora were compared to the intact, contralateral femora, as well as to rats whose defects had been allowed to heal with continuous use of ExFixLow, ExFixMed or ExFixHigh fixators. Healing was monitored by weekly radiologic evaluation. Eight weeks after surgery, final X-rays were taken and the animals euthanized; 2 femurs were harvested and fixed for histology in 4 % ice cold paraformaldehyde and the remaining specimens were wrapped in a gauze soaked with 0.9% saline solution and frozen at -20°C for physical testing. The quality of the healed defects were evaluated DXA, µCT, histology and biomechanical testing. All these methods were described in the Chapter Four, Materials and Methods Section.

Animal care and experimental protocols were followed in accordance with NIH guidelines and approved by the Beth Israel Deaconess Medical Center Institutional Animal Care and Use Committee. Following a minimum 48-hour acclimatization period, the animals were transported to a dedicated surgical procedure room.



### **5.2.1.3 Statistical Analysis**

Comparisons of continuous variables between five treatment groups were performed using a two-tailed t-test, and by analysis of variance (One Way-ANOVA) to determine significant difference.

The power level for all the data was found to be from 0.8 to 1. Thus the numbers of animals per group used in these studies is enough to determine a 5% difference between the test groups. All tests were two-tailed, with differences considered significant at  $p < 0.05$ . Data are presented as mean $\pm$ SE, unless otherwise noted.

## **5.3 RESULTS**

### **5.3.1 Histological Evolution of Defects during the First 2 Weeks of Healing under Different Stiffness Regimens**

Representative micrographs of tissues within defects stabilized with ExFixLow, ExFixMed and ExFixHigh at day 6, 9 and 14 are presented in Figures 5.1 and 5.2. The hematoxylin and eosin-stained sections (Figure 5.1) demonstrate the general appearance of the tissues within the segmental defect, whereas safranin O-fast green-stained sections (Figure 5.2) show the presence of proteoglycans, which is the precursor to endochondral bone formation.

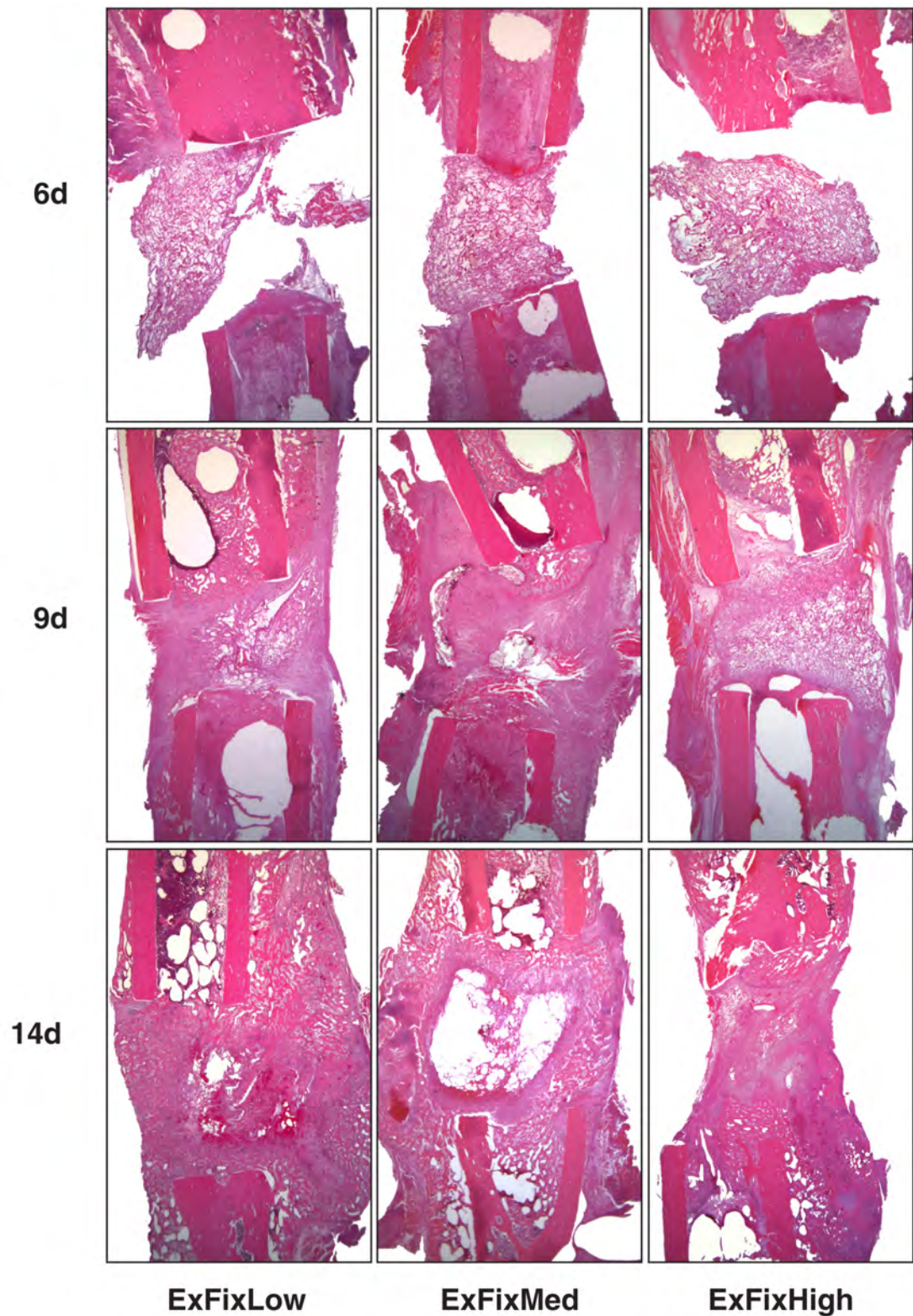


**Figure 5.1** Representative longitudinal histological sections of femoral segmental defects after 6, 9 and 14 days of treatment with rhBMP-2 with three different stiffness fixators. Paraffin embedded sections stained with hematoxylin & eosin at 16x magnification.

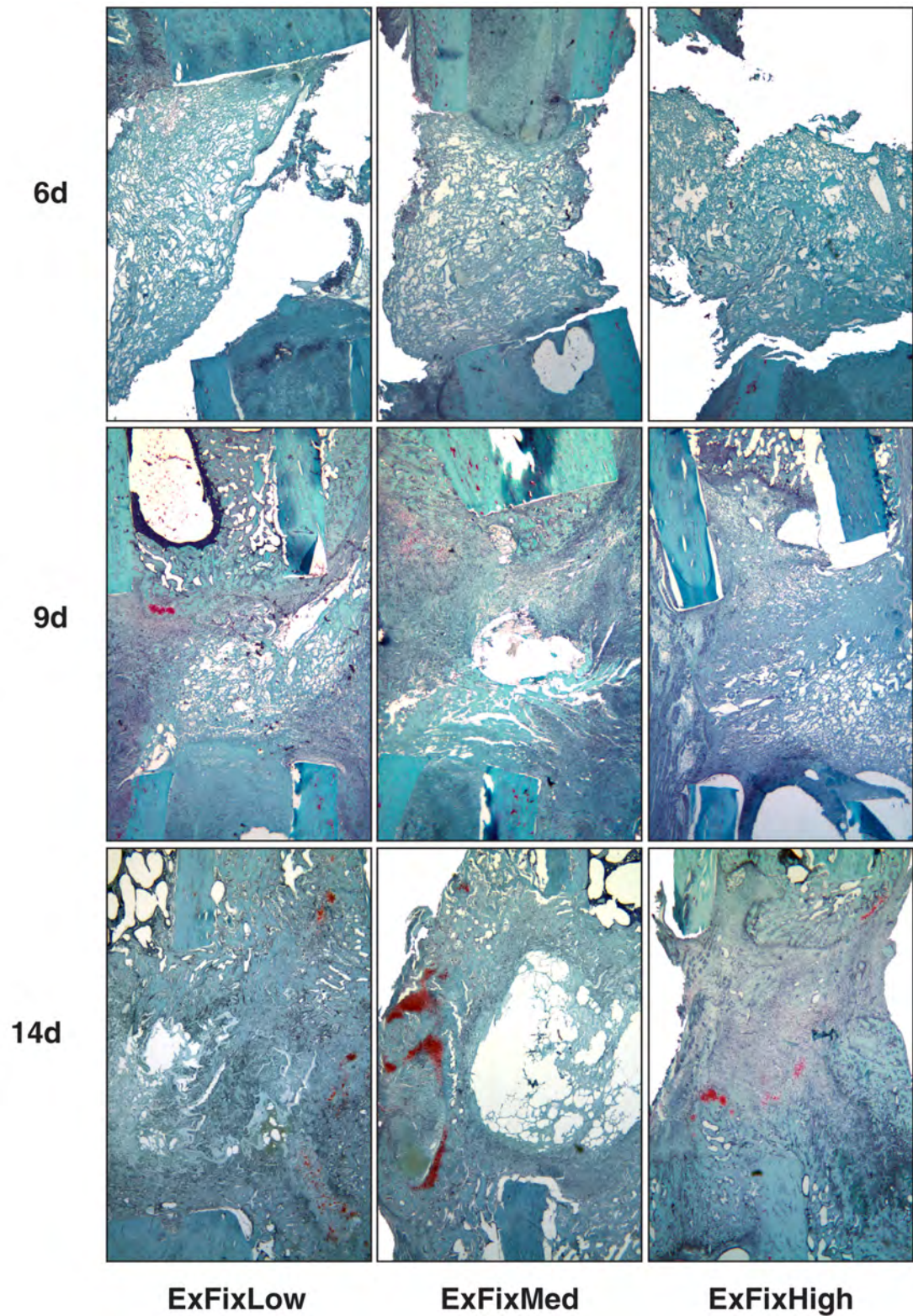


**Figure 5.2** Representative longitudinal histological sections of femoral segmental defects after 6, 9 and 14 days of treatment with rhBMP-2 with three different stiffness fixators. Paraffin embedded sections stained with safranin orange- fast green at 25x magnification.

Evaluation of the CSD in the longitudinal sections six days post-surgery showed no evidence of tissue formation, within the defects, which contained only the implanted collagen sponge no matter which stiffness external fixator was used. In the groups with two lower stiffness fixators, there was evidence of a periosteal reaction adjacent to the defect gap around the periosteum (Figure 5.3).

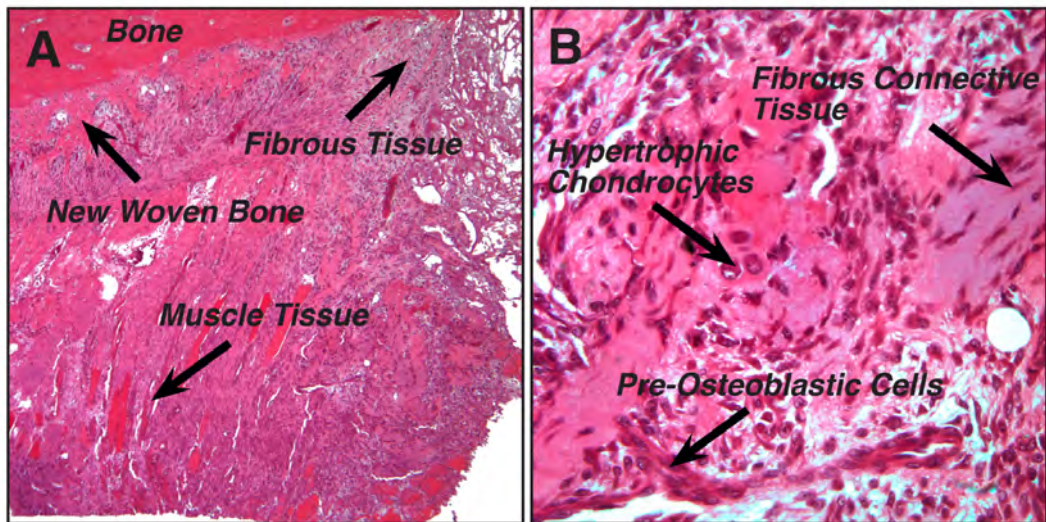


**Figure 5.3** Representative longitudinal histological sections of femoral segmental defects after 6 days of treatment with rhBMP-2 with lower stiffness external fixator. Paraffin embedded sections stained with hematoxylin & eosin. (A) Periosteum reaction with new woven bone formation, muscle atrophy and regeneration (shown with arrows). Also, fibrous connective tissue adjacent to the defect 50x magnification; (B) Hypertrophic chondrogenic cells, evidence of pre-osteoblastic cells and fibrous connective tissue adjacent to the defect at 400x magnification.

Interestingly, three days later there was unmistakable deposition of new tissue in the defects of the two groups with the lowest stiffness external fixators. This presented as the formation of external callus, with the defect gap completely filled with soft tissue. In both groups there was marked thickening of the periosteum, which appeared to spread across the defect forming a bridge. This was more prominent on the side opposite the fixator. Bone, but not cartilage was visible in this area (Figure 5.4).

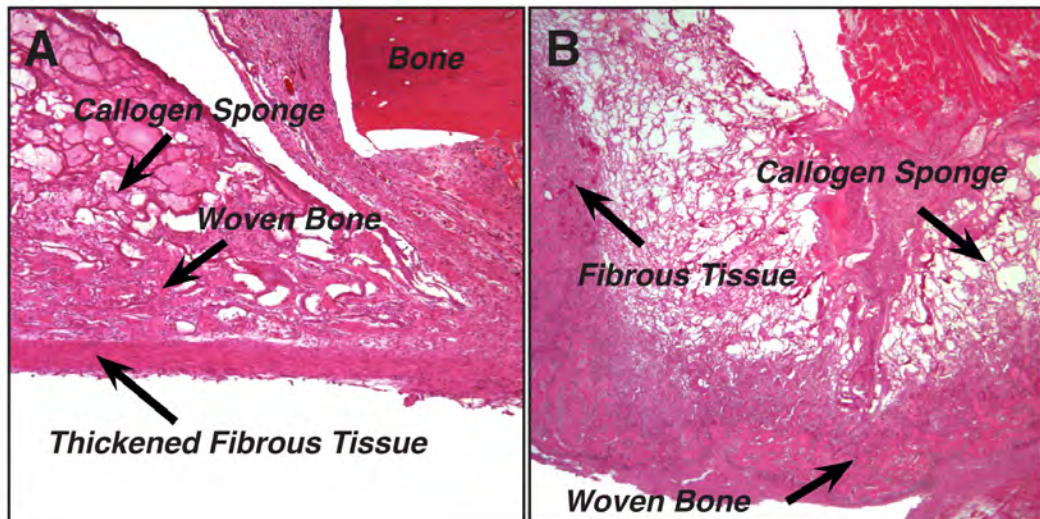


**Figure 5.4** Representative longitudinal histological sections of femoral segmental defect after 9 days of treatment with rhBMP-2 with lower stiffness external fixator. Paraffin embedded sections stained with hematoxylin & eosin. (A) Thickened fibrous tissue bridging the defect, adjacent to that new woven bone and remaining parts of collagen sponge (shown with arrows) at 400x magnification; (B) New bone formation around the edges of new callus covered with the layer of fibrous tissue. In the center of the defect collagen sponge (shown with arrows) 400x magnification.

Furthermore, evidence of new bone formation, often around the scaffolds of the sponge material was seen and periosteal new bone formation on the bone adjacent to the defect. However and there was no real evidence of cartilage beyond a few flecks of safranin-O staining material in the ExFixLow group (Figure 5.2).

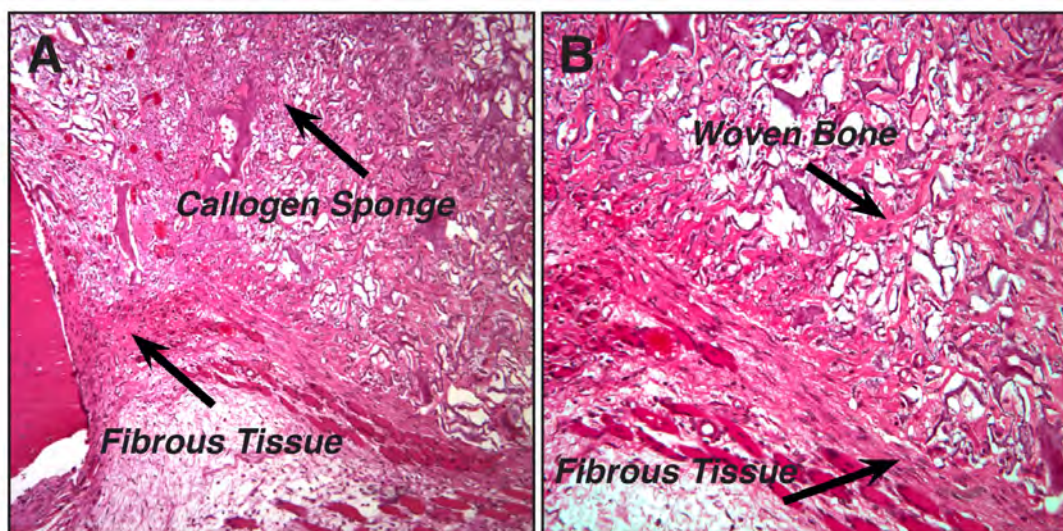


**Figure 5.5** Representative longitudinal histological sections of femoral segmental defects after 9 days of treatment with rhBMP-2 with ExFixHigh external fixator. Paraffin embedded sections stained with hematoxylin & eosin. (A) Fibrous and sponge material adjacent to the

defect at 100x magnification; (B) Fibrous and sponge material in the defect at 200x magnification.

In contrast, in the group with the most rigid external fixator, ExFixHigh, the defect showed continued presence of ACS and the defect was surrounded with fibrous connective tissue. Although, as in the other groups there was marked woven bone formation along the periosteum adjacent to the defect, but the defect did not bridge (Figure 5.5).

Two weeks post-surgery, the defects from the animals that had been treated with two lower stiffness fixators were filled with extensive amount of new woven bone around the residual sponge scaffold (Figure 5.6A&B).

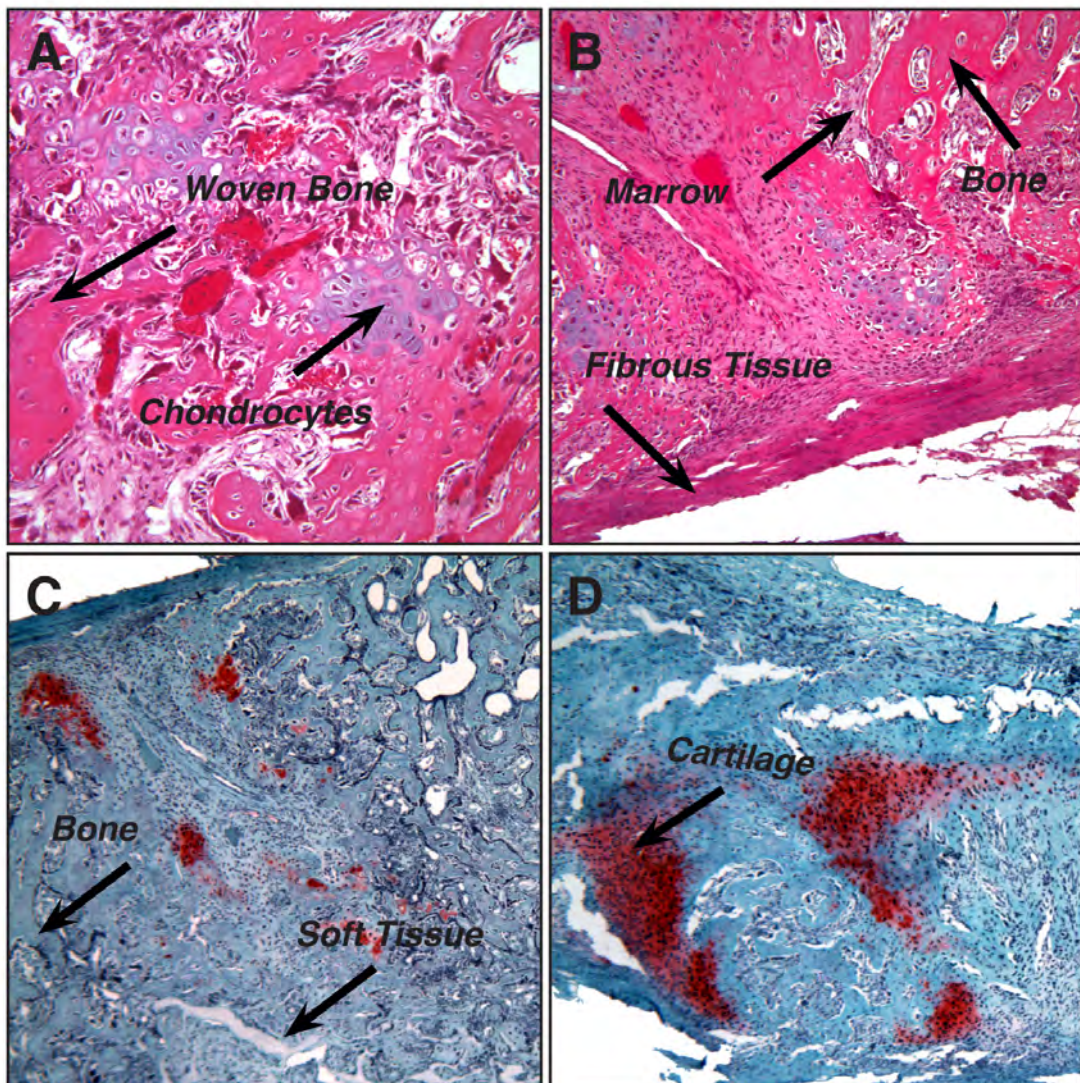


**Figure 5.6** Representative longitudinal histological sections of femoral segmental defects after 2 weeks of treatment with rhBMP-2 with ExFixMed external fixator. Paraffin embedded sections stained with hematoxylin & eosin (top row) and safranin orange-fast green (bottom row). (A) New woven bone formation and a few remaining chondrocyte cells in the defect at 200x magnification; (B) Thickened fibrous tissue bridging the defect and some areas of new woven bone at 100x magnification; (C&D) Traces of cartilage on the edges of callus at 50x magnification).

Interestingly, in both of these groups the gap was completely bridged not by a new bone tissue, but by a thick band of fibrous tissue that looked like periosteum. Surprisingly, two weeks post surgery only very small areas of cartilage was observed with the lower stiffness fixators (Figure 5.6C&D). The defects stabilized with ExFixMed group had a gap in the middle of the defect. This finding can not be explained at the current time and needs further investigation, but the same phenomenon was also observed on the  $\mu$ CT.

The group with the highest stiffness external fixator had no external callus at 14 days. Although the defect gap was filled, there was relatively little bone and most of the tissue appeared to be fibrous. This fibrous tissue had an appearance of thickened periosteum, which spanned across the defect. In addition, only very small foci of cartilage were also observed (Figure 5.7A&B).

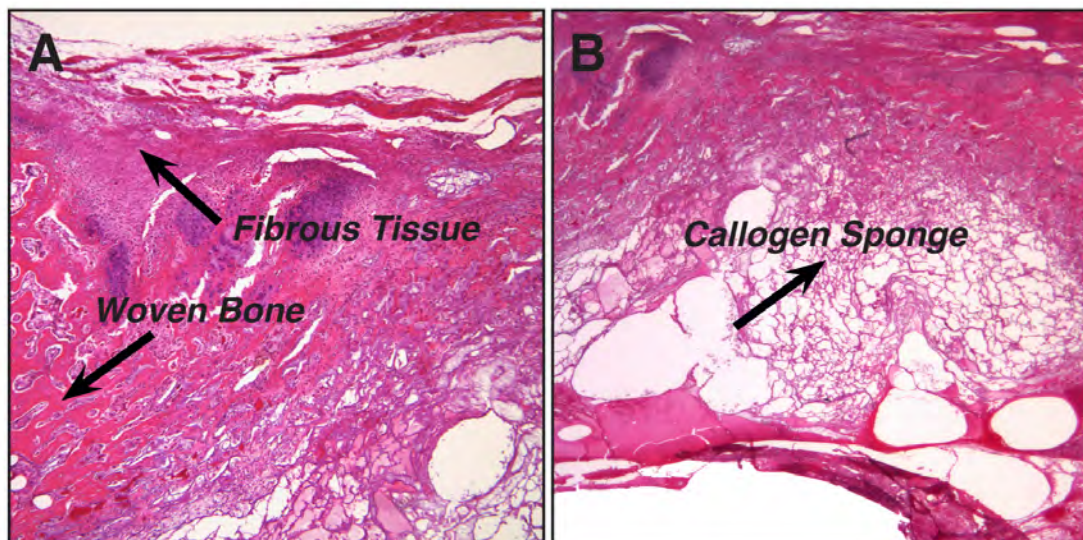


**Figure 5.7** Representative longitudinal histological sections of femoral segmental defects after 14 of treatment with rhBMP-2 with ExFixHigh external fixator. Paraffin embedded sections stained with hematoxylin & eosin. (A) Fibrous tissue and traces and areas of new woven bone in the defect at 50x magnification; (B) Presence of sponge scaffold and fibrous tissue along the edge of the defect at 50x magnification.

## **5.3.2 Evaluation of an Improved Healing Regimen using Mechanical Modulation**

### **5.3.2.1 Radiographic Evaluation**

As noted in Chapter 4, weekly X-rays confirmed traces of callus formation already after 9 days of treatment with ExFixLow. Two weeks post-surgery the 5mm defect area was mostly filled with calcified tissue as shown in the x-ray image (Figure 5.8A&B). After this was confirmed, the fixator stiffness was changed from ExFixLow to ExFixHigh; from now on this group will be referred to as the Modulated group and compared to the X-ray images from the ExFixLow, Med and High groups already shown in the Chapter 4. One week after the external fixator stiffness was changed, which was 3 weeks after the initial surgery, the x-rays revealed complete callus bridging with bony tissue and no evidence of radioopaque lines in the defect. In contrast, soft tissue persisted in those defects stabilised with ExFixLow and ExFixMed until 4 weeks after the surgery, and with ExFixHigh for at least 6 weeks post-surgery. As described later, persistence of cartilage was seen histologically after 8 weeks of stabilisation with ExFixHigh.

Four weeks, post-surgery, i.e. two weeks after the fixator stiffness was changed to more rigid, the callus size of the Modulated group appeared to be at its maximum. X-rays taken one week later revealed that the callus size started to decrease and this change was evident weekly until the end of 8 weeks treatment. In contrast, this phenomenon was not observed in the groups where the defect had been stabilized constantly with ExFixLow, ExFixMed or ExFixHigh. In fact, in the groups with the two lower stiffness fixators, the size of external callus appeared to increase as healing progressed until the end of treatment, whereas in the group with the most rigid fixator, callus size stayed unchanged (Figure 5.8A&B).



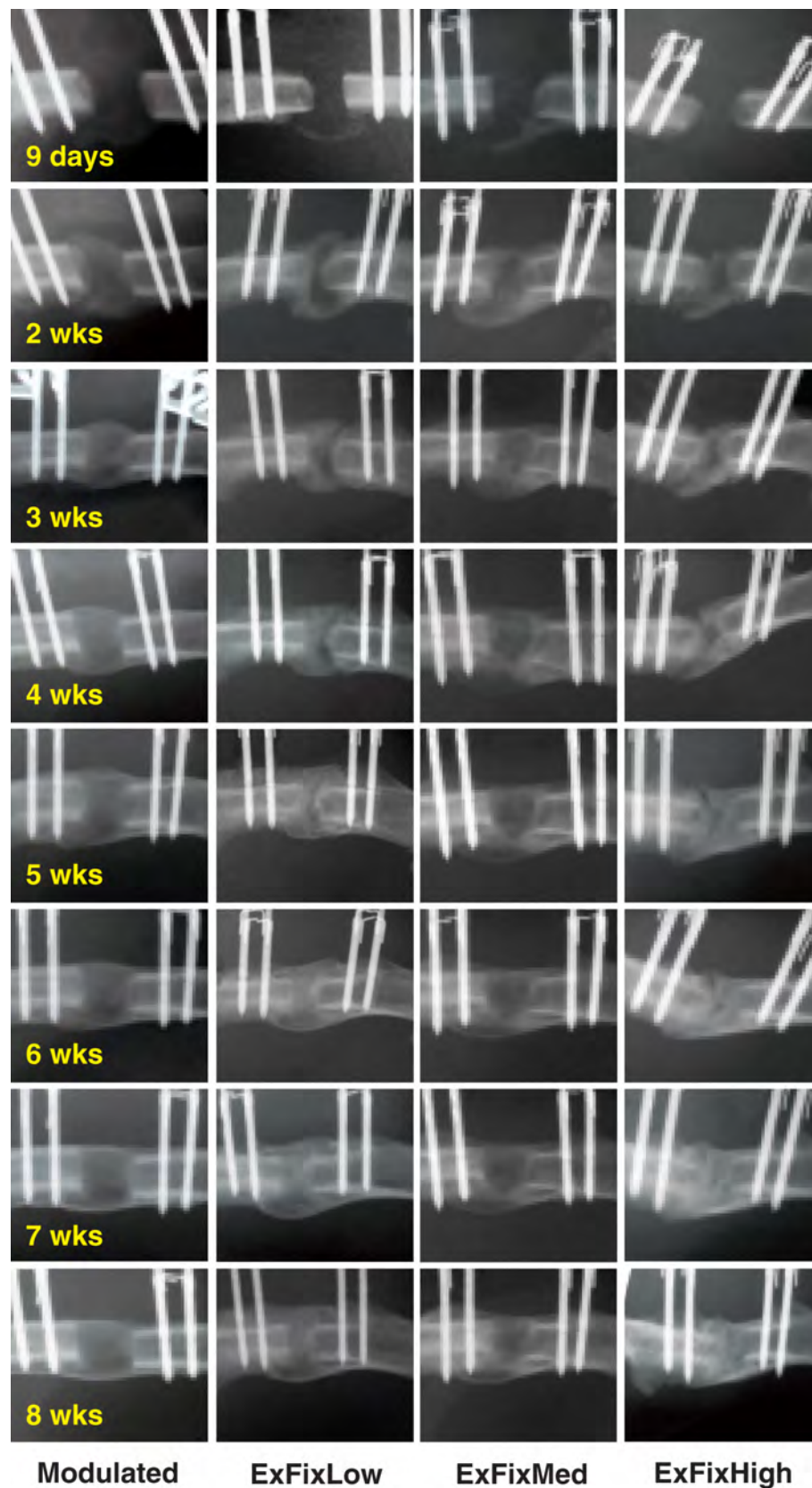


**Figure 5.8A** First set of representative radiographic images in the groups with ExFixLow, ExFixMed and ExFixHigh and the improved group 9 days, 2, 3, 4, 5, 6, 7 and 8 post-surgery. In the Modulated group, ExFixLow was changed to ExFixHigh after 2 weeks.

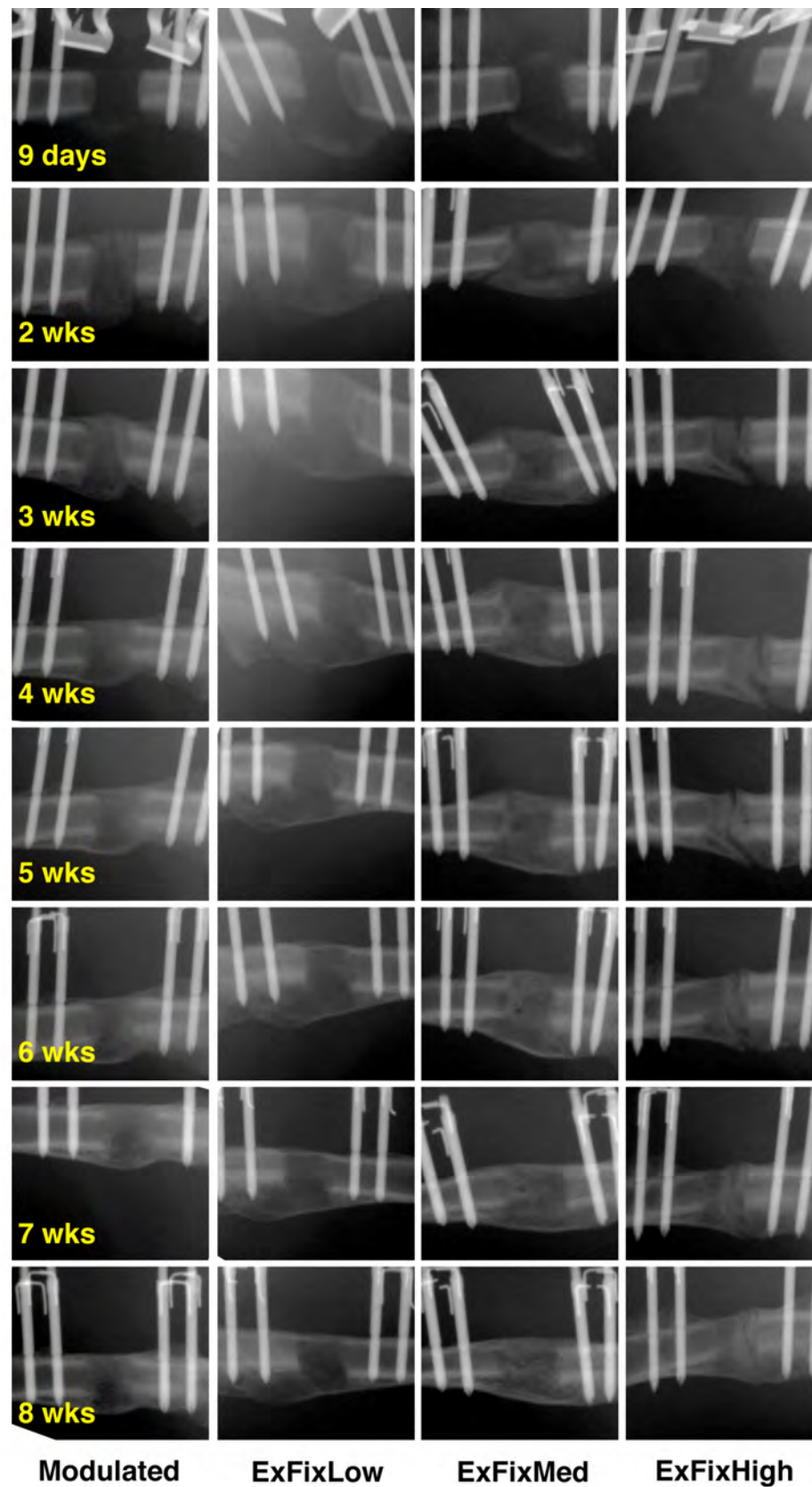


**Figure 5.8B** Second set of representative radiographic images in the groups with ExFixLow, ExFixMed and ExFixHigh and the improved group 9 days, 2, 3, 4, 5, 6, 7 and 8 post-surgery. In the Modulated group, ExFixLow was changed to ExFixHigh after 2 weeks.

### 5.3.2.2 Dual-energy X-ray absorptiometry (DXA)

After 8 weeks of treatment bone mineral content (BMC, g), as described in the chapter four, was highest with ExFixLow as compared with all the other groups. However, there was no significant difference observed when ExFixLow was compared to ExFixMed and ExFixHigh, although there was a trend downward with the two higher stiffness fixators. Interestingly, the “Modulated” group where the external fixator stiffness was changed from ExFixLow to ExFixHigh 2 weeks post-surgery, had the same BMC as the intact contralateral femur. This finding suggest that the group with the Modulated treatment is at a more advanced stage of bone healing and remodelling than the other groups. Furthermore, a statistically significant difference was only observed when intact contralateral femur and Modulated treatment was compared to all other external fixator stiffness groups as shown in figure 5.9 and table 5.1 and 5.3.

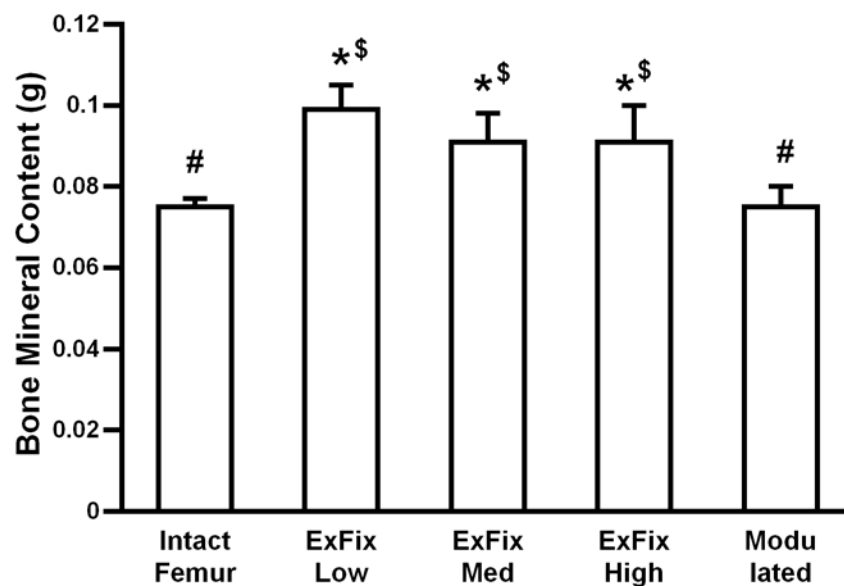


**Figure 5.9** Bone Mineral Content (BMC, g) in the segmental defect region after 8 weeks of treatment with rhBMP-2 was measured by DXA. Values given are means  $\pm$  SEM; Asterisks indicate statistically significant from intact, contralateral femur, dollar signs indicate statistical significant difference from Modulated, and hash signs indicate significant difference from ExFixHigh ( $p < 0.05$ ,  $n=9-10$  per group).

<i>Variable</i>	Intact Femur (n=10)	Modulated (n=9)	ExFixLow (n=10)	ExFixMed (n=9)	ExFixHigh (n=9)
BMC (g)	0.075±0.01 <sup>#</sup>	0.099±0.02* <sup>\$</sup>	0.091±0.02* <sup>\$</sup>	0.091±0.03* <sup>\$</sup>	0.091±0.03* <sup>\$</sup>

**Table 5.1** Bone Mineral Content (BMC, g) segmental healing characteristic of intact femur, Optimized, ExFixLow, ExFixMed and ExFixHigh treated with rhBMP-2 as measured by MicroCT (mean ± SD). Asterisks indicate statistical significance from intact, contralateral femur, dollar signs indicate statistical significant difference from Modulated group, and hash signs indicate significant difference from ExFixHigh ( $p < 0.05$ ).

### 5.3.2.3 Micro-computed tomography ( $\mu$ CT)

The findings seen in the radiographic images were confirmed with high-resolution  $\mu$ CT data. The total cross-sectional area (TA,  $\text{mm}^2$ ) or callus size in the Modulated group was smaller when compared to the ExFixLow group and this difference was significant ( $p < 0.032$ ). Also, a statistically significant difference was seen when the modulated group was compared to the Intact Femur, ExFixMed and ExFixHigh groups,  $p < 0.001$  as shown in the figure 5.10 and table 5.3.

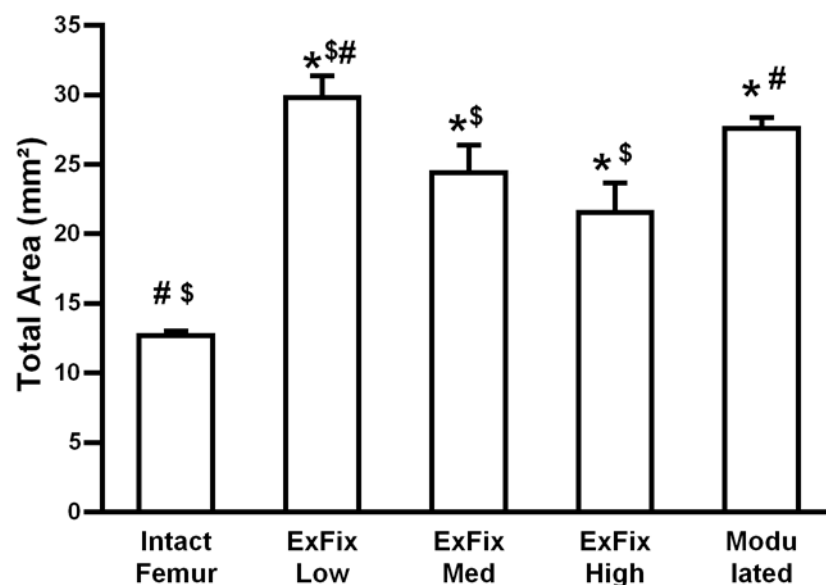


**Figure 5.10** MicroCT was used to measure Total area/Callus size (TA,  $\text{mm}^2$ ) in four different groups treated with rhBMP-2 (mean ± SEM) and compared to the Intact femur. Asterisks indicate statistical significance from intact, contralateral femur, dollar signs

indicate statistical significant difference from Modulated group, and hash signs indicate significant difference from ExFixHigh ( $p < 0.05$ ,  $n=9-10$  per group).

Bone area (BA,  $\text{mm}^2$ ) in the defect region in the modulated group was lower than in the other three groups with various stiffness external fixators. However, when the Modulated group was compared to the intact contralateral femur the BA 19% increase and this difference was significant ( $p < 0.04$ ), but not as big as with ExFixLow, ExFixMed or ExFixHigh fixators (Figure 5.11 and Table 5.3).

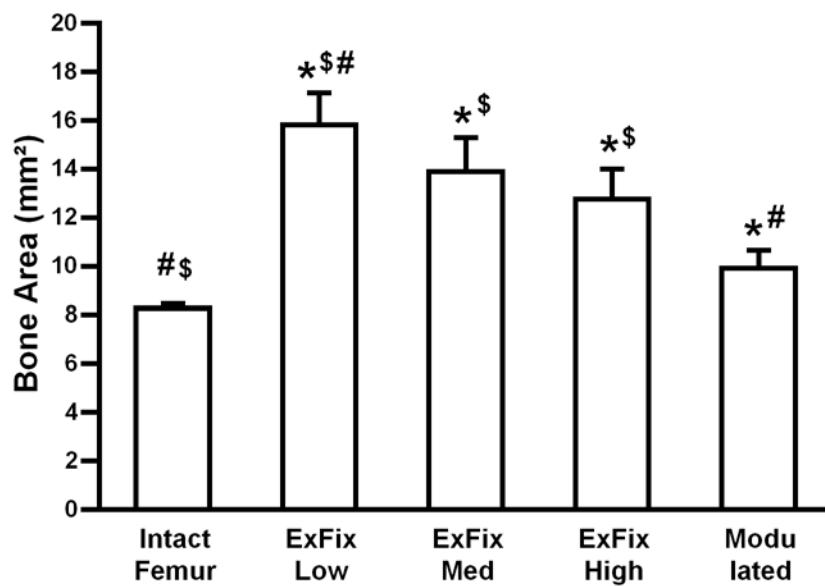


**Figure 5.11** MicroCT was used to measure Bone Area ( $\text{mm}^2$ ) in four different groups: ExFixLow, ExFixMed and ExFixHigh and the Modulated group (mean  $\pm$  SEM) and compared to the Intact Femur. Asterisks indicate statistical significance from intact, contralateral femur, dollar signs indicate statistical significant difference from Modulated group, and hash signs indicate significant difference from ExFixHigh ( $p < 0.05$ ,  $n=9-10$  per group).

Surprisingly, Bone area/Total Area or Callus size (BA/TA, %) or so called bone area fraction in the defect region was the lowest in the Modulated treatment group as compared with all other groups and this difference was significant ( $p < 0.001$ , Figure 5.12 and Table 5.3). Furthermore, when the Intact Femur group was compared to the Modulated group, the BA/TA%, was twice as high.

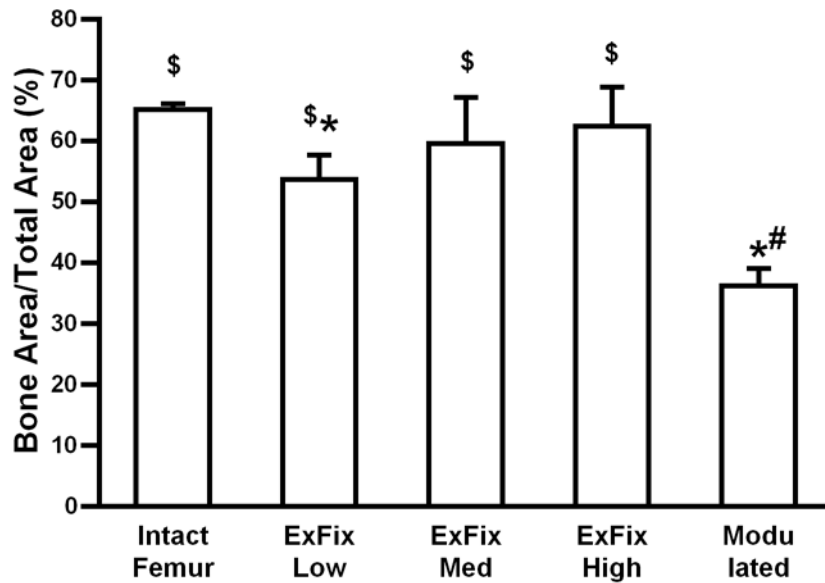


**Figure 5.12** MicroCT was used to measure Bone Area/Total Area (%) in defects treated with rhBMP-2 and stabilised with various stiffness fixator and Modulated group (mean  $\pm$  SEM) and compared to the Intact Femur. Asterisks indicate statistical significance from intact, contralateral femur, dollar signs indicate statistical significant difference from Modulated, and hash signs indicate significant difference from ExFixHigh ( $p < 0.05$ ,  $n=9-10$  per group).

The polar moment of inertia (pMOI,  $\text{mm}^4$ ) is a quantity used to predict an object's ability to resist torsion. This applies to all the engineering structures including bones. The larger pMOI is, the less the beam will twist, when subjected to a given torque, although this does not include material properties which would change the outcome of the object's strength.

In the treatment group subjected to the Modulated stiffness, the pMOI was 2.5 fold higher than in the intact contralateral femur, this difference was significant,  $p < 0.001$  as shown in the figure 5.13. In contrast, the pMOI in the Modulated group was lower than the ExFixLow group, where stiffness of the external fixator was the lowest and this difference was significant, ( $p < 0.0001$ , Figure 5.13 and Table 5.2 and 5.3). There was no difference observed between the two other groups with higher stiffness external fixators.

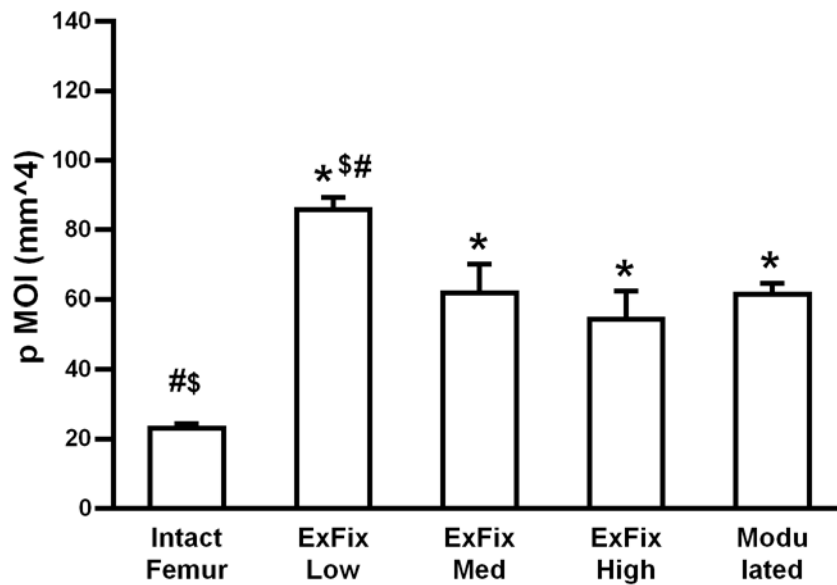


**Figure 5.13** MicroCT was used to measure polar moment of inertia (pMOI, mm<sup>4</sup>) with various stiffness fixators and the modulated group (mean  $\pm$  SEM) and compared to the Intact Femur. Asterisks indicate statistical significance from intact, contralateral femur, dollar signs indicate statistical significant difference from modulated, and hash signs indicate significant difference from ExFixHigh ( $p < 0.05$ ,  $n=9-10$  per group).

The results of the physical testing are collated in Table 5.2

<i>Variables</i>	Intact Femur (n=10)	ExFixLow (n=10)	ExFixMed (n=9)	ExFixHigh (n=9)	Modulated (n=9)
TA (mm <sup>2</sup> )	12.71 $\pm$ 0.3 <sup># \$</sup>	29.8 $\pm$ 1.5 <sup>*# \$</sup>	24.4 $\pm$ 2.0 <sup>*\$</sup>	21.5 $\pm$ 2.1 <sup>*\$</sup>	27.6 $\pm$ 0.8 <sup>*#</sup>
BA (mm <sup>2</sup> )	8.27 $\pm$ 0.2 <sup># \$</sup>	15.8 $\pm$ 1.3 <sup>*# \$</sup>	13.8 $\pm$ 1.4 <sup>*\$</sup>	12.8 $\pm$ 1.2 <sup>*\$</sup>	10.0 $\pm$ 0.7 <sup>*#</sup>
BA/TA (%)	65.1 $\pm$ 0.9 <sup>\$</sup>	53.6 $\pm$ 4.1 <sup>*\$</sup>	59.6 $\pm$ 7.6 <sup>\$</sup>	62.4 $\pm$ 6.4 <sup>\$</sup>	36.2 $\pm$ 2.8 <sup>*#</sup>
pMOI (mm <sup>4</sup> )	23.1 $\pm$ 1.2 <sup># \$</sup>	85.9 $\pm$ 3.5 <sup>*\$#</sup>	61.8 $\pm$ 8.2 <sup>*</sup>	54.4 $\pm$ 8.1 <sup>*</sup>	61.4 $\pm$ 3.0 <sup>*</sup>

**Table 5.2** Segmental healing characteristics of Intact femur, Modulated, ExFixLow, ExFixMed and ExFixHigh treated with rhBMP-2 as measured by MicroCT (mean  $\pm$  SEM). Asterisks indicate statistical significance from intact, contralateral femur, dollar signs indicate statistical significant difference from Modulated, and hash signs indicate significant difference from ExFixHigh ( $p < 0.05$ ,  $n=9-10$  per group).

Representative longitudinal 2D and 3D  $\mu$ CT images in the Modulated treatment group show more advanced healing as compared to the other groups where various stiffness external fixators were used (Figure 5.14A&B).

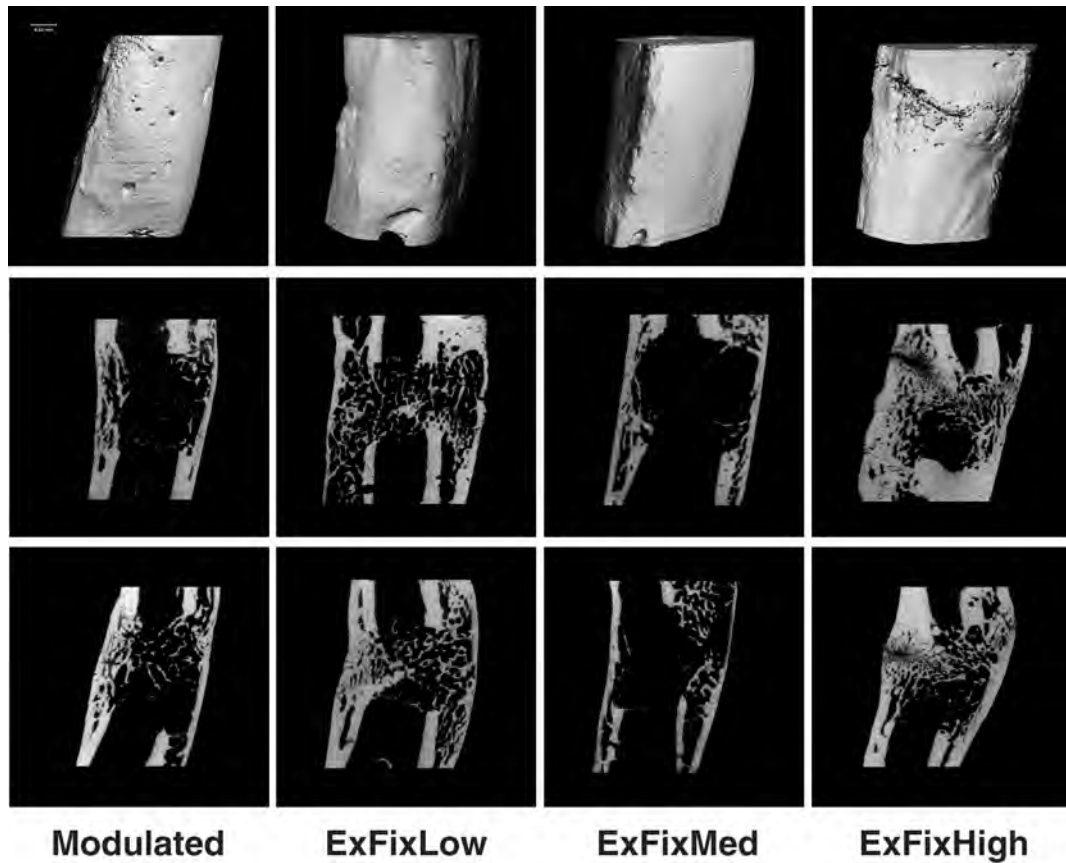


**Figure 5.14A** First set of representative 3D (top row) and 2D (second and third rows) longitudinal  $\mu$ CT images of femora 8 weeks post-surgery in the Modulated group and three different stiffness fixators.



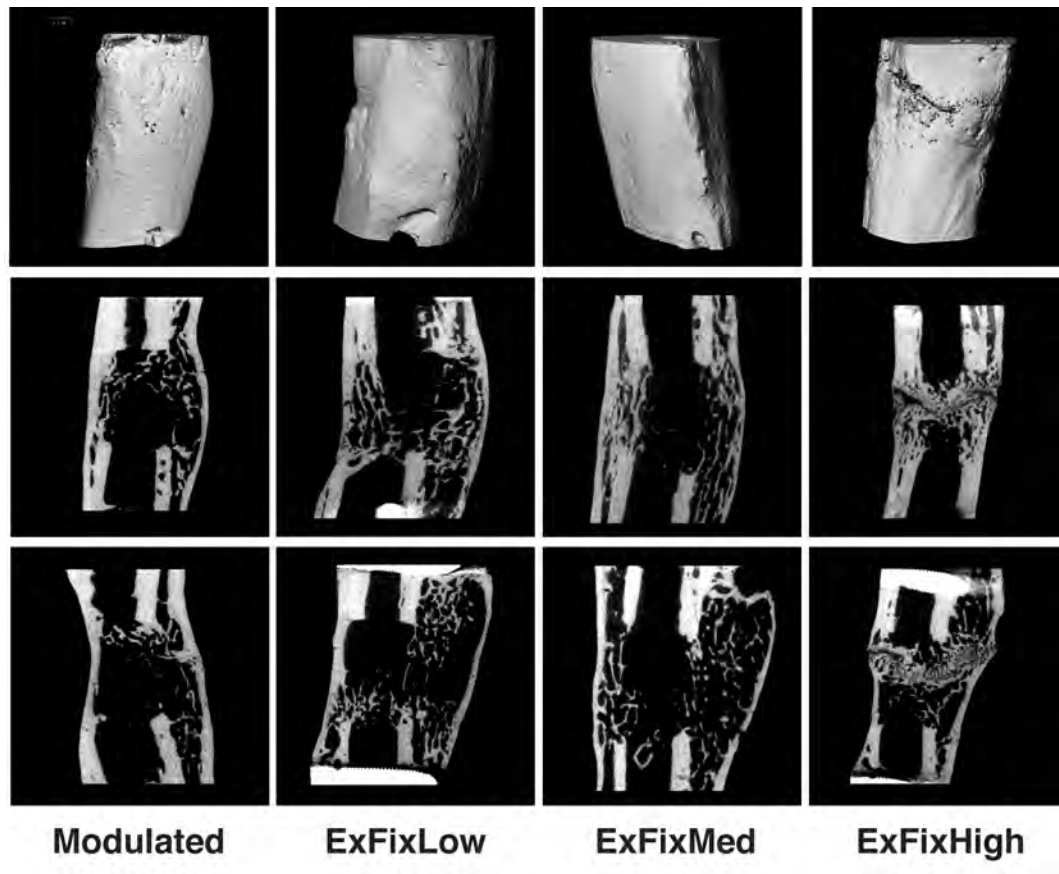


**Figure 5.14B** Second set of representative 3D (top row) and 2D (second and third rows) longitudinal  $\mu$ CT images of femora 8 weeks post-surgery in the Modulated group and three different stiffness fixators.

In the figure 5.15A&B representative 2D transverse images also confirm this finding. In fact, despite having the smallest amount of bone, the Modulated group, showed more organized structure and advanced healing in the defect after 8 weeks of treatment with rhBMP-2. This translated into thicker cortical bone and smaller amount of trabecular bone when compared to the ExFixLow, ExFixMed and ExFixHigh groups. Furthermore, in the Modulated group formation of new cortical bone had even circumference distribution of the healed callus over entire length of the segmental defect, which was not observed in the groups with different stiffnesses. The ExFixLow group had the biggest callus, but the neocortex around the callus was thicker and had a less symmetrical distribution than defects stabilised according to the conditions of the Modulated group.

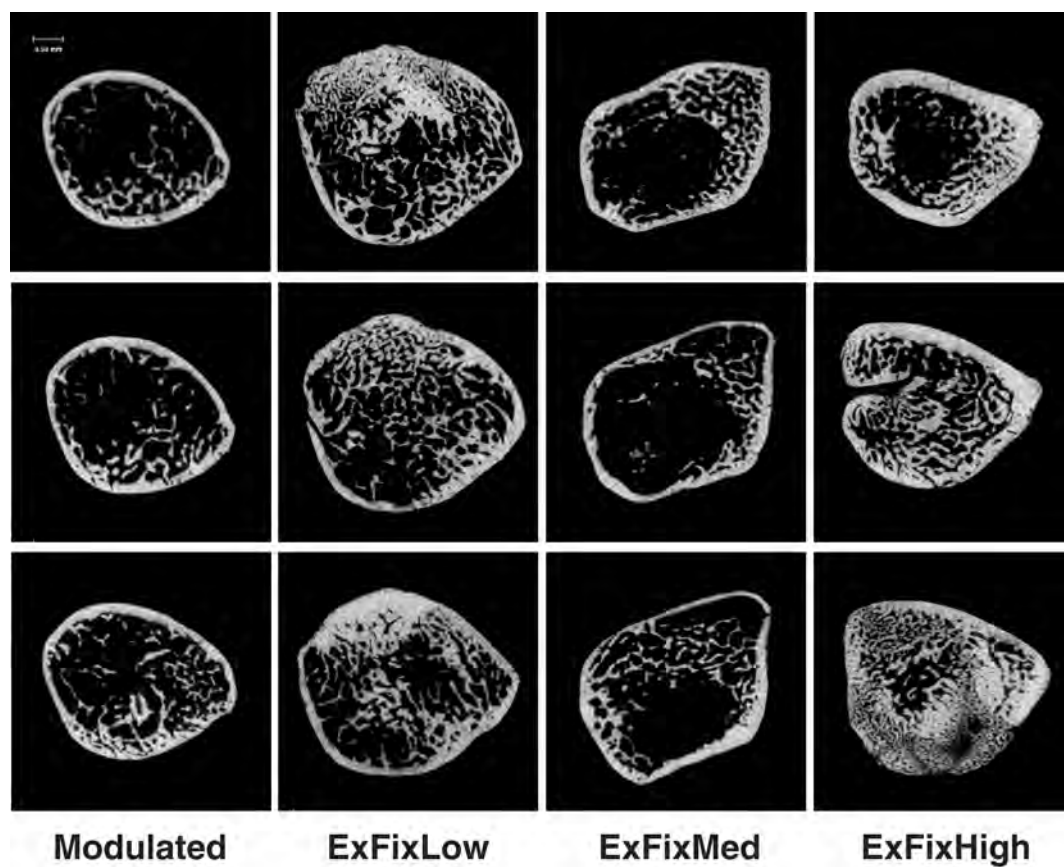


**Figure 5.15A** First set of representative transverse 2D  $\mu$ CT images of femora 8 weeks post-surgery in the Modulated group and three different stiffness fixators.

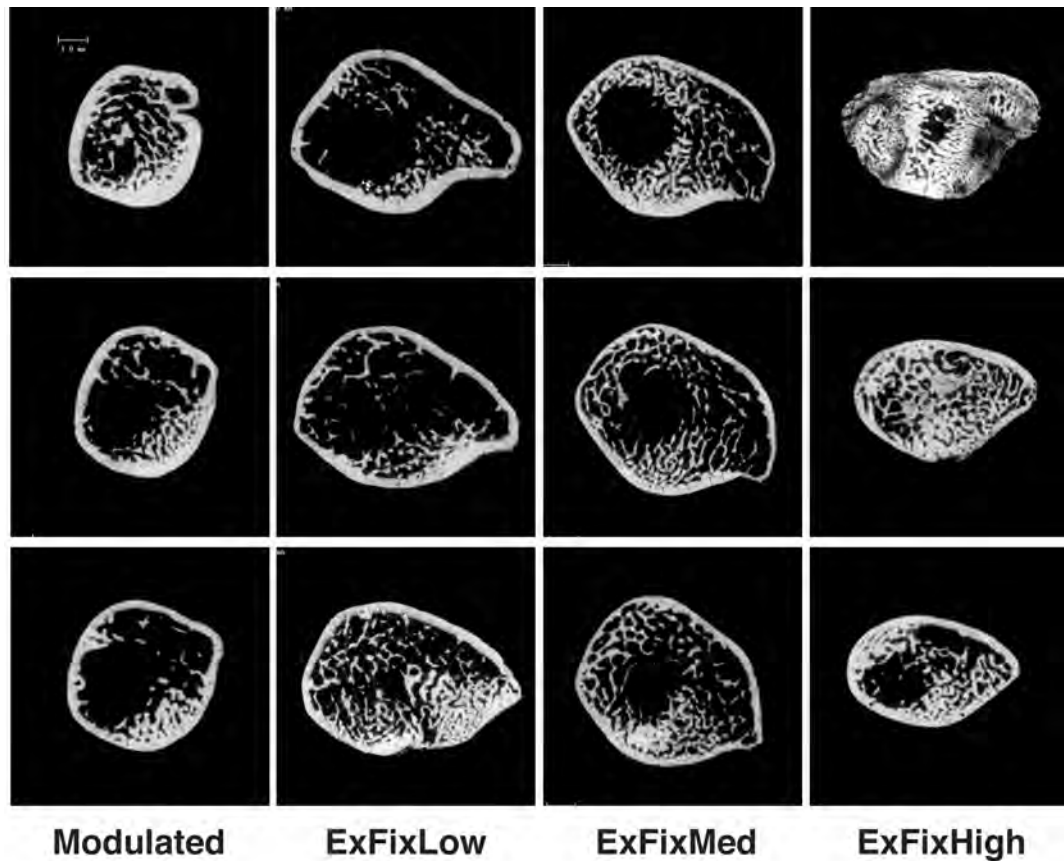


**Figure 5.15B** Second set of representative transverse 2D  $\mu$ CT images of femora 8 weeks post-surgery in the Modulated group and three different stiffness fixators.

#### 5.3.2.4 Histology

Representative histological images of CSD 8 weeks post-surgery under the different fixator conditions are shown in the Figure 5.16. These images clearly show advanced CSD healing in the Modulated group as compared to the other three groups. Defects healed under Modulated conditions had more organization and better architecture, which resulted in evenly distributed neocortical continuity throughout the defect and smaller amount of trabecular bone in the marrow canal. This is probably due to more advanced remodelling process. Defects stabilised with ExFixLow, which were a control to a Modulated group, also formed considerable amount of bone, but this was less well organized and the neocortices were less well developed. Defects stabilised with ExFixMed had large areas of unmineralised tissue in the central area, while those stabilised with ExFixHigh contained residual cartilage (Figure 5.16).

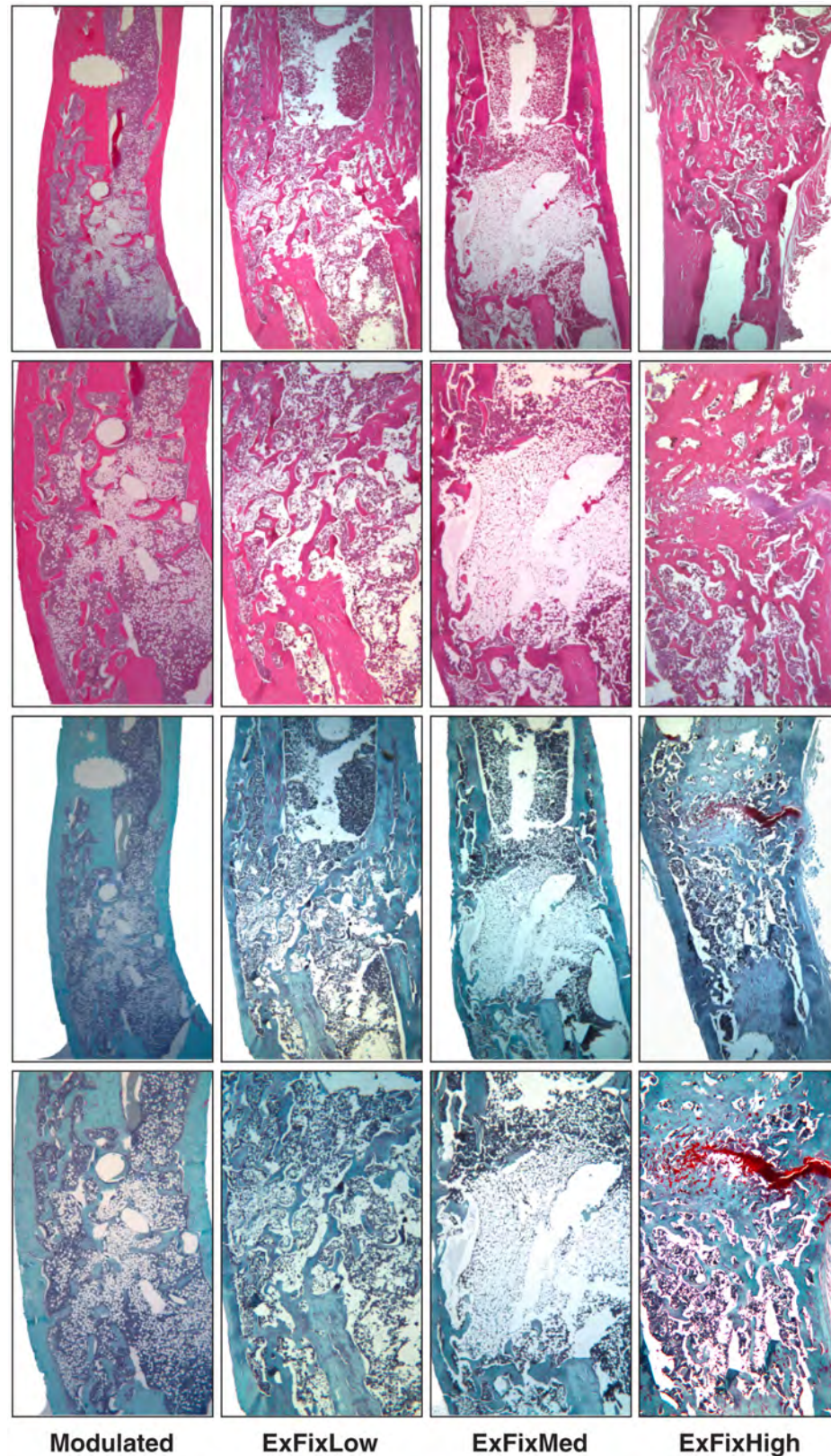


**Figure 5.16** Representative histological sections from femoral mid-defect region 8 weeks post-surgery and stabilized with ExFixLow, ExFixMed, ExFixHigh and in a Modulated group. Paraffin embedded sections stained with hematoxylin & eosin (two top row) and Safranin Orange (two bottom row). First and third row at 16x magnification and second and fourth row at 25x magnification.

### 5.3.2.5 *Ex-Vivo* Torsion Testing

The femoral defect stiffness following healing under modulated conditions was about significantly higher than the intact contralateral femur and in the group stabilised with ExFixHigh. In addition, the torsional stiffness in the Modulated group was 14% lower than in the ExFixLow group, however this difference was not statistically significant. There were no other differences observed between the treatment groups (Figure 5.17 and Table 5.3).

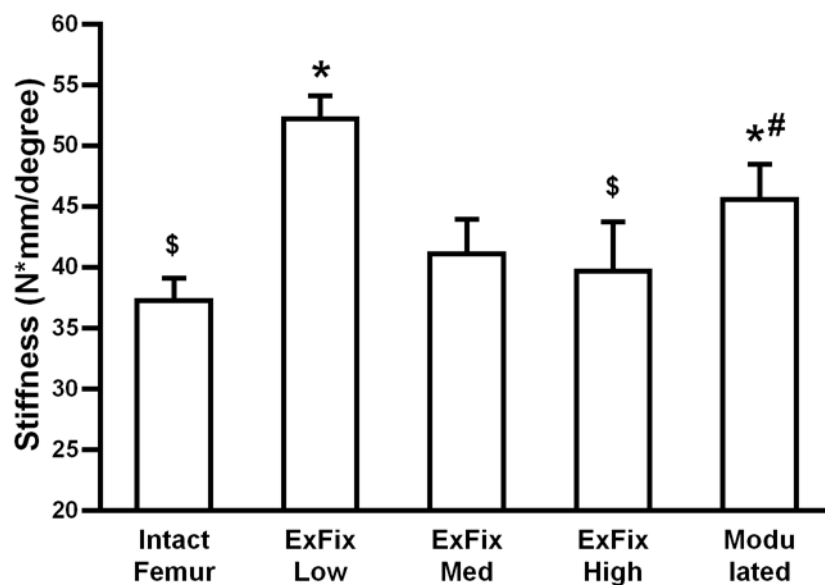


**Figure 5.17** Torsional stiffness of femurs treated with rhBMP-2 in four different groups 8 weeks post-surgery, compared to the intact contralateral femur (mean  $\pm$  SEM). Asterisks indicate statistical significance from intact, contralateral femur, dollar signs indicate statistical significant difference from Modulated, and hash signs indicate significant difference from ExFixHigh ( $p < 0.05$ ,  $n=7-8$  per group).

Interestingly, defects healed under modulated conditions were considerably stronger than the intact femur and defects stabilised with ExFixLow, ExFixMed and ExFixHigh (Figure. 5.18 and Table 5.3). However, this only reached statistical significance when the Modulated group was compared to the intact femur and the ExFixHigh group. This is probably due to the small sample size.

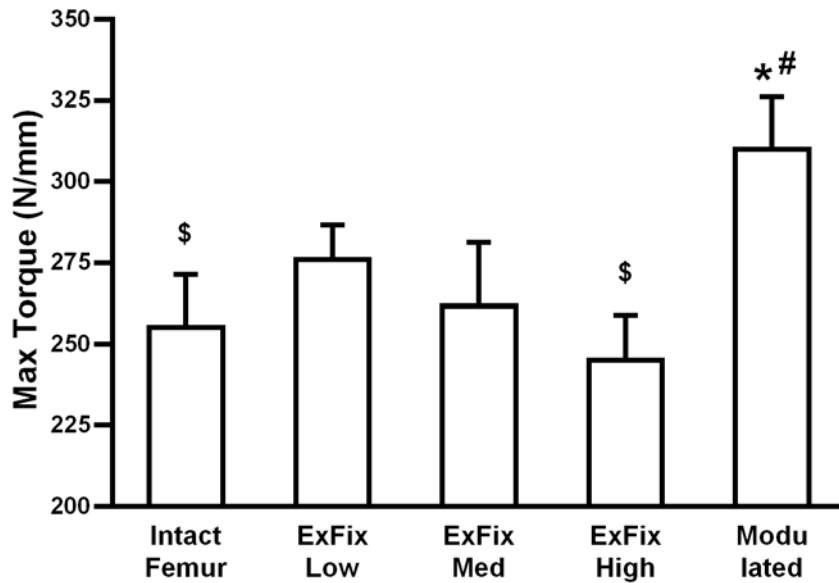


**Figure 5.18** Maximum Torque of femurs 8 weeks post-surgery compared to the intact contralateral femur (mean  $\pm$  SEM). Asterisks indicate statistical significance from intact, contralateral femur, dollar signs indicate statistical significant difference from Modulated, and hash signs indicate significant difference from ExFixHigh ( $p < 0.05$ ,  $n=7-8$  per group).

### 5.3 DISCUSSION

The experiments described in this Chapter stemmed from the results discussed in Chapter 4 where the lower stiffness fixators accelerated the early stages of defect healing by stimulating the formation and mineralization of callus. By two weeks, there was clear evidence of mineralization, which was assumed to reflect endochondral ossification. Because of data from the fracture repair literature showing that excess motion inhibits endochondral ossification by impairing angiogenesis [34, 41, 88, 91, 92, 95, 106, 108, 131, 136, 155], it was decided to increase the stiffness of the fixator two weeks post-operatively. The results described in this Chapter confirm that initial stabilisation with ExFixLow followed at two weeks by ExFixHigh indeed improves defect healing both in terms of the speed of healing and the quality of the healed bone. However, histological examination of the defects within the first two post-operative weeks provided no evidence of an endochondral process. This surprising result needs further study. Nevertheless the data are in general agreement with several studies showing that the early stages of

fracture healing are especially sensitive to mechanical conditions and that these might direct the entire healing process [35, 83, 120, 131, 134, 142].

Histological inspection revealed that six days post-surgery no healing was evident, regardless of the fixation. The collagen sponge used as a carrier for the rhBMP-2 was still present in the defect and there was a slight periosteal reaction adjacent to the defect in the two lowest stiffness external fixator groups (Figure 5.6). By day nine the histological appearance of the defects changed. Defects stabilized with two lowest stiffness fixators had evidence of new bone formation and surprisingly the defect was bridged with a thickened layer of fibrous tissue that looked like periosteum (Figure 5.2), which was not seen in the group with rigid fixator. Five days later, two weeks post surgery, the appearance of defects changed dramatically. Defects in the groups with lower stiffness fixators were largely filled with new woven bone (Figure 5.4) although the layer that bridged the defect was fibrous tissue with appearance of periosteum. Only small cartilaginous areas were present, consistent with the formation of bone through an endochondral process. However, this must have happened very quickly, within a period of 5 days. An alternative explanation is that the bone formed by direct osteogenesis, without a cartilaginous intermediate. Further experiments are needed to distinguish between these two possibilities. Remarkably, defects stabilised with the most rigid fixator, lacked external callus, and showed no evidence of ossification. Small areas of cartilage were visible and ACS was still present (Figure 5.5).

The histological data confirm the radiologic data of Chapter 4 in demonstrating that healing of the defects is favoured by the lowest stiffness fixator. However, contrary to expectation, no cartilaginous callus was seen at any time point. At 9 days the defects stabilised by ExFixLow contained fibrous tissue, and at 2 weeks they were mostly filled with new bone. As noted, the biological changes that occur during the interim 5 days merit further scrutiny. There are almost no prior published data to aid consideration of this point. Yasko et al. [61] showed that, under the conditions imposed by their fixators, healing of rat segmental defects occurred via an endochondral process. The purpose for their study was to determine whether implants of rhBMP-2 cause bone formation in an osseous bone location and whether the activity of this protein promotes functional angiogenesis at the site of

implantation, and whether a segmental defect created at the length that predictably precludes union, can be healed by the bone that is formed. They used two different doses 1.4 or 11  $\mu\text{g}$  of rhBMP-2 protein implanted in each defect together with guanidine-hydrochloride extracted demineralized rat bone matrix as a carrier and compared this to the matrix carrier only. They found that both doses of rhBMP-2 induced formation of endochondral bone in the osseous defect, in a dose dependent manner. The high dose yielded significant bone formation resulting in radiographic, histological and mechanical evidence of union. On the contrary, lower dose of protein failed to show any new bone formation until the third or fourth week and the scant bone that formed in the defect failed to progress resulting in a non-union in all instances. Most importantly they found that no specimen had formation of bone in the defect without evidence of formation of cartilage as observed by a time course histological study. They also found that implantation of rhBMP-2 did not exhibit enhanced functional blood flow in the defect seven days post surgery. Even though, determining the mechanical environment was not one of the aims of this study, they also observed that in several specimens bone formed eccentrically along the region opposite the plate. They postulate that the ultimate shape and size of the resultant bone that formed in the defect may have followed the pattern related to the mechanical environment of fixation device they used.

The premise for the change to a much stiffer fixator at 2 weeks (fixator “Modulation”) was to potentiate the more rapid calcification of a cartilaginous callus, which would then be replaced by a woven bone and then remodelled into lamellar bone. Although this premise was shown to be incorrect, it nevertheless produced a dramatically beneficial effect on defect healing. Radiographic images revealed that one week after modulation there was complete osseous union with no evidence of soft tissue, unlike in the other groups. Furthermore, as healing progressed weekly X-rays showed decrease in the external callus and at the end of eight weeks treatment the callus size appeared to be smaller and resembled the shape of the native femur (Figure 5.8A&B). These findings were supported by 3D high-resolution  $\mu\text{CT}$  images (Figure 5.14A&B and 5.15A&B), where the decrease in the external callus was found to be significantly smaller than in defects where the ExFixLow had not been exchanged for a high stiffness fixator. Interestingly, the bone



area of the healed defect was also significantly lower. In fact, in the Modulated group, the bone area was significantly lower than in any other stiffness group, but it had more bone than the intact, contralateral femur. In addition, transverse images from the healed defects in the Modulated group appeared to have a more uniform and symmetrical distribution of circumferential callus and smaller numbers of trabeculae, than in the other treatment groups. Transverse  $\mu$ CT revealed that formation of a new cortex was especially well developed in the Modulated group (Figure 5.15A&B). This conclusion is supported by the histological data showing thicker and uniform distribution of neocortical callus (Figure 5.16).

The marrow cavity of defects healed under Modulated conditions contained far fewer trabecular struts than those of the other groups, further suggesting enhanced osseous remodelling and maturation. Defects stabilised with lowest stiffness fixator for the entire 8 weeks of the experiment had a bigger external callus, thinner and asymmetric distribution of neocortical bone, and much higher amounts of trabecular bone inside the marrow cavity. In the two higher stiffness groups the repair process appeared to be even slower. Histological slides stained with safranin O-fast green revealed the presence of residual cartilage within the defect area (Figure 5.15 third and forth row). This may imply that, in these two groups, the healing process after eight weeks is incomplete.

The radiographic,  $\mu$ CT and histologic findings were further supported by additional analyses. For example, BMC, as measured by DXA, returned to the untreated contralateral femur values within the eight weeks after Modulation treatment. On the contrary, in all other groups where different stiffness external fixators were used, BMC remained significantly higher than normal at 8 weeks. This might suggest slower remodelling, associated with the accumulation of more mineralized tissue, which would make bones more brittle and could jeopardize the mechanical integrity of repaired defect. This conclusion is supported by the results of biomechanical testing, which showed that torsional stiffness in these groups were significantly lower than in the Modulated and lowest stiffness fixator groups, but reached the same values as the contralateral femur. Interestingly, the maximum torque, which is the amount of force needed to break the bone in torsion, was significantly higher than contralateral femur in all groups, except ExFixHigh group. The higher

maximum torque in the Modulated group might have been attributed to the more advanced healing of the CSD defect. This finding is reflected by smaller callus, the formation of which appeared to be accelerated, and enhanced remodelling resulting in a more rapid reduction of periosteal and endosteal callus, especially when compared to the group with lowest stiffness external fixator. The enhanced repair and remodelling of the Modulated group is also reflected in a higher strength and lower bone mineral content. These effects might have been caused by smaller IFM in the defect, although this was not measured in this study, which might have prevented disruption of vascular supply, hence allowed faster repair process and increased remodelling of the repaired defects. Furthermore, the effect of natural weight bearing on defect healing was not investigated in this study and needs to be addressed in the future experiments.

In conclusion, this current experiment revealed that early axial modulation, from lower to more rigid fixation, resulted in accelerated callus maturation, which presented with more organized bone architecture of healed defects. In addition, the Modulated group appeared to induce faster remodelling of endosteal and periosteal callus tissue, which exhibited with reduced callus size at the end of treatment as compared with the Low external fixator group. Moreover, the torsional strength of the 5mm healed defect was significantly increased. These factors could be also associated with a secondary effect of early weight bearing related to decreased pain in the injured femur due to a more stable defect gap conditions with more rigid fixator, which allowed healing of defect in more efficient and timely manner. Surprisingly, we were not able to obtain strong histological evidence of endochondral ossification as a mechanism of defect repair. Further investigation is needed to determine the pathway of bone healing in CSDs and how this is modulated by the ambient mechanical environment.

Summary of *in-vivo* and *in-vitro* results of the physical testing are collated in Table 5.3

<i>Variables</i>	<b>Intact Femur</b> (n=10)	<b>ExFixLow</b> (n=10)	<b>ExFixMed</b> (n=9)	<b>ExFixHigh</b> (n=9)	<b>Modulated</b> (n=9)
<b><i>In-Vivo Data</i></b>					
TA (mm <sup>2</sup> )	12.7±0.3 <sup>#</sup> \$	29.8±1.5* <sup>#</sup> \$	24.4±2.0* <sup>\$</sup>	21.5±2.1* <sup>\$</sup>	27.6±0.8* <sup>#</sup>
BA (mm <sup>2</sup> )	8.3±0.2 <sup>#</sup> \$	15.8 ± 1.3* <sup>#</sup> \$	13.8 ± 1.4* <sup>\$</sup>	12.8 ± 1.2* <sup>\$</sup>	10.0±0.7* <sup>#</sup>
BA/TA (%)	65.1±0.9 <sup>\$</sup>	53.6±4.1* <sup>\$</sup>	59.6±7.6 <sup>\$</sup>	62.4±6.4 <sup>\$</sup>	36.2±2.8* <sup>#</sup>
pMOI (mm <sup>4</sup> )	23.1±1.2 <sup>#</sup> \$	85.9±3.5* <sup>\$#</sup>	61.8±8.2* <sup>\$</sup>	54.4±8.1* <sup>\$</sup>	61.4±3.0* <sup>\$</sup>
BMC (g)	0.08±0.01 <sup>#</sup>	0.1±0.02* <sup>\$</sup>	0.09±0.02* <sup>\$</sup>	0.09±0.03* <sup>\$</sup>	0.1±0.02* <sup>\$</sup>
Torsion Stiffness (N/mm)	n=9 37.3±1.7	n=7 52.2±4.4	n=8 42.7±2.8	n=7 39.7±4.0	n=8 45.6±2.9
Max Torque (N*mm/ degree)	255.1±16	275.9±11	261.7±24	244.9±14	309.8±26
<b>Stiffness (N/mm)</b>	<b><i>In- Vitro Data – Axial Compression Construct Testing (n=6)</i></b>				
No Defect	N/A	33.6±0.9 <sup>\$</sup>	36.0±0.9 <sup>\$#</sup>	39.6±0.6 <sup>#</sup>	N/A
5mm Defect	N/A	33.6±0.9 <sup>\$</sup>	36.0±0.9 <sup>\$#</sup>	39.6±0.6 <sup>#</sup>	N/A
Rubber	N/A	38.7±0.7 <sup>\$</sup>	42.7±0.5 <sup>\$#</sup>	46.2±0.8 <sup>#</sup>	N/A
LDPE	N/A	214.8±9.6	220.0±6.8	263.2±9.5	N/A
Wood	N/A	315.9±36 <sup>#</sup>	351.4±24 <sup>#</sup>	368.2±21	N/A

**Table 5.3** *In-vivo* segmental healing characteristics of Intact femur, Modulated, ExFixLow, ExFixMed and ExFixHigh treated with rhBMP-2 as measured by MicroCT (n=9-10), DXA (n=9-10), Torsional testing (n=7-8), (mean ± SEM); and *in-vitro* results from axial compression construct testing: no defect, 5mm empty defect and with different inserts such as rubber, LDPE, wood (mean ± SEM, n=6). Asterisks indicate statistical significance from intact, contralateral femur, dollar signs indicate statistical significant difference from Modulated, and hash signs indicate significant difference from ExFixHigh (p < 0.05).

## **CHAPTER SIX**

### ***GENERAL DISCUSSION***

The overall aims of this project were to determine whether the healing of CSDs in response to rhBMP-2 is responsive to the ambient mechanical environment and, if so, whether this information could be used to improve healing. Although the effects of mechanics on the spontaneous repair of sub-critical sized, osseous defects have been studied extensively, there is almost no prior literature concerning CSDs. Moreover, the intersection of mechanical signals and biological signals in the context of bone healing *in-vivo* has not been studied in detail. Thus, the novelty of this study is that it is the first to demonstrate interactions between the mechanical environment and the ability of a locally applied growth factor to enhance CSD healing *in-vivo*.

In many cell types the mechanical environment critically influences cellular behaviour [156-159]. Several studies using different cell types found that BMPs and their antagonists are regulated by mechanical stimulation and influence BMP signalling in an autocrine or paracrine fashion [160-163]. Furthermore, responses of endogenous and exogenous BMPs to mechanical stimulation have been demonstrated in several studies, and it has been reported that there is optimal magnitude and type of loading for BMP-2 expression [75, 76, 145]. In one *in-vitro* study,, for example, static tensile force enhanced the osteoblastic differentiation of MSCs in response to BMP-2, while tensile force alone increased cell proliferation [76]. In light of studies such as these, it is not surprising that my data demonstrate such a powerful effect of the mechanical environment on the healing of CSDs in response to BMP-2.

The data presented in this thesis confirm the high responsiveness of CSD healing to mechanical influences, but suggest that there are important differences between the responses of CSDs and sub-critical sized defects. Importantly, it proved possible to enhance dramatically the healing of CSDs in the rat femur by modulating the stiffness of fixation during the healing process. If also true for humans, this could have important clinical implications.

Investigation of these issues required the design and manufacture of novel fixators of known stiffness, and whose stiffness could be reliably modulated in a precise, quantitative fashion at will. As described in Chapter 2, the newly developed external fixator has several unique features. Firstly, unlike alternatives found in the literature

[77, 164], including one I have used in the past (ExFixOld) [54, 55, 60], the new fixator was designed to have a minimal mass to avoid uncontrolled motion due to inertia. In addition, to create a reproducible 5mm defect with the minimal trauma to the bone and surrounding soft tissue, conventional and rotating saws were not considered. Instead a saw guide was created and used in conjunction with a gigly (wire) saw. Connecting elements of various stiffnesses were created for the external fixator to produce different mechanical environments. This configuration also allows the connecting elements to be changed *in-vivo* while still attached to the animal, thereby allowing the mechanical environment to be changed during the healing process. This is important, because it is likely that different stages of healing respond differently to mechanical stimuli. In many of the experiments described in this thesis, the novel fixator was compared to an earlier model, ExFixOld, with which our laboratory has much experience and a wealth of historical data.

Only three different connective elements were created for this project, allowing study of three different stiffnesses, but additional stiffnesses could be created easily depending on the requirements of future studies. Furthermore, the fixator was made so that a preset offset of exactly 6mm was reproducibly and reliably achieved using precisely manufactured titanium screws designed specifically for this fixator. This is in contrast to the majority of previously published fixators, including ExFixOld, where investigators have used K-wires to secure the fixators [54-56, 59-61, 165]. Descriptions of previous devices, moreover, do not mention the preset offset from the bone surface to the plate or external fixator, which makes it difficult to determine the local mechanical conditions. In addition, K-wires are known to have poor rotational stability, and the type of motion this creates has been shown to inhibit the process of bone healing, especially when it is used as an intramedullary nail [97]. Knowing the precise local mechanical conditions is essential to the interpretation of the outcome of bone healing studies.

These observations raise another important issue -- fixator stability. Although mechanical properties can be easily determined experimentally, surprisingly few investigators have characterized the *in-vitro* and *in-vivo* mechanical properties of the fixation devices used for their studies. The most important mechanical factors are the

axial and shear IFMs in the plane of the fracture surface. These movements are influenced by the load applied to the fixation device (weight bearing and muscle forces) and the stiffness of the device. Although, due to limited resources, we were not able to perform torsional stiffness testing, the axial test is sufficient enough to answer the key question proposed in this thesis. The mechanical properties of the newly designed external fixators were examined at three levels. First, *in-vitro* three point bending tests were carried out to determine the rigidity of the stability bars. Fixators were then installed on excised rat femurs, with and without 5mm defects, and tested in axial compression to imitate weight bearing. Finally, to approximate the alterations in the mechanical properties of the defect as it heals, rubber, plastic and wood were inserted into the defects to simulate different phases of healing. The results of these studies showed convincingly that the mechanical environment cannot be explained solely in terms of the properties of the components used to construct the fixator. It is essential to measure the overall mechanical properties of the entire fixator construct attached to bone, and to take into account mechanical contributions from the defect tissue itself as it heals. These issues were most dramatically illustrated with ExFixOld, which has an extremely stiff stability bar, yet provided minimal support to a fresh defect because of its offset (distance) from the bone and because it was secured with K-wires. However, according to my mechanical testing simulation data, as healing progressed and contributed increasingly to the overall stability of the defect, femora stabilised with ExFixOld became extremely stiff. This further indicates the need to appreciate temporal changes in the mechanical environment that occur as healing progresses. Besides the parameters tested in this study, which determine the *in-vitro* stability of the fixation, other factors are important for *in-vivo* success. To prevent a screw from pulling out from the bone, a certain depth of thread (core diameter) and thickness between the threads were chosen specifically for the cortical bone material. Also, the ratio of drill diameter to the screw diameter, that determines the pre-stress in bone due to insertion of the threaded pins, was also carefully calculated to prevent bone fractures through the pinholes. The possible contribution of surrounding soft tissues to the mechanical environment within the defect was not considered in my studies, although this should be investigated in the future. Having constructed and characterised the novel

fixators, their effects on the healing of a 5mm femoral defect in the rat were investigated.

The *in-vivo* studies showed that earlier and bigger callus was formed with the lower stiffness external fixators. On the contrary the more rigid device produced significantly smaller callus, with delayed appearance of external callus over the same time period. Nevertheless, all defects healed and after 8 weeks the material properties (bone mineral content, g) of the new bone formed with the different stiffness fixators were not significantly different. However, the structure of the healed defect, as assessed by  $\mu$ CT and histology, differed considerably. With the highest stiffness fixator, ExFixHigh, the new bone was irregular in morphology and contained discontinuities, which appear histologically as areas of cartilage. Such discontinuities were less evident using the fixator of medium stiffness, ExFixMed, but the transverse  $\mu$ CT images suggested in each case a “hole” in the centre of the healed bone. Histology did not reveal extensive areas of cartilage in this region, so they are best explained as areas of unmineralised fibrous tissue. Surprisingly, the most impressive healing was accomplished with the lowest stiffness fixator, ExFixLow: defects were filled with bone, no cartilage was seen and the neo-cortex was regular and continuous. This result was unexpected, because data from studies of sub-critical defects and fractures suggest that low stiffness generates abundant cartilage that fails to undergo endochondral ossification because excessive IFM disrupts the formation of new blood vessels. This indicates that the mechano-biology of the healing of CSDs is either dissimilar from that of fractures or sub-critical sized defects, or that stiffness needs to be further reduced before it becomes detrimental to the healing process.

Based upon these data, it was decided to attempt to improve outcome by modulating the stiffness of the fixator during healing. The original hypothesis, consistent with the radiological data shown in Chapter 4, was that low stiffness accelerated healing during the first two weeks, at which time mineralization was first evident. At the time, we considered this to be the beginning of endochondral ossification, a process thought to be favoured by high stiffness. Accordingly, two weeks post-surgery the connection elements of the fixator stability bar were changed from lowest to highest



stiffness. The results of this experiment, described in Chapter 5, are quite provocative.

As hypothesised, healing was dramatically enhanced by modulating the stiffness during healing, in the manner described above. Compared to defects stabilised with an invariable stiffness fixator for the entire 8 weeks, healing was accelerated and the newly formed bone had far more uniform new cortices and fewer trabeculae within the marrow cavity; no cartilage was present. The external callus was significantly smaller in the Modulated group as compared to the ExFixLow group, but significantly higher than in all other stiffness groups including the contralateral femur. In contrast, the amount of bone within the callus was significantly lower in the Modulated group than in all different stiffness experimental groups. Indeed, the amount of bone within the callus was only 19% above the bone content of the contralateral femur. In addition, the stiffness of the healed defects in the Modulated group was significantly different from that of the intact femur and ExFixHigh, and the healed defects of the Modulated group were markedly stronger than all other tested groups. Furthermore, the bone mineral content of the healed defect, as determined by DXA, in the Modulated group were significantly lower than in all other stiffness groups, but were the same as the contralateral femur. Hence, this observation might suggest a more advanced healing and remodelling process in this group. Translated into a clinical setting, such an effect might allow weight bearing at a far earlier time than is presently the case.

Histological examination of defects at 6, 9 and 14 days gave surprising results. Based upon the supposition that healing would proceed via an endochondral process and that the first signs of radioopacity would indicate the beginning of cartilage mineralization, we expected to see cartilage at days 9 and 14. Instead, there was very little cartilage in any of the specimens. Instead, defects stabilised under low and moderate fixation had little evidence of new bone formation in the defect 9 days post surgery, yet extensive areas of woven bone after 14 days of treatment. In contrast, those stabilised under high stiffness had only fibrous tissue. Surprisingly, at days 9 and 14 in the two lowest stiffness groups, the defects were bridged by the thickened layer of what appeared histologically to be periosteal fibrous tissue. However from the X-ray images, this region appeared either as calcified cartilage or newly

mineralized bone. Further research, including the examination of undecalcified tissue sections, is needed to resolve this issue.

The formation of bone at low and medium stiffness appeared to have been rapid. At 6 days there was almost no evidence of repair activity. The defects were acellular and filled only with the collagen sponge used to deliver the rhBMP-2, although at the lowest two stiffnesses there was evidence of a marked periosteal reaction adjacent to the defects. At 9 days, however, there was extensive ingrowth of fibrous tissue into the defects, which at the lowest two stiffnesses had become woven bone by day 14. The absence of cartilage is puzzling and forces us to consider the possibility that healing occurred by the direct differentiation of precursor cells into osteoblasts rather than by endochondral ossification. If this were so, its apparent enhancement by low stiffness is highly surprising. Clearly, more research into the mechano-biology of healing under these conditions is warranted.

Relevant to our data is a recent report of a study by Claes et al. [149] where the investigators “dynamized” a rat osteotomy one week post-surgery, having first stabilised the defect with a high stiffness fixator. In their experiments switching from stiff to flexible fixation did not improve healing of the defect. This is compatible with research by other investigators [98, 166] showing that when fixation stability was changed from rigid to more flexible as healing progressed, there was no significant improvement in the biomechanical properties of the bone at the end of study. In some cases, it was even detrimental, no matter whether early or late dynamization was applied. Similarly, axial passive and active dynamisation under external fixation in stable and unstable fracture types seemed to provide an increased amount, and a more uniform distribution of, periosteal callus. However, changing fixator stiffness by removal of excessive pins or connecting sidebars did not enhance bone fracture healing. In contrast, only one study in dogs by Larrson et al. [151] found that early dynamisation appeared to accelerate callus maturation, as reflected by higher periosteal new bone formation and greater torsional stiffness. Importantly, weight bearing, without exception, proved to be the most important stimulus in restoring fractured bone to its original mechanical strength [167].

As noted, nearly all the literature on bone healing comes from studies of fractures and sub-critical sized defects. A major difference between these settings and the CSDs studied here is the ready availability of periosteal cells in fractures and sub-critical defects. This may be the crucial difference between sub-critical size and critical size defects that explains their different abilities to heal. Recent transplantation studies by the O’Keefe group [168-171] have confirmed the importance of the periosteum to the healing of fractures. By undertaking segmental cortical graft transplantations between wild-type and ROSA mice., where all cells are LacZ<sup>+</sup>, these investigators were able to distinguish host cells from donor cells. Zhang et al. [171] used this model to show the essential role of periosteal progenitor cell in bone graft healing. They noted that the surrounding periosteum is the first tissue to respond to injury. It undergoes a large proliferative response and cells from the cambial layer differentiate into chondrocytes to form a cartilaginous soft callus that subsequently undergoes endochondral ossification. They found that approximately 70% of osteogenesis on the graft was attributed to the expansion and differentiation of donor periosteal progenitor cells. Furthermore, engraftment of BMP-2 producing bone marrow stromal cells on nonvital allografts showed marked increases in cortical graft incorporation and neovascularization.

The above mechanism of periosteally initiated healing is not available to a CSD. Of possible high significance, our histological observations suggest that, in our model, periosteal cells spread along the surface of the collagen sponge, eventually forming a continuous bridge. This may be in response to a BMP-2 chemotactic gradient formed as BMP-2 leaches from the sponge. The study of Zhang et al. [171] and the present study both suggest that direct activation of the local periosteal progenitor cells is necessary to induce an early healing response. Intriguingly, this migration of periosteal cells in our models appears to occur first on the side furthest away from the fixator, which is also the side where radio-opacity is first noted. Periosteum is known to contain multipotent progenitor cells, and it is tempting to speculate that, under the mechanical conditions created by the external fixators, these cells undergo osteoblastic differentiation within the defect. Interestingly, an *in-vitro* study by Mitsui et al. [145] investigated BMP expression in cultured osteoblastic cells subjected to mechanical compression force. They used 0.5, 1, 2 and 3 g/cm<sup>2</sup>

compressive force on the cells and found that the highest BMP expression was seen when they used  $1\text{g/cm}^2$  force. This was associated with decreased expression of BMP antagonist such as chordin, noggin, and gremlin. This study identified an optimal force magnitude for supporting a BMP response, and demonstrates one way in which external fixator stiffness could help determine responses to BMP and induced osteogenesis.

The only other published report on the biology of CSD healing in response to rhBMP-2 is that of Yasko et al. [61]. Using a rat model similar to ours, stabilized with high-density polyethylene plate fixed with four K-wires, they demonstrated that healing occurred via a classical endochondral mechanism. The difference between our findings and theirs presumably resides with the different mechanical environments generated by the different fixation devices used in the two studies. Healing through endochondral ossification in the studies of Yasko et al could be also related to a different carrier [61]. They used demineralized rat-bone matrix (DBM) to delivery rhBMP-2. Although not able to induce bone healing by itself, DMB may nevertheless have provided additional growth factors that contributed to a chondrogenic response during the early the healing process.

Collectively, my data and those in the literature indicate the importance of mechanical forces in determining cell fate, as first suggested by Roux [37] and later in experimental data by Pauwels [36]. These hypotheses are consistent with data from multiple studies in fracture healing which showed that the mechanical strength, stiffness and the size of the fracture callus is related to the degree of fixation stability [81, 88, 133, 143]. Moreover, it has been observed that certain loading conditions inhibit the process of healing, both in animal models and clinically. For instance, monitoring of patients has demonstrated that the fixation systems in clinical use create complex load situations resulting in a mixture of different movements such as axial compression, translational shear, bending and axial torsion [87, 117, 172]. It is therefore essential to define boundaries of fixation stability for optimal healing on the basis of both clinically relevant fixation and loading conditions.

My data strongly suggest that healing of CSDs does not follow the rules established for fractures and sub-critical sized defects, and needs to be experimentally

investigated in its own right. In further agreement with this, histological data suggest that healing of CSDs does not occur by forming a double cortex [54-56, 59-61, 173], as is the case with rodent fracture healing [174-178].

The major conclusion from my work, that the healing of CSDs in response to BMPs, is exquisitely sensitive to the ambient mechanical environment, which can be manipulated to accelerate and improve repair, harks back to the pioneering studies of Roux over 100 years ago. Roux [37] was one of the first scientists to perform laboratory experiments, measuring strain transfer in bone models with photoelasticity equipment. He compared the mechanical environment on cells in a fracture callus with fracture repair patterns, and he proposed that deformation of shape is the specific stimulus for the formation of collagenous fibrils and hydrostatic compression is the specific stimulus for the formation of cartilaginous tissue; for osteogenesis to occur would require that the mechanical environment first becomes stabilized by the presence of fibrous tissue. Since the time of Roux, Pauwels and many other scientist, the mechanical conditions of bone repair have been widely studied by many scientists and clinicians, but many fundamental issues concerning the relationship between the mechanical environment and cellular response remain unclear, especially when the fracture gap is too large to heal spontaneously. While there exists an extensive literature, involving both clinical and experimental animal studies, reporting the effects on fracture repair of the local mechanical environment using various fixation devices with and without biologic therapies [35, 38, 41, 66, 73, 81, 83, 84, 87, 88, 91, 92, 98, 117, 120, 134-136, 138, 142, 143, 151, 164, 166, 172, 179-181], there are none concerning the healing of CSDs. This might be related to the false assumption that CSD healing is governed by the same rules as those that govern the healing of different types of fractures and osteotomies.

In Conclusion, this study clearly shows that critical size segmental defects treated with rhBMP-2 heal differently from fractures and this should be taken into consideration not only when planning new experimental studies but also when developing strategies for improving the clinical outcome. Careful selection of not only the biologic treatment but also the type of fixation device is required. More studies are required to establish the mechanisms through which biology and biomechanics interact at the tissue and cellular level. Once these are adequately

understood and translated into clinical practice, it will be possible to heal bones more quickly, inexpensively and reliably than is presently the case.

## FUTURE WORK

Several of the research areas touched upon in this study would benefit from further investigation. Because only 3 different stiffnesses and one modulation were compared in this study, we do not know whether healing could be enhanced further by using a greater range of stiffnesses, or by different modulation patterns. It would be a straightforward matter to produce fixators with a greater range of stiffnesses and to perform the necessary experiments.

A fully optimized repair protocol might reduce the need for rhBMP-2. Because rhBMP-2 is so costly, any reduction in its consumption would be of great socio-economic benefit. As noted, extremely large, wildly supra-physiological doses of rhBMP-2 are presently used. A protocol in which the mechanical environment is optimized could well reduce the rhBMP-2 requirement by log orders of magnitude.

A third fruitful area of further investigation is to understand the mechano-biology of healing under the conditions described in this thesis. The histological data are tantalising and provide evidence that healing under the conditions tested in this project may not follow the classical route of endochondral ossification. Clearly, there is much that could be done to study this. At a minimum, precise histological and imaging studies are needed to monitor, in a detailed fashion, the formation of bone within the defects. *In-vivo*  $\mu$ CT and other sophisticated *in-vivo* imaging techniques would be very helpful here. Coupled to such studies is the need to determine the origin of the osteoprogenitors that ultimately differentiate into bone within the defect. Preliminary histological data point to the periosteum as an important source, but bone marrow, adjacent muscle and circulating osteoprogenitors are additional possibilities that need evaluation.

Finally, because the ultimate goal of all experimental investigations of this type is to improve clinical outcome, conditions that have been optimised in the rat model need to be evaluated in a large animal, such as the sheep. Any reasonable procedures that allow CSDs to heal quicker and better, and which permit earlier weight bearing, while eliminating the need for bone grafting and, perhaps, reducing the need for rhBMP-2, should form the basis of future clinical trials.

## **GRADUATE SCHOOLS SKILLS PROGRAMME**

### **Completed Training:**

1. Introduction to Work as a Lecture
2. Using feedback efficiently and effectively



---

## REFERENCES

1. Jee, W.S., *Integrated Bone Tissue Physiology: Anatomy and Physiology*. Bone Mechanics Handbook, ed. S.C. Cowin. 2001: CRC Press.
2. Alamy.
3. Hert, J., *A new attempt at the interpretation of the functional architecture of the cancellous bone*. J Biomech, 1994. 27(2): p. 239-42.
4. Journals.Prous.com.  
[http://journals.prous.com/journals/dnp/20041701/html/dn170019/images/Tro en\\_fl.gif](http://journals.prous.com/journals/dnp/20041701/html/dn170019/images/Tro en_fl.gif).
5. Duncan, R.L. and C.H. Turner, *Mechanotransduction and the functional response of bone to mechanical strain*. Calcif Tissue Int, 1995. 57(5): p. 344-58.
6. Mikuni-Takagaki, Y., et al., *Distinct responses of different populations of bone cells to mechanical stress*. Endocrinology, 1996. 137(5): p. 2028-35.
7. Tan, S.D., et al., *Fluid shear stress inhibits TNFalpha-induced osteocyte apoptosis*. J Dent Res, 2006. 85(10): p. 905-9.
8. Cowin, S.C., *Bone stress adaptation models*. J Biomech Eng, 1993. 115(4B): p. 528-33.
9. SurgeonGeneral.gov, <http://www.surgeongeneral.gov/library/bone health/images /Figure2-3.gif>.
10. UWO.ca, <http://www.uwo.ca/pathol/cases /Skeletal/fracture4.jpg>.
11. Matsumoto, T., et al., *Circulating endothelial/skeletal progenitor cells for bone regeneration and healing*. Bone, 2008. 43(3): p. 434-9.
12. V.H.F., *Gavril A. Ilizarov, M.D., PH.D., D.SC. 1921-1992* J Bone Joint Surg Am, 1993. 75: p. 953.
13. *Who's Who in Orthopedics*. Gavriil Abramovich Ilizarov 1921–1992 2005: Springer London.
14. Aberdeenquest.com,  
<http://www.aberdeenquest.com/web/MultimediaFiles/ABDMS069413.JPG>.
15. Welch, R.D., et al., *Effect of recombinant human bone morphogenetic protein-2 on fracture healing in a goat tibial fracture model*. J Bone Miner Res, 1998. 13(9): p. 1483-90.

16. den Boer, F.C., et al., *Effect of recombinant human osteogenic protein-1 on the healing of a freshly closed diaphyseal fracture*. Bone, 2002. 31(1): p. 158-64.
17. Bouxsein, M.L., et al., *Recombinant human bone morphogenetic protein-2 accelerates healing in a rabbit ulnar osteotomy model*. J Bone Joint Surg Am, 2001. 83-A(8): p. 1219-30.
18. Li, G., et al., *Bone consolidation is enhanced by rhBMP-2 in a rabbit model of distraction osteogenesis*. J Orthop Res, 2002. 20(4): p. 779-88.
19. Einhorn, T.A., et al., *A single percutaneous injection of recombinant human bone morphogenetic protein-2 accelerates fracture repair*. J Bone Joint Surg Am, 2003. 85-A(8): p. 1425-35.
20. Seeherman, H.J., et al., *Recombinant human bone morphogenetic protein-2 delivered in an injectable calcium phosphate paste accelerates osteotomy-site healing in a nonhuman primate model*. J Bone Joint Surg Am, 2004. 86-A(9): p. 1961-72.
21. Seeherman, H., et al., *rhBMP-2/calcium phosphate matrix accelerates osteotomy-site healing in a nonhuman primate model at multiple treatment times and concentrations*. J Bone Joint Surg Am, 2006. 88(1): p. 144-60.
22. Boden, S.D., et al., *The use of rhBMP-2 in interbody fusion cages. Definitive evidence of osteoinduction in humans: a preliminary report*. Spine, 2000. 25(3): p. 376-81.
23. Burkus, J.K., et al., *Anterior lumbar interbody fusion using rhBMP-2 with tapered interbody cages*. J Spinal Disord Tech, 2002. 15(5): p. 337-49.
24. Dimar, J.R., et al., *Clinical outcomes and fusion success at 2 years of single-level instrumented posterolateral fusions with recombinant human bone morphogenetic protein-2/compression resistant matrix versus iliac crest bone graft*. Spine, 2006. 31(22): p. 2534-9; discussion 2540.
25. Johnsson, R., B. Stromqvist, and P. Aspenberg, *Randomized radiostereometric study comparing osteogenic protein-1 (BMP-7) and autograft bone in human noninstrumented posterolateral lumbar fusion: 2002 Volvo Award in clinical studies*. Spine, 2002. 27(23): p. 2654-61.
26. Kanayama, M., et al., *A prospective randomized study of posterolateral lumbar fusion using osteogenic protein-1 (OP-1) versus local autograft with ceramic bone substitute: emphasis of surgical exploration and histologic assessment*. Spine, 2006. 31(10): p. 1067-74.
27. Suh, D.Y., et al., *Delivery of recombinant human bone morphogenetic protein-2 using a compression-resistant matrix in posterolateral spine fusion in the rabbit and in the non-human primate*. Spine, 2002. 27(4): p. 353-60.

28. Vaccaro, A.R., et al., *A pilot safety and efficacy study of OP-1 putty (rhBMP-7) as an adjunct to iliac crest autograft in posterolateral lumbar fusions*. Eur Spine J, 2003. 12(5): p. 495-500.
29. Vaccaro, A.R., et al., *A 2-year follow-up pilot study evaluating the safety and efficacy of op-1 putty (rhbmp-7) as an adjunct to iliac crest autograft in posterolateral lumbar fusions*. Eur Spine J, 2005. 14(7): p. 623-9.
30. Vaccaro, A.R., et al., *A pilot study evaluating the safety and efficacy of OP-1 Putty (rhBMP-7) as a replacement for iliac crest autograft in posterolateral lumbar arthrodesis for degenerative spondylolisthesis*. Spine, 2004. 29(17): p. 1885-92.
31. Govender, S., et al., *Recombinant human bone morphogenetic protein-2 for treatment of open tibial fractures: a prospective, controlled, randomized study of four hundred and fifty patients*. J Bone Joint Surg Am, 2002. 84-A(12): p. 2123-34.
32. Swiontkowski, M.F., et al., *Recombinant human bone morphogenetic protein-2 in open tibial fractures. A subgroup analysis of data combined from two prospective randomized studies*. J Bone Joint Surg Am, 2006. 88(6): p. 1258-65.
33. Jones, A.L., et al., *Recombinant human BMP-2 and allograft compared with autogenous bone graft for reconstruction of diaphyseal tibial fractures with cortical defects. A randomized, controlled trial*. J Bone Joint Surg Am, 2006. 88(7): p. 1431-41.
34. O'Sullivan, M.E., E.Y. Chao, and P.J. Kelly, *The effects of fixation on fracture-healing*. J Bone Joint Surg Am, 1989. 71(2): p. 306-10.
35. Aro, H.T., H.T. Wahner, and E.Y. Chao, *Healing patterns of transverse and oblique osteotomies in the canine tibia under external fixation*. J Orthop Trauma, 1991. 5(3): p. 351-64.
36. Pauwels, F., *[A new theory on the influence of mechanical stimuli on the differentiation of supporting tissue. The tenth contribution to the functional anatomy and causal morphology of the supporting structure.]*. Z Anat Entwicklungsgesch, 1960. 121: p. 478-515.
37. Roux, W., *Der Zuchtende Kampf der Teile, oder die "Teilauslese" im Organismus*. 1891(See also: Roux, W. Anpassungslehre, Histomechanik, Histochemie. Mit Bemerkungen über die Entwicklung und Formgestaltung der Gelenke (Adaptation, Histomechanics and Histochemistry, with a notation about the development and formation of bones) Virchows Archiv 207:168-209;1912.).
38. Carter, D.R., P.R. Blenman, and G.S. Beaupre, *Correlations between mechanical stress history and tissue differentiation in initial fracture healing*. J Orthop Res, 1988. 6(5): p. 736-48.

39. Perren, S.M., Cordey J., *The Concept of Interfragmentary Strain*. In Uthoff HK(ed). *Internal fixation of Fractures*. 1980, Berlin: Springer-Verlag. 63-77.
40. Claes, L., et al., *Influence of size and stability of the osteotomy gap on the success of fracture healing*. J Orthop Res, 1997. 15(4): p. 577-84.
41. Lacroix, D. and P.J. Prendergast, *A mechano-regulation model for tissue differentiation during fracture healing: analysis of gap size and loading*. J Biomech, 2002. 35(9): p. 1163-71.
42. Schmitz, J.P. and J.O. Hollinger, *The critical size defect as an experimental model for craniomandibulofacial nonunions*. Clin Orthop Relat Res, 1986(205): p. 299-308.
43. Bruder, S.P., et al., *The effect of implants loaded with autologous mesenchymal stem cells on the healing of canine segmental bone defects*. J Bone Joint Surg Am, 1998. 80(7): p. 985-96.
44. Quarto, R., et al., *Repair of large bone defects with the use of autologous bone marrow stromal cells*. N Engl J Med, 2001. 344(5): p. 385-6.
45. Kusumoto, K., et al., *Comparative study of bone marrow induced by purified BMP and recombinant human BMP-2*. Biochem Biophys Res Commun, 1995. 215(1): p. 205-11.
46. Wang, E.A., *Bone morphogenetic proteins (BMPs): therapeutic potential in healing bony defects*. Trends Biotechnol, 1993. 11(9): p. 379-83.
47. Wozney, J.M. and V. Rosen, *Bone morphogenetic protein and bone morphogenetic protein gene family in bone formation and repair*. Clin Orthop Relat Res, 1998(346): p. 26-37.
48. Bostrom, M., et al., *Use of bone morphogenetic protein-2 in the rabbit ulnar nonunion model*. Clin Orthop Relat Res, 1996(327): p. 272-82.
49. Cook, S.D., et al., *The effect of recombinant human osteogenic protein-1 on healing of large segmental bone defects*. J Bone Joint Surg Am, 1994. 76(6): p. 827-38.
50. Gerhart, T.N., et al., *Healing segmental femoral defects in sheep using recombinant human bone morphogenetic protein*. Clin Orthop Relat Res, 1993(293): p. 317-26.
51. Sciadini, M.F. and K.D. Johnson, *Evaluation of recombinant human bone morphogenetic protein-2 as a bone-graft substitute in a canine segmental defect model*. J Orthop Res, 2000. 18(2): p. 289-302.
52. Cook, S.D., et al., *Recombinant human bone morphogenetic protein-7 induces healing in a canine long-bone segmental defect model*. Clin Orthop Relat Res, 1994(301): p. 302-12.

53. Cook, S.D., et al., *Effect of recombinant human osteogenic protein-1 on healing of segmental defects in non-human primates*. J Bone Joint Surg Am, 1995. 77(5): p. 734-50.
54. Betz, O.B., et al., *Direct percutaneous gene delivery to enhance healing of segmental bone defects*. J Bone Joint Surg Am, 2006. 88(2): p. 355-65.
55. Betz, V.M., et al., *Healing of segmental bone defects by direct percutaneous gene delivery: effect of vector dose*. Hum Gene Ther, 2007. 18(10): p. 907-15.
56. Hsu, W.K., et al., *Lentiviral-mediated BMP-2 gene transfer enhances healing of segmental femoral defects in rats*. Bone, 2007. 40(4): p. 931-8.
57. Hu, J., et al., *Callus formation enhanced by BMP-7 ex vivo gene therapy during distraction osteogenesis in rats*. J Orthop Res, 2007. 25(2): p. 241-51.
58. Brick, K.E., et al., *rhBMP-2 Modulation of Gene Expression in Infected Segmental Bone Defects*. Clin Orthop Relat Res, 2008.
59. Chu, T.M., et al., *Segmental bone regeneration using a load-bearing biodegradable carrier of bone morphogenetic protein-2*. Biomaterials, 2007. 28(3): p. 459-67.
60. Glatt, V., et al., *Ability of recombinant human bone morphogenetic protein 2 to enhance bone healing in the presence of tobramycin: evaluation in a rat segmental defect model*. J Orthop Trauma, 2009. 23(10): p. 693-701.
61. Yasko, A.W., et al., *The healing of segmental bone defects, induced by recombinant human bone morphogenetic protein (rhBMP-2). A radiographic, histological, and biomechanical study in rats*. J Bone Joint Surg Am, 1992. 74(5): p. 659-70.
62. Einhorn, T.A., et al., *The healing of segmental bone defects induced by demineralized bone matrix. A radiographic and biomechanical study*. J Bone Joint Surg Am, 1984. 66(2): p. 274-9.
63. Gomez-Benito, M.J., et al., *A 3D computational simulation of fracture callus formation: influence of the stiffness of the external fixator*. J Biomech Eng, 2006. 128(3): p. 290-9.
64. Carter, D.R., et al., *Mechanobiology of skeletal regeneration*. Clin Orthop Relat Res, 1998(355 Suppl): p. S41-55.
65. Claes, L.E., et al., *Effects of mechanical factors on the fracture healing process*. Clin Orthop Relat Res, 1998(355 Suppl): p. S132-47.
66. Kenwright, J. and T. Gardner, *Mechanical influences on tibial fracture healing*. Clin Orthop Relat Res, 1998(355 Suppl): p. S179-90.

67. Yasuda, I., *Dynamic callus and electric callus*. Bone Joint Surg, 1955. 37A: p. 1292-1299.
68. Yang, K.H., et al., *Exposure to low-intensity ultrasound increases aggrecan gene expression in a rat femur fracture model*. J Orthop Res, 1996. 14(5): p. 802-9.
69. Rubin, C.T. and L.E. Lanyon, *Regulation of bone formation by applied dynamic loads*. J Bone Joint Surg Am, 1984. 66(3): p. 397-402.
70. Rubin, C.T. and L.E. Lanyon, *Kappa Delta Award paper. Osteoregulatory nature of mechanical stimuli: function as a determinant for adaptive remodeling in bone*. J Orthop Res, 1987. 5(2): p. 300-10.
71. Isaksson, H., et al., *Comparison of biophysical stimuli for mechano-regulation of tissue differentiation during fracture healing*. J Biomech, 2006. 39(8): p. 1507-16.
72. Rubin, C., et al., *Anabolism. Low mechanical signals strengthen long bones*. Nature, 2001. 412(6847): p. 603-4.
73. Goodship, A.E., J.L. Cunningham, and J. Kenwright, *Strain rate and timing of stimulation in mechanical modulation of fracture healing*. Clin Orthop Relat Res, 1998(355 Suppl): p. S105-15.
74. Tsuji, K., et al., *BMP2 activity, although dispensable for bone formation, is required for the initiation of fracture healing*. Nat Genet, 2006. 38(12): p. 1424-9.
75. Sato, M., et al., *Mechanical tension-stress induces expression of bone morphogenetic protein (BMP)-2 and BMP-4, but not BMP-6, BMP-7, and GDF-5 mRNA, during distraction osteogenesis*. J Bone Miner Res, 1999. 14(7): p. 1084-95.
76. Kim, I.S., et al., *Synergistic action of static stretching and BMP-2 stimulation in the osteoblast differentiation of C2C12 myoblasts*. J Biomech, 2009. 42(16): p. 2721-7.
77. Mark, H., et al., *An external fixation method and device to study fracture healing in rats*. Acta Orthop Scand, 2003. 74(4): p. 476-82.
78. Feighan, J.E., et al., *Induction of bone by a demineralized bone matrix gel: a study in a rat femoral defect model*. J Orthop Res, 1995. 13(6): p. 881-91.
79. Hunt, T.R., J.R. Schwappach, and H.C. Anderson, *Healing of a segmental defect in the rat femur with use of an extract from a cultured human osteosarcoma cell-line (Saos-2). A preliminary report*. J Bone Joint Surg Am, 1996. 78(1): p. 41-8.
80. Jazrawi, L.M., et al., *Bone and cartilage formation in an experimental model of distraction osteogenesis*. J Orthop Trauma, 1998. 12(2): p. 111-6.

81. Probst, A., et al., *Callus formation and fixation rigidity: a fracture model in rats*. J Orthop Res, 1999. 17(2): p. 256-60.
82. Richards, M., et al., *Marrow-derived progenitor cell injections enhance new bone formation during distraction*. J Orthop Res, 1999. 17(6): p. 900-8.
83. Aro, H.T. and E.Y. Chao, *Bone-healing patterns affected by loading, fracture fragment stability, fracture type, and fracture site compression*. Clin Orthop Relat Res, 1993(293): p. 8-17.
84. Augat, P., et al., *Shear movement at the fracture site delays healing in a diaphyseal fracture model*. J Orthop Res, 2003. 21(6): p. 1011-7.
85. Augat, P., et al., *Local tissue properties in bone healing: influence of size and stability of the osteotomy gap*. J Orthop Res, 1998. 16(4): p. 475-81.
86. Claes, L., K. Eckert-Hubner, and P. Augat, *The fracture gap size influences the local vascularization and tissue differentiation in callus healing*. Langenbecks Arch Surg, 2003. 388(5): p. 316-22.
87. Duda, G.N., et al., *Interfragmentary motion in tibial osteotomies stabilized with ring fixators*. Clin Orthop Relat Res, 2002(396): p. 163-72.
88. Goodship, A.E., et al., *The role of fixator frame stiffness in the control of fracture healing. An experimental study*. J Biomech, 1993. 26(9): p. 1027-35.
89. Schell, H., et al., *The course of bone healing is influenced by the initial shear fixation stability*. J Orthop Res, 2005. 23(5): p. 1022-8.
90. Williams, E.A., et al., *The early healing of tibial osteotomies stabilized by one-plane or two-plane external fixation*. J Bone Joint Surg Am, 1987. 69(3): p. 355-65.
91. Wu, J.J., et al., *Comparison of osteotomy healing under external fixation devices with different stiffness characteristics*. J Bone Joint Surg Am, 1984. 66(8): p. 1258-64.
92. Grundnes, O. and O. Reikeras, *Effects of instability on bone healing. Femoral osteotomies studied in rats*. Acta Orthop Scand, 1993. 64(1): p. 55-8.
93. Molster, A.O., *Effects of rotational instability on healing of femoral osteotomies in the rat*. Acta Orthop Scand, 1984. 55(6): p. 632-6.
94. Utvag, S.E., D.B. Rindal, and O. Reikeras, *Effects of torsional rigidity on fracture healing: strength and mineralization in rat femora*. J Orthop Trauma, 1999. 13(3): p. 212-9.
95. Molster, A.O. and N.R. Gjerdet, *Effects of instability on fracture healing in the rat*. Acta Orthop Scand, 1984. 55(3): p. 342-6.

96. Molster, A.O., et al., *Controlled bending instability in the healing of diaphyseal osteotomies in the rat femur*. J Orthop Res, 1987. 5(1): p. 29-35.
97. Schoen, M., et al., *Introduction of a new interlocked intramedullary nailing device for stabilization of critically sized femoral defects in the rat: A combined biomechanical and animal experimental study*. J Orthop Res, 2008. 26(2): p. 184-9.
98. Utvag, S.E., et al., *Influence of flexible nailing in the later phase of fracture healing: strength and mineralization in rat femora*. J Orthop Sci, 2001. 6(6): p. 576-84.
99. Pacicca, D.M., D.C. Moore, and M.G. Ehrlich, *Physiologic weight-bearing and consolidation of new bone in a rat model of distraction osteogenesis*. J Pediatr Orthop, 2002. 22(5): p. 652-9.
100. Radomisli, T.E., et al., *Weight-bearing alters the expression of collagen types I and II, BMP 2/4 and osteocalcin in the early stages of distraction osteogenesis*. J Orthop Res, 2001. 19(6): p. 1049-56.
101. Sato, K. and M.R. Urist, *Induced regeneration of calvaria by bone morphogenetic protein (BMP) in dogs*. Clin Orthop Relat Res, 1985(197): p. 301-11.
102. Sato, M., et al., *Expression of bone matrix proteins mRNA during distraction osteogenesis*. J Bone Miner Res, 1998. 13(8): p. 1221-31.
103. Seebach, C., et al., *Intermittent parathyroid hormone (1-34) enhances mechanical strength and density of new bone after distraction osteogenesis in rats*. J Orthop Res, 2004. 22(3): p. 472-8.
104. Sojo, K., et al., *Immunohistochemical study of vascular endothelial growth factor (VEGF) and bone morphogenetic protein-2, -4 (BMP-2, -4) on lengthened rat femurs*. J Craniomaxillofac Surg, 2005. 33(4): p. 238-45.
105. Yasui, N., et al., *Three modes of ossification during distraction osteogenesis in the rat*. J Bone Joint Surg Br, 1997. 79(5): p. 824-30.
106. Harrison, L.J., et al., *Controlled induction of a pseudarthrosis: a study using a rodent model*. J Orthop Trauma, 2003. 17(1): p. 11-21.
107. Kaspar, K., et al., *An easily reproducible and biomechanically standardized model to investigate bone healing in rats, using external fixation*. Biomed Tech (Berl), 2007. 52(6): p. 383-90.
108. Mark, H., et al., *Effects of fracture fixation stability on ossification in healing fractures*. Clin Orthop Relat Res, 2004(419): p. 245-50.
109. Mark, H. and B. Rydevik, *Torsional stiffness in healing fractures: influence of ossification: an experimental study in rats*. Acta Orthop, 2005. 76(3): p. 428-33.



110. McCann, R.M., et al., *Effect of osteoporosis on bone mineral density and fracture repair in a rat femoral fracture model*. J Orthop Res, 2008. 26(3): p. 384-93.
111. Smith-Adaline, E.A., et al., *Mechanical environment alters tissue formation patterns during fracture repair*. J Orthop Res, 2004. 22(5): p. 1079-85.
112. Cullinane, D.M., et al., *The effect of recombinant human osteogenic protein-1 (bone morphogenetic protein-7) impregnation on allografts in a canine intercalary bone defect*. J Orthop Res, 2002. 20(6): p. 1240-5.
113. Cullinane, D.M., et al., *Effects of the local mechanical environment on vertebrate tissue differentiation during repair: does repair recapitulate development?* J Exp Biol, 2003. 206(Pt 14): p. 2459-71.
114. Dickson, G.R., et al., *Microcomputed tomography imaging in a rat model of delayed union/non-union fracture*. J Orthop Res, 2008. 26(5): p. 729-36.
115. Jager, M., et al., *The critical size bony defect in a small animal for bone healing studies (II): implant evolution and surgical technique on a rat's femur*. Biomed Tech (Berl), 2005. 50(5): p. 137-42.
116. Willie, B., et al., *Mechanical characterization of external fixator stiffness for a rat femoral fracture model*. J Orthop Res, 2009. 27(5): p. 687-93.
117. Gardner, T.N., M. Evans, and J. Kenwright, *The influence of external fixators on fracture motion during simulated walking*. Med Eng Phys, 1996. 18(4): p. 305-13.
118. Morgan, E.F., et al., *Mechanotransduction and fracture repair*. J Bone Joint Surg Am, 2008. 90 Suppl 1: p. 25-30.
119. Leong, P.L. and E.F. Morgan, *Measurement of fracture callus material properties via nanoindentation*. Acta Biomater, 2008. 4(5): p. 1569-75.
120. Carter, D.R. and M. Wong, *The role of mechanical loading histories in the development of diarthrodial joints*. J Orthop Res, 1988. 6(6): p. 804-16.
121. Perren, S.M. and B.A. Rahn, *Biomechanics of fracture healing*. Can J Surg, 1980. 23(3): p. 228-32.
122. Anderson, L.D., W.S. Gilmer, Jr., and R.E. Tooms, *Experimental fractures treated with loose and tight fitting medullary nails*. Surg Forum, 1962. 13: p. 455-7.
123. Yamagishi, M. and Y. Yoshimura, *The biomechanics of fracture healing*. J Bone Joint Surg Am, 1955. 37-A(5): p. 1035-68.
124. Peterson, B., et al., *Healing of critically sized femoral defects, using genetically modified mesenchymal stem cells from human adipose tissue*. Tissue Eng, 2005. 11(1-2): p. 120-9.

125. Ridler, T.W., Calvard S., *Picture thresholding using an iterative selection method*. Trans Sys Cybern, 1978. 8(8): p. 629-632.
126. Hildebrand, T., et al., *Direct three-dimensional morphometric analysis of human cancellous bone: microstructural data from spine, femur, iliac crest, and calcaneus*. J Bone Miner Res, 1999. 14(7): p. 1167-74.
127. Hildebrand, T. and P. Ruegsegger, *Quantification of Bone Microarchitecture with the Structure Model Index*. Comput Methods Biomech Biomed Engin, 1997. 1(1): p. 15-23.
128. Cheline, A.J., A.H. Reddi, and R.B. Martin, *Bone morphogenetic protein-7 selectively enhances mechanically induced bone formation*. Bone, 2002. 31(5): p. 570-4.
129. Pekkarinen, T., et al., *Reindeer BMP extract in the healing of critical-size bone defects in the radius of the rabbit*. Acta Orthop, 2006. 77(6): p. 952-9.
130. Vogelín, E., et al., *Healing of a critical-sized defect in the rat femur with use of a vascularized periosteal flap, a biodegradable matrix, and bone morphogenetic protein*. J Bone Joint Surg Am, 2005. 87(6): p. 1323-31.
131. Klein, P., et al., *The initial phase of fracture healing is specifically sensitive to mechanical conditions*. J Orthop Res, 2003. 21(4): p. 662-9.
132. Bishop, N.E., et al., *Shear does not necessarily inhibit bone healing*. Clin Orthop Relat Res, 2006. 443: p. 307-14.
133. White, A.A., 3rd, M.M. Panjabi, and W.O. Southwick, *Effects of compression and cyclical loading on fracture healing--a quantitative biomechanical study*. J Biomech, 1977. 10(4): p. 233-9.
134. Augat, P., et al., *Early, full weightbearing with flexible fixation delays fracture healing*. Clin Orthop Relat Res, 1996(328): p. 194-202.
135. Cheal, E.J., et al., *Role of interfragmentary strain in fracture healing: ovine model of a healing osteotomy*. J Orthop Res, 1991. 9(1): p. 131-42.
136. Epari, D.R., et al., *Instability prolongs the chondral phase during bone healing in sheep*. Bone, 2006. 38(6): p. 864-70.
137. Chao, E.Y. and N. Inoue, *Biophysical stimulation of bone fracture repair, regeneration and remodelling*. Eur Cell Mater, 2003. 6: p. 72-84; discussion 84-5.
138. Claes, L., et al., *Temporary distraction and compression of a diaphyseal osteotomy accelerates bone healing*. J Orthop Res, 2008. 26(6): p. 772-7.
139. Cullinane, D.M., et al., *Induction of a neoarthrosis by precisely controlled motion in an experimental mid-femoral defect*. J Orthop Res, 2002. 20(3): p. 579-86.

140. Epari, D.R., et al., *Timely fracture-healing requires optimization of axial fixation stability*. J Bone Joint Surg Am, 2007. 89(7): p. 1575-85.
141. Garcia-Aznar, J.M., et al., *Computational simulation of fracture healing: Influence of interfragmentary movement on the callus growth*. J Biomech, 2007. 40(7): p. 1467-76.
142. Gilbert, J.A., L.E. Dahners, and M.A. Atkinson, *The effect of external fixation stiffness on early healing of transverse osteotomies*. J Orthop Res, 1989. 7(3): p. 389-97.
143. Goodship, A.E. and J. Kenwright, *The influence of induced micromovement upon the healing of experimental tibial fractures*. J Bone Joint Surg Br, 1985. 67(4): p. 650-5.
144. Isaksson, H., et al., *Bone regeneration during distraction osteogenesis: Mechano-regulation by shear strain and fluid velocity*. J Biomech, 2006.
145. Mitsui, N., et al., *Optimal compressive force induces bone formation via increasing bone morphogenetic proteins production and decreasing their antagonists production by Saos-2 cells*. Life Sci, 2006. 78(23): p. 2697-706.
146. Augat, P., et al., *Mechanics and mechano-biology of fracture healing in normal and osteoporotic bone*. Osteoporos Int, 2005. 16 Suppl 2: p. S36-43.
147. Einhorn, T.A., *Clinically applied models of bone regeneration in tissue engineering research*. Clin Orthop Relat Res, 1999(367 Suppl): p. S59-67.
148. Probst, A. and H.U. Spiegel, *Cellular mechanisms of bone repair*. J Invest Surg, 1997. 10(3): p. 77-86.
149. Claes, L., et al., *Early dynamization by reduced fixation stiffness does not improve fracture healing in a rat femoral osteotomy model*. J Orthop Res, 2009. 27(1): p. 22-7.
150. Claes, L.E., et al., *Effect of dynamization on gap healing of diaphyseal fractures under external fixation*. Clin Biomech (Bristol, Avon), 1995. 10(5): p. 227-234.
151. Larsson, S., et al., *Effect of early axial dynamization on tibial bone healing: a study in dogs*. Clin Orthop Relat Res, 2001(388): p. 240-51.
152. Marsh, J.L., et al., *Unilateral external fixation until healing with the dynamic axial fixator for severe open tibial fractures*. J Orthop Trauma, 1991. 5(3): p. 341-8.
153. Domb, B.G., et al., *Comparison of dynamic versus static external fixation for pediatric femur fractures*. J Pediatr Orthop, 2002. 22(4): p. 428-30.
154. Siguier, T., et al., *[External fixation in fractures of the lower limb in children]*. Rev Chir Orthop Reparatrice Appar Mot, 1995. 81(2): p. 157-62.

- 
155. Le, A.X., et al., *Molecular aspects of healing in stabilized and non-stabilized fractures*. J Orthop Res, 2001. 19(1): p. 78-84.
  156. Discher, D.E., P. Janmey, and Y.L. Wang, *Tissue cells feel and respond to the stiffness of their substrate*. Science, 2005. 310(5751): p. 1139-43.
  157. Giannone, G. and M.P. Sheetz, *Substrate rigidity and force define form through tyrosine phosphatase and kinase pathways*. Trends Cell Biol, 2006. 16(4): p. 213-23.
  158. Janmey, P.A. and C.A. McCulloch, *Cell mechanics: integrating cell responses to mechanical stimuli*. Annu Rev Biomed Eng, 2007. 9: p. 1-34.
  159. Kadow, C.E., et al., *Polyacrylamide hydrogels for cell mechanics: steps toward optimization and alternative uses*. Methods Cell Biol, 2007. 83: p. 29-46.
  160. Aspenberg, P., et al., *Reduced expression of BMP-3 due to mechanical loading: a link between mechanical stimuli and tissue differentiation*. Acta Orthop Scand, 2000. 71(6): p. 558-62.
  161. Lau, K.H., et al., *Up-regulation of the Wnt, estrogen receptor, insulin-like growth factor-I, and bone morphogenetic protein pathways in C57BL/6J osteoblasts as opposed to C3H/HeJ osteoblasts in part contributes to the differential anabolic response to fluid shear*. J Biol Chem, 2006. 281(14): p. 9576-88.
  162. Mitsui, F.H., et al., *Influence of thermal and mechanical load cycling on microtensile bond strengths of total and self-etching adhesive systems*. Oper Dent, 2006. 31(2): p. 240-7.
  163. Sharp, L.A., Y.W. Lee, and A.S. Goldstein, *Effect of low-frequency pulsatile flow on expression of osteoblastic genes by bone marrow stromal cells*. Ann Biomed Eng, 2009. 37(3): p. 445-53.
  164. Strube, P., et al., *A new device to control mechanical environment in bone defect healing in rats*. J Biomech, 2008. 41(12): p. 2696-702.
  165. Lee, F.Y., et al., *Repair of bone allograft fracture using bone morphogenetic protein-2*. Clin Orthop Relat Res, 2002(397): p. 119-26.
  166. Aro, H.T., et al., *The effects of physiologic dynamic compression on bone healing under external fixation*. Clin Orthop Relat Res, 1990(256): p. 260-73.
  167. Wolff, J., *The Law of Bone Remodeling*. 1986, Berlin: Springer.
  168. Xie, C., et al., *COX-2 from the injury milieu is critical for the initiation of periosteal progenitor cell mediated bone healing*. Bone, 2008. 43(6): p. 1075-83.

- 
169. Xie, C., et al., *Structural bone allograft combined with genetically engineered mesenchymal stem cells as a novel platform for bone tissue engineering*. Tissue Eng, 2007. 13(3): p. 435-45.
  170. Zhang, X., et al., *A perspective: engineering periosteum for structural bone graft healing*. Clin Orthop Relat Res, 2008. 466(8): p. 1777-87.
  171. Zhang, X., et al., *Periosteal progenitor cell fate in segmental cortical bone graft transplantations: implications for functional tissue engineering*. J Bone Miner Res, 2005. 20(12): p. 2124-37.
  172. Duda, G.N., et al., *Interfragmentary movements in the early phase of healing in distraction and correction osteotomies stabilized with ring fixators*. Langenbecks Arch Surg, 2003. 387(11-12): p. 433-40.
  173. Lane, J.M., et al., *Bone marrow and recombinant human bone morphogenetic protein-2 in osseous repair*. Clin Orthop Relat Res, 1999(361): p. 216-27.
  174. Ashraf, N., et al., *Evidence for overgrowth after midfemoral fracture via increased RNA for mitosis*. Clin Orthop Relat Res, 2007. 454: p. 214-22.
  175. Desai, B.J., et al., *The effect of age on gene expression in adult and juvenile rats following femoral fracture*. J Orthop Trauma, 2003. 17(10): p. 689-98.
  176. Gerstenfeld, L.C., et al., *Three-dimensional reconstruction of fracture callus morphogenesis*. J Histochem Cytochem, 2006. 54(11): p. 1215-28.
  177. Isaksson, H., et al., *Remodeling of fracture callus in mice is consistent with mechanical loading and bone remodeling theory*. J Orthop Res, 2008.
  178. Meyer, R.A., Jr., et al., *Gene expression in older rats with delayed union of femoral fractures*. J Bone Joint Surg Am, 2003. 85-A(7): p. 1243-54.
  179. Kenwright, J. and A.E. Goodship, *Controlled mechanical stimulation in the treatment of tibial fractures*. Clin Orthop Relat Res, 1989(241): p. 36-47.
  180. Ulstrup, A.K., *Biomechanical concepts of fracture healing in weight-bearing long bones*. Acta Orthop Belg, 2008. 74(3): p. 291-302.
  181. Utvag, S.E. and O. Reikeras, *Effects of nail rigidity on fracture healing. Strength and mineralisation in rat femoral bone*. Arch Orthop Trauma Surg, 1998. 118(1-2): p. 7-13.

Glatt, V. (May 2008) "Influence of Mechanical Environment upon the Healing of Segmental Bone Defects in the Rat Model. Preliminary Report": *Biologic Science Postgraduate Symposium, Warwick University, Coventry, UK.*

## **Abstract**

### **Influence of the Mechanical Environment upon the Healing of Segmental Bone Defects: Evaluation in a Rat Femoral Model**

Despite the intrinsic ability of bone to heal, there are numerous clinical circumstances where bone healing is defective. My research focuses on the loss of large segments of bone after traumatic injury. If these defects are too large, they will not heal spontaneously. Surgical approaches to healing such defects can be supplemented with recombinant, human bone morphogenetic proteins -2 and -7 (BMP-2 and BMP-7). Despite this, the clinical management of critical-sized defects remains problematic. Our project is based on the hypothesis that the healing of critical-sized defects in response to BMP-2 can be dramatically improved by manipulating the mechanical environment within the defect. To study this, we have developed custom external fixators, which allow the mechanical environment of a segmental defect in the rat femur to be manipulated experimentally *in vivo*. Experiments are in progress to determine the effect of fixator stiffness on the healing of these defects in response to BMP-2. The early results show a large difference in callus size depending on the stiffness of the fixator.

Glatt, V., Matthys, R., Ivkovic, A., Evans, C. (June 2008) "Influence of Mechanical Environment upon the Healing of Segmental Bone Defects in the Rat Model Studied with a Novel, Customized, External Fixator. Preliminary data": 8<sup>th</sup> Annual European Cells and Materials Conference, Davos Switzerland.

## Abstract

### Influence of the Mechanical Environment upon the Healing of Segmental Bone Defects in a Rat Model Studied with a Novel, Customized, External fixator

<sup>1</sup>V. Glatt, <sup>2</sup>R. Matthys, <sup>1</sup>A.Ivkovic, <sup>1</sup>C. Evans

<sup>1</sup>Department of Orthopaedic Surgery, Harvard Medical School, Boston, MA, US,

<sup>2</sup>AO Development Institute, Davos Platz, Switzerland

**Introduction:** Despite the intrinsic ability of bone to heal, there are still numerous clinical circumstances where bone healing is defective and demands the attention of the physician. Common examples include the delayed and non-union of fractures, and the loss of large segments of bone after traumatic injury, tumor resection and failed arthroplasty. There are several surgical approaches to enhance the healing of human bones, and these have been supplemented in recent years by the introduction of recombinant, human bone morphogenetic proteins -2 and -7 (BMP-2 and BMP-7) into clinical practice in combination with different fixation devices. Over the years there have been many advances in technology, which helped to improve the fixation for critical sized defects. Despite these improvements, the clinical management of critical-sized defects remains problematic for surgeons today because it isn't clear how stiff or flexible the fixation device should be to optimize bone healing. Our project is based on the hypothesis that the healing of critical-sized defects in response to BMP-2 can be dramatically improved by manipulating the mechanical environment within the defect. Accordingly, this project aims to investigate the influence of the mechanical environment on bone healing in response to BMP-2 in a rat, critical-sized defect model. The mechanical environment of the defect is altered with a custom made external fixator whose stiffness can be changed in a reliable, quantitative fashion.

**Materials and Methods:** Novel, second generation, external fixators that can be adjusted to provide three different stiffnesses were designed specifically for the rat femur. All materials in the fixator were chosen to be the same as used clinically for human implants. The screws for a new external fixator are made out of titanium (Ti). The stability bars are made out of polyetheretherketones (PEEK). The diameter of the screws is 1mm and the length is 12.75mm. The distance between the screws is 4mm and the distance between the middle screws is 11mm. All holes are predrilled using a 0.79mm drill bit. The screws are locked in the corresponding holes of the fixator, which is parallel to bone surface and set at the distance of 5mm. The fixator stiffness can be changed by changing the stability bars to provide stiffnesses of 40, 70 or 100%, as required. To create reproducible 5mm defects in all rats the guide was designed for a 0.22mm wire saw that clips on the external fixator in between the two middle screws. A rat, femoral, critical-sized defect model was used to test this fixator *in-vivo*. A 5mm defect was created in 6 Sprague-Dawley rats and treated with rhBMP-2 applied on a collagen sponge with external fixators providing 40, 70, 100% stiffness. Animals were x-rayed weekly for 8 weeks to monitor bone healing.

**Results:** A second generation external fixator prototype was successfully created and manufactured for testing *in-vivo* (Figure 1). An *in-vivo* pilot study showed that there is a difference in bone healing depending on external fixator stiffness. Weekly x-rays revealed that bone callus size was biggest in the group with the lowest stiffness (40%) fixator. Furthermore, early callus formation was seen in this group and 70% stiffness group after 9 days of treatment. However, the group with 100% stiffness external fixator had no callus formation after 9 days of treatment. In this group callus formation was delayed until after two weeks of treatment. By the third week defects were bridged with all fixation methods with the biggest callus in 40 and 70% stiffness fixators and smaller callus with 100% stiffness (Figure 2).

**Discussion:** Loss of large segments of bone leads to critical-sized defects that fail to heal spontaneously. Although healing can be induced by recombinant, human bone morphogenetic protein-2 (rhBMP-2), the clinical response is modest. The current project focuses on the influence of the mechanical environment on the healing of critical sized segmental defects in response to rhBMP-2. In preliminary studies, using a first generation external fixator to stabilize the defect, we have been able to achieve osseous union using rhBMP2 and BMP-2 gene transfer with an adenovirus vector. However the rate of healing and the mechanical properties of the healed bone are inconsistent. We hypothesized that this is due to insufficiencies in the rigid external fixator, which generates an unfavorable local mechanical environment. Therefore, we have designed a new, second generation external fixator which allows us to control and measure with precision, the mechanical environment within the critical-sized segmental defect *in-vivo*. Our pilot study shows that fixator stiffness is important in the biologic process of healing bone. In fact, from the weekly x-rays we observed that with 40 and 70% stiffness fixator callus formation was seen already after 9 days of treatment, whereas defects subjected to 100% stiffness had no callus. Furthermore, after two weeks bone regeneration was seen in all groups, but two lower stiffness groups had bigger callus formation as compared to the stiffest fixator. This confirms findings in the literature that if there is too much micro motion during healing, bone bigger callus forms (1) Material, structural and mechanical testing will be performed to determine how important early callus formation and size is to the physical properties of the healed bone. We will apply this knowledge to manipulate fixator stiffness through the course of healing to get rapid bone regeneration and best quality of healed bone. The findings from this study will be highly relevant to the surgical management of patients with segmental bone defects and, possibly, delayed and non-union fractures.

**Reference:** 1. Gomez-Benito MJ, Garcia-Aznar JM, Kuiper JH, Doblare M 2006 A 3D computational simulation of fracture callus formation: influence of the stiffness of the external fixator. J Biomech Eng 128(3):290-9.

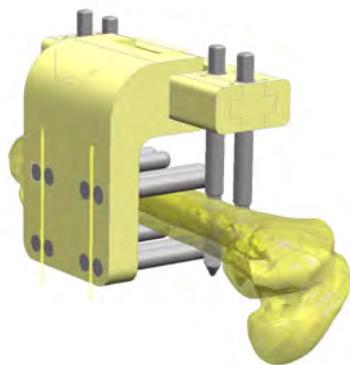


Figure 1 External Fixator with saw guide

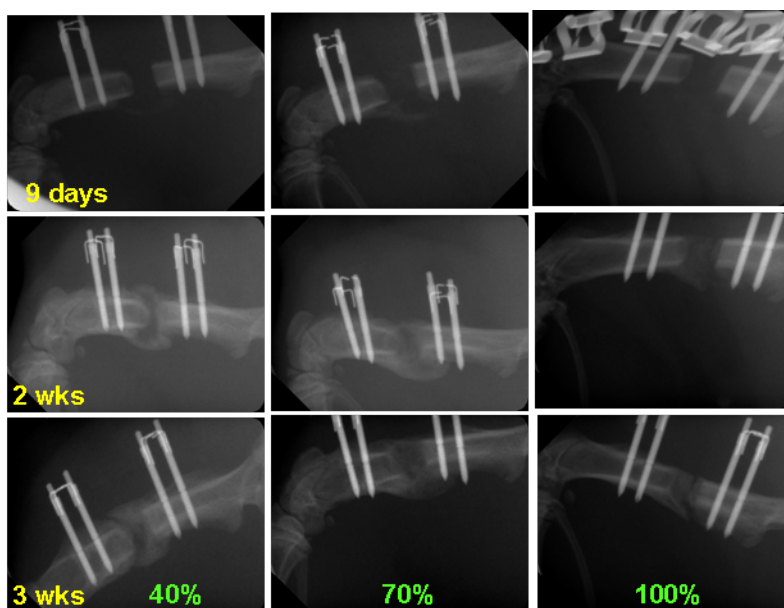


Figure 2 Representative x-ray images with 40, 70 and 100% stiffness external fixator after 9 days, 2 and 3 weeks of treatment with rhBMP-2.